Major intracontinental strike-slip faults and contrasts in lithospheric strength

Peter Molnar
Katherine E. Dayem
Department of Geological Sciences, Cooperative Institute for Research in Environmental Sciences (CIRES), University of Colorado, Boulder, Colorado 80309-0399, USA

ABSTRACT

A large fraction of major intracontinental strike-slip faults, defined here as those slipping at rates of ~10 mm/yr or more, lie adjacent to relatively strong regions, such as oceanic lithosphere or Precambrian shields. We suggest that such faults form adjacent to discontinuities in strength, because strain in a continuous medium must concentrate near such strong objects. Concentration in strain is enhanced in deforming continua where viscosity is non-Newtonian, and hence where strain rates vary with deviatoric stress raised to a power greater than one, as is the case for rock-forming minerals at low temperatures characteristic of the lithosphere. Conversely, in regions where deformation is spread over a wide region, such as in the Basin and Range Province of the western United States or in the high interior of the Tibetan Plateau, the absence of strong objects may allow deformation to be diffuse without the development of rapidly slipping faults.

INTRODUCTION

Almost by definition, transform faults between oceanic plates pass through the entire lithosphere as narrow shear zones, but the nature of strike-slip faults within continents remains a subject of discussion. Some imagine that major strike-slip faults in continents also act as plate boundaries and can be defined as narrow shear zones beneath the much thicker crust of continents than that of oceanic regions (e.g., Peltzer and Tapponnier, 1988; Tapponnier et al., 1986, 1990, 2001). Others see strike-slip faults, including major ones, not only marking discontinuities in the velocity field, but also serving as passive markers in the deformation field of the brittle upper part of lithosphere, which deforms continuously at depth (e.g., Davis et al., 1997; England and Houseman, 1986; England and Molnar, 1990, 1997; Flesch et al., 2001, 2005; Holt, 2000; Holt et al., 1991). Both views can be seen as end members. Minor faults separating small blocks of crust almost surely do not pass straight down into the lithosphere as narrow shear zones. Slip on many major intracontinental strike-slip faults, however, absorb large fractions of relative plate movement between lithospheric plates and deforming regions, e.g., the Alpine fault in New Zealand, the San Andreas fault in California, and the North Anatolian fault in Turkey. Thus, if these different views are to be tested, major, not minor, strike-slip faults are likely to provide the necessary evidence (leaving aside for the moment how one decides what defines a major fault).

Strain will concentrate near the boundaries of relatively strong regions immersed within a deforming medium, with the degree to which strain rates concentrate dependent on the constitutive law that relates stress and strain rate (e.g., Bell et al., 1977; Dayem et al., 2009). Thus, some degree of localization should develop within a homogeneous viscous substance near its boundaries with more viscous material. We tested the idea that deformation near the Altyn Tagh fault, which bounds the rigid Tarim Basin on the north from the deforming Tibetan Plateau to the south, occurs without additional weakening such as by dissipative heating or grain-size reduction, and hence that the material properties of lithosphere beneath Tibet and beneath the Tarim Basin remained constant as deformation accumulated (Dayem et al., 2009). Although localized deformation occurs along the boundary between material with different viscosity coefficients (Fig. 1), we found that additional weakening must occur to localize deformation in order to mimic the extent to which strain has been concentrated in a narrow zone along the Altyn Tagh fault (Dayem et al., 2009). Thus, we cannot reject the idea that strain localizes in the mantle beneath major faults, as Peltzer and Tapponnier (1988; see also Tapponnier et al., 1986, 1990, 2001) have argued.

The need for such localization of strain and the evolving development of lateral variations in material properties along the Altyn Tagh fault poses another question: are heterogeneities in strength a necessary prerequisite for localization of strain within the mantle? To address this question, we summarize data concerning major strike-slip faults with the view of asking, to what extent do major strike-slip faults develop adjacent to marked heterogeneities in strength? Answering this question requires answering a number of somewhat arbitrary questions, not just, what defines a major fault?

Before pursuing these questions, we review the basic reasoning that underlies asking such questions in the first place. We first give a brief discussion of how nonlinear viscosity can enhance the concentration of strain near a strong region in a continuously deforming medium. We then digress to discuss how localization of strain can develop once a shear zone is present and dissipative heating allows localized weakening. This form of localization is not the process that we consider here, but the process that allows strain to be localized in narrow zones once some concentration of strain has begun. We then consider brittle faulting in the upper crust, which also is not the main motivation of our study. As faults result from brittle deformation, and they clearly are important in the deformation that we see at the surface, we do not neglect them. Brittle fracturing of the upper crust, however, cannot alone account for the existence of major faults. Given that most faults are minor, we see them as surface manifestations of deeper processes, and following the discussion of brittle processes, we ignore them. The main part of the paper is a discussion of evidence of major faults and their tectonic settings, most of which is relegated to the Appendix.

Geosphere; August 2010; v. 6; no. 4; p. 444–467; doi: 10.1130/GES00519.1; 3 figures; 1 table; 13 appendix figures.

Localization of Strain Near Heterogeneity in Strength (or Viscosity)

Simple arguments show that, in a viscously deforming solid that obeys a nonlinear relationship between deviatoric stress, τ, and strain rate, $\dot{\varepsilon}$; e.g., $\dot{\varepsilon} \sim \tau^n$, where $n > 1$, strain localizes near a strong region. The state of stress is governed by the equation of equilibrium, or Stokes's equation, which may be written as

$$\nabla \cdot \tilde{\sigma} + \rho g \hat{z} = 0. \quad (1)$$

Here $\tilde{\sigma} = \tilde{\tau} - P$ is the stress tensor; $\tilde{\tau}$ is the deviatoric stress tensor, P is pressure, ρ is density, g is gravity, and $\hat{z}$ is the unit vector pointing upward (tensile stresses are positive.) Let us consider the simple case in which the boundary of a strong region is parallel to the y axis, and deformation occurs largely in response to shear, τ_{xy}, on vertical planes parallel to that axis. To a good approximation, we may ignore variations in the y direction. In the simple case of largely strike-slip deformation with no body force, only one of the three components of equation 1 need be considered:

$$\frac{\partial \tau_{xy}}{\partial x} + \frac{\partial \sigma_{yy}}{\partial y} + \frac{\partial \tau_{yz}}{\partial z} \approx \frac{\partial \tau_{xy}}{\partial x} = 0. \quad (2)$$

Thus, the shear stress τ_{xy} is nearly constant with distance away from the strong region. A more precise statement is that τ_{xy} decreases slowly with distance from it; presumably, all components of stress vanish at a large distance from the strong region.

The constitutive law relating stress and strain is commonly written as:

$$\tau_{xy} = B\dot{E}^{(1-n)/n}\dot{\varepsilon}_{xy} \quad (3)$$

Here $\dot{\varepsilon}_{xy}$ is the xy component of strain rate, $\dot{E}$ is the second invariant of the strain rate tensor, and n and B are material parameters. (In the case of Newtonian viscosity, $n = 1$ and B is twice the coefficient of viscosity.) In the simple case that we have considered, there is only one important component of strain rate, $\dot{\varepsilon}_{xy}$. Thus, $\dot{E} = \dot{\varepsilon}_{xy}$, and equation 3 becomes

$$\tau_{xy} = B\ \dot{\varepsilon}_{xy}^{1/n}. \quad (4)$$

If τ_{xy} decreases slowly with increasing x, and B is constant, $\dot{\varepsilon}_{xy}^{1/n}$ also decreases slowly with distance. For $n = 3$, for example, if τ_{xy} decreased to half its value at $x = 0$ over some sensible geological distance x_0, the strain rate would decrease by 8 times. If stress decreased linearly with distance, the strain rate would drop from its value at $x = 0$ to half that value at $x = 0.406x_0$. For $n > 10$, as might be appropriate for mantle lithosphere colder than ~700 °C (e.g., Evans and Goetze, 1979; Raterron et al., 2004), strain is yet more localized near the boundary between regions of different strength (e.g., Dayem et al., 2009). Where τ_{xy} decreased by 2 times, strains would be $2^{10} = 1024$ times smaller than at the boundary, and for linear decrease in stress, the strain rate would drop to half its maximum value at $x = 0.134x_0$. Thus, the nonlinear viscosity that we expect for rock-forming minerals and for the lithosphere in general should enhance localization of strain near strong regions.

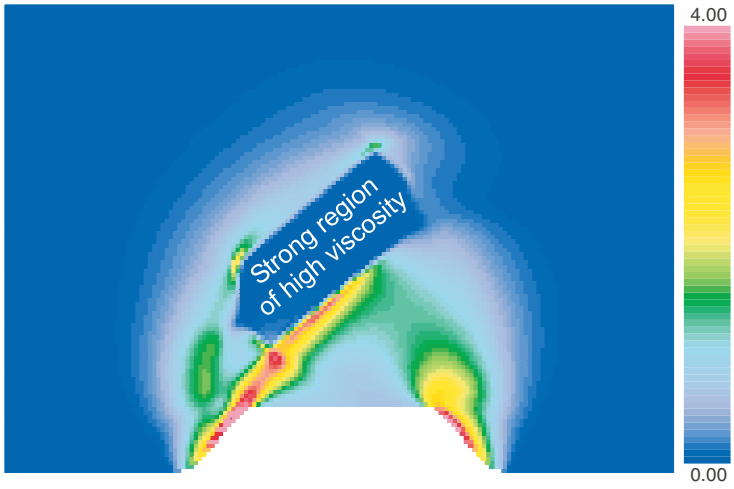

Figure 1. Maximum shear strain rate of a thin viscous sheet with a strong region immersed within a region of constant viscosity coefficient and indented by a rigid object. This simulation is meant to mimic conditions in Asia, where India indents the rest of Eurasia, and the Tarim Basin, which is north of the Tibetan Plateau, behaves as a strong object. The calculation is controlled by two dimensionless parameters, n (see equation 3) and the Argand number, Ar, which is a measure of stress due to crustal thickness variations relative to viscous stress. For the calculation shown, n = 10, Ar = 6, and the sheet has been indented 40% the width of the indenting boundary.

Dissipative Heating and Localization of Strain

Slip on most faults in the upper crust occurs during earthquakes, and some of the strain energy that is released during the earthquakes is radiated away by elastic waves, but most suppose that the radiated energy is a small fraction (<~10%) of the total strain energy released. At the shallow depths where earthquakes occur, some strain energy is dissipated in the comminution of particles and the creation of new surfaces. Hence, strain energy is lost as surface energy, but most consider this also to be small (e.g., Chester et al., 2005; Lockner and Okubo, 1983; Olgaard and Brace, 1983; see Wilson et al. 2005, for a different view). Most dissipation leads to heating of the surrounding rock. That heating can, in turn, weaken the adjacent rock and reduce the resistance to slip, so that the fault zone develops into a zone of weakness within intact, stronger rock.

In the simple case of a fault separating two half-spaces that slide past one another at a constant rate, shear heating of the fault will raise the temperature there, and heat will diffuse into the adjacent half-spaces. If the strength of the material decreases with increasing temperature, as the temperature rises, the stress and rate of heating will decrease. Concurrently, as heat diffuses laterally from the fault, the weakened zone near the fault grows wider. Thus, dissipation will be spread over an increasingly wider zone. For this idealized case, the shear zone will widen continuously (e.g., Fleitout and Froidevaux, 1980; Yuen et al., 1978).

If a strike-slip fault separates two quarter-spaces, and the top surface is maintained at a fixed temperature, as in the Earth, then heat will diffuse not only horizontally outward from the fault, but also upward to the top surface. Initially, such a shear zone would widen, as heat diffused laterally, and as the rock surrounding the fault warmed and became weaker. Eventually, however, upward diffusion of heat would occur faster than laterally outward diffusion,

and the temperature structure would approach a steady state in which all dissipative heating were lost by flow through the top surface in a region near the initial fault (e.g., Thatcher and England, 1998; Yuen et al., 1978). The width of the region with elevated heat flux would scale with the depth distribution of dissipative heating, so that deeper concentrations of dissipative heating would require longer times to reach steady state and would be overlain by wider zones of high heat flux. It follows that shear zones through the lithosphere, for which dissipative heating was concentrated at depths of a few tens of kilometers, would in turn be only ~100 km wide (e.g., Leloup et al., 1999; Thatcher and England, 1998).

Brittle Deformation Above a Continuously Deforming Substratum

The preceding discussion is meant to consider the case in which most of the strain in a large region, hundreds of kilometers in dimension, occurs by slip on a single fault at the surface and within a relatively narrow zone (<~100 km) at depth. The opposite situation seems to characterize some regions, like the Basin and Range Province of the United States or the Tibetan Plateau, where strain is spread over regions ~1000 km in dimension by slip on faults that are tens to a couple of hundred of kilometers apart. In such regions, particularly where slip occurs on normal (or reverse) faults that do not dip vertically, the common image includes such faults widening into diffuse shear zones at depth within the crust and not penetrating the Moho. The Moho beneath the Basin and Range Province, for example, seems to be flat and not cut by faults (Klemperer et al., 1986), a fact that has been used to buttress the supposition that strain is continuous in the lower crust and upper mantle (e.g., Fletcher and Hallet, 1983; Froidevaux, 1986). Although strain cannot be laterally invariant in the upper mantle beneath such regions, a description of deformation that includes blocks of lithosphere ~100 m in thickness, but only tens of kilometers in lateral dimensions moving with respect to one another seems unlikely.

MAJOR INTRACONTINENTAL STRIKE-SLIP FAULTS

Deforming regions many hundreds of kilometers to ~1000 km in dimension, like the Basin and Range Province or most of Tibet, can accommodate ~10–20 mm/yr of movement across them, but in general faults that slip as fast as 10 mm/yr do not occur within such regions. By contrast, in many regions where relative movement is concentrated on a single fault, slip on that fault reaches, if not exceeds, 10 mm/yr. Thus, we use slip rates of ~10 mm/yr or more to identify major faults that could be underlain by narrow shear zones penetrating the entire lithosphere, not just upper crust. Of course, there are notable exceptions to this criterion for identifying major faults; for example, slip on the Dead Sea fault between the eastern Mediterranean and the Arabian shield is <~5 mm/yr (Alchalbi et al., 2010; Gomez et al., 2007; Le Beon et al., 2008; Reilinger et al., 2006; Wdowinski et al., 2004), but although some deformation clearly does occur adjacent to the fault (e.g., Alchalbi et al., 2010), it serves as a good example of plate boundary within a continental region.

We compiled a list of major strike-slip faults, including all of those assigned a rate of 10 mm/yr or higher (Table 1; Fig. 2), and we assessed evidence for slip rates on them. Both dating of Quaternary offsets and geodetic measurements, particularly using global positioning system (GPS), place constraints on slip rates. In the Appendix, we offer summaries of the relevant data that constrain slip rates and other aspects of the faults tabulated in Table 1. To the best of our knowledge, Table 1 contains all intracontinental strike-slip faults with slip rates as large as 10 mm/yr, as well as other faults that seem worthy of note. The discussions in the Appendix are built around regions, beginning in Alaska, continuing through western North America and Central America to South America, and then from Anatolia eastward across Asia, to Indonesia and other islands of the western Pacific, to New Zealand. Here we summarize faults and slip rates in the context of their relationships to strong regions and to marked viscosity contrasts.

Major intracontinental strike-slip faults have developed in a variety of settings, but only some of them have formed adjacent to regions that are obviously strong. Prominent examples of such a faults are the Fairweather fault, which is the continuation of the Queen Charlotte Islands fault and serves as the North America–Pacific plate boundary along the west coast of Canada and southeast Alaska (Figs. 2 and A1); the San Andreas fault in California, which is near the Pacific plate (Fig. A2); the El Pilar fault in northern Venezuela, which serves as the Caribbean–South America plate boundary (Fig. A4); the North Anatolian fault in Turkey, which is near the Black Sea coastline and hence near oceanic lithosphere (Fig. A5); the Chaman fault in Pakistan and Afghanistan, which is along the western margin of the India plate, and on which slip absorbs virtually all of the plate motion between the India and Eurasia plates (Fig. A7); the Altyn Tagh fault, which follows the northern edge of the Tibetan Plateau and the southern edge of the Tarim Basin (Fig. A7), which is largely underlain by Precambrian basement and has behaved as a stable platform since Paleozoic time (e.g., Yin and Nie, 1994); and the Alpine fault along the west coast of the South Island of New Zealand and adjacent to relatively strong lithosphere (Fig. A13), which is oceanic in the southern part and is capped by thin crust in the northern part. We contend that some other faults that slip at ~10 mm/yr also are bounded by strong regions, but aspects of them make this association less convincing than for those mentioned above. For example, the western end of the Garlock fault (Fig. A2), the slip rate of which seems to be slightly <10 mm/yr, is adjacent to the Sierra Nevada block, which seems to behave as a strong object (Argus and Gordon, 1991). The Boconó fault, the slip rate of which might be slightly <10 mm/yr, is adjacent to the crest of the Mérida Andes in Venezuela, which in turn is bounded on the southeast by the Guyana shield of Precambrian rock (Fig. A4). The East Anatolian fault in eastern Turkey (Fig. A5), with slip apparently ~10 mm/yr (e.g., Reilinger et al., 2006), is near the northwest end of the Arabian plate, though perhaps not close enough to be affected by it. The slip rate for the Dead Sea fault is not >~5 mm/yr, but that slip absorbs relative motion between the Arabian and African plates. For much of its length, the Kunlun fault in northern Tibet lies along the southern edge of the Qaidam Basin (Fig. A7), which seems to have undergone only mild deformation compared to its surroundings and appears to be underlain by Precambrian basement (Yin et al., 2007, 2008a, 2008b). Moreover, deformation becomes distributed at the ends of this fault, where it dies out, and where it is not adjacent to the Qaidam Basin. Strike slip along the Longitudinal Valley fault in Taiwan (Fig. A9), at least in places, seems to be rapid, if the data that we have compiled contain inconsistencies (see Appendix). In any case, it lies along the western edge of the Philippine Sea plate. The Sorong and Yapen faults in northwestern New Guinea are near the coastline of the Pacific Ocean, and serve as the boundary to the Pacific plate, if not to the Australian plate hundreds of kilometers to the south (Fig. A12). Impressive as most of these faults might be, they comprise only half of the intracontinental strike-slip faults slipping at ~10 mm/yr listed in Table 1.

For at least one obvious example, the Polochic-Montagua fault zone in Guatemala (Figs. 2 and A3), the high slip rate may give a misleading impression of how continental lithosphere deforms in this region. The Cayman Trough to the east (Figs. 2 and A3) acts as a transform fault and marks the plate boundary between the North America and Caribbean

TABLE 1. LIST OF MAJOR INTRACONTINENTAL STRIKE-SLIP FAULTS

Region	Fault*	Rate (mm/yr)	Comments
North America	**Fairweather**	**46**	**Bounded by Pacific plate**
North America	*Denali*	~4–14	*Underlain by underthrust lithosphere*
North America	**San Andreas**	**30–37**	**Bounded by Pacific plate**
North America	San Gregorio–Hosgri	~3–8	Rate varies along fault
North America	Garlock	~5–10	**Bounded by Sierra Nevada block**
Guatemala	Polochic-Montagua	**20**	Fault splays on land
South America	**El Pilar**	**20**	**Bounded by Caribbean plate**
South America	**Boconó**	6–**10**	**Bounded by Guyana shield**
South America	Oca	2	Bounded by the Caribbean plate
Turkey	**North Anatolian**	**24**	**Bounded by Black Sea**
Turkey	**East Anatolian**	**~10**	**Bounded by the Arabian shield (?)**
Middle East	**Dead Sea**	~5	**Arabia-Africa plate boundary**
Iran	Main Recent	~3 (<12)	
Iran	North Tabriz	3–6	
Iran	Main Kopet Dagh	~2	
Iran	Bakharden-Quchan	9	Five strands, with each <5 mm/yr
Iran	Doruneh	2–3	
Iran	Deshir	2	
Iran	Anar	0.8	
Iran	Minab-Zendan	5–7	Short length
Iran	Sabzevaran-Jiroft	6	Very short length
Iran	Gowk-Nayband	1.4	
Iran	East and West Neh	3–8	Several strands
Afghanistan-Pakistan	**Chaman**	**28**	**Bounded by Indian plate**
Tajikistan	Darvaz-Karakul	11	Bounded by Tajik Depression (?)
Tien Shan	Talas-Ferghana	<1–3	
Tibet	Karakorum	3–5	
Tibet	**Altyn Tagh**	~**10**	**Bounded by Tarim Basin**
Tibet	**Kunlun**	~**10**	**Bounded by Qaidam Basin**
China	Haiyuan	~5	
China	**Xianshuihe**	~**10**	**Within deforming crust**
China	**Garzê-Yushu**	~**10**	**Within deforming crust**
China	Red River	< 5	
Myanmar	*Sagaing*	**18**	*Underlain by underthrust lithosphere*
Indonesia	*Sumatra*	5–**25**	*Underlain by underthrust lithosphere*
Taiwan	**Longitudinal Valley**	0–**20**	**Bounded by Philippine Sea plate**
Philippines	*Philippine*	**20–25**	*Underlain by underthrust lithosphere*
Sulawesi	Palu-Koro	~**40**	Several strands over wide area
	Gorontalo	**11**	Very short length
Irian Jaya	**Sorong and Yapen**	~**20**	**Part of wide shear zone**
New Zealand	**Alpine**	**23–27**	**Bounded by Australian plate**
	Marlboro: Wairau	3–5	*Part of wide complex shear zone*
	Marlboro: Awatere	~6	*Part of wide complex shear zone*
	Marlboro: Clarence	3.5–5	*Part of wide complex shear zone*
	Marlboro: Hope	**18–23**	*Part of wide complex shear zone*
	Marlboro: Porters Pass	3–4	*Part of wide complex shear zone*

*Bold text shows faults that are bounded by strong lithosphere. Italics indicate faults associated with oblique subduction, and that absorb a large fraction of the component of relative plate motion.

plates. The Cayman Trough contains two narrow strike-slip fault zones with a short segment of spreading between them. Deformation clearly is localized on the strike-slip faults. Where the western of these faults reaches the continental lithosphere of Central America, however, it splays into at least two, and apparently three separate strands. Moreover, the slip rate decreases westward (Lyon-Caen et al., 2006). Thus, where the transform fault between oceanic plates passes into a continent without strong lithosphere, the fault splays out and deformation occurs over a broad zone (DeMets et al., 2007; Lyon-Caen et al., 2006; Rodriguez et al., 2009; Rogers and Mann, 2007). In some ways, the Polochic-Montagua fault zone illustrates how deformation within continental regions tends not be localized when a strong region is absent.

Similarly, ~100 mm/yr of left-lateral shear must be accommodated across western New Guinea (Fig. A12), but only the Sorong and Yapen faults seem to be major. The apparent absence of major strike-slip faults within the region where the remaining ~80 mm/yr of strike-slip shear must be absorbed (e.g., Stevens et al., 2002) is consistent with there being no major strength contrasts within the lithosphere beneath the region.

None of the faults discussed above is near a subduction zone, but as Fitch (1972) noted, major strike-slip faults can absorb deformation associated with oblique subduction (Fig. 3). In such cases, slabs of oceanic lithosphere plunge beneath accretionary wedges of material and adjacent lithosphere seaward of the volcanic arcs. The strike-slip faults strike parallel to trenches, and in many cases they follow closely the belt of volcanoes. Thus, regardless of the nature of the lithosphere landward of the belt of volcanoes, strong oceanic lithosphere underlies the wedge of material seaward of the volcanoes. Two of the major faults listed in Table 1, the Sumatran fault (Figs. 2 and A8) and the Sagaing fault in Myanmar (Figs. 2 and A7), illustrate these characteristics well.

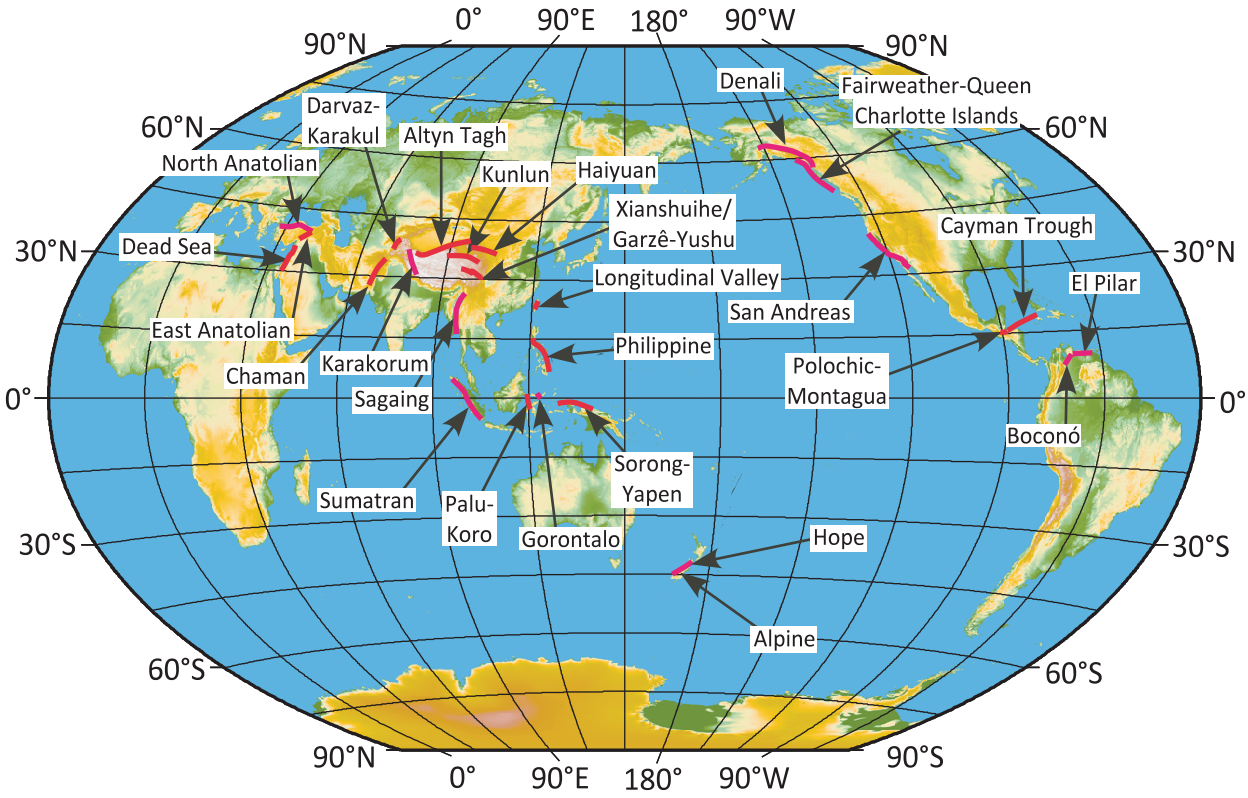

Figure 2. Map of the world showing locations of most of the major strike-slip faults discussed in the Appendix. We omit here the many faults in Iran (Fig. A6), all of which seem to slip <10 mm/yr, and we omit other faults with comparably low rates, in part to avoid cluttering the figure. Purple lines show right-lateral faults, and red lines show left-lateral faults.

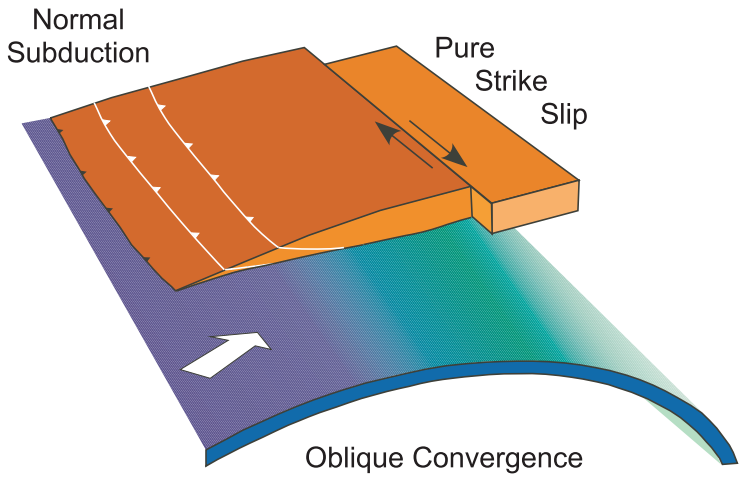

Figure 3. Simple illustration of strike-slip faults at subduction zones where convergence is oblique. Oceanic crust, in blue that shades into green with depth, forms the top part of oceanic lithosphere that moves obliquely toward the overriding plate (brown). The overriding plate includes an accretion wedge of offscraped material. The subducting lithosphere dips at a gentle angle beneath this material, and in most regions where active arc volcanism occurs, the subducting plate reaches a depth of ~100 km beneath the volcanoes (e.g., England et al., 2004). Thus the wedge-shaped fragment of the overriding plate is underlain immediately below by oceanic lithosphere. Where subduction is oblique, the strike-slip component commonly is absorbed not by oblique underthrusting, but by pure strike-slip faulting on a fault that passes near the belt of volcanoes.

Fitch (1972) recognized this relationship in a study of earthquakes in Indonesia and from the style of deformation in Sumatra. The Australia plate moves nearly due north relative to the Sunda block, but subduction of the Australia plate includes a large northeastward component of slip. To compensate for that obliquity, the wedge of lithosphere above the downgoing Australian plate and southwest of the volcanoes slides northwest, relative to Sundaland to the northeast, along the Sumatran fault (Fig. A8). McCaffrey (1991, 1992) showed further that the variation in slip vectors of earthquakes along the Sunda arc adjacent to Sumatra required that the forearc wedge deform and the slip rate on the Sumatran fault increase toward the northwest, a result corroborated by GPS measurements (e.g., Bock et al., 2003; Genrich et al., 2000; Prawirodirdjo et al., 1997, 2000) and by estimates of slip rates on segments of the fault (e.g., Bellier and Sébrier, 1995; Bellier et al., 1999; Sieh and Natawidjaja, 2000).

The Sumatran fault differs from most of strike-slip faults considered here by being somewhat less linear and by following the volcanic arc. Sieh and Natawidjaja (2000) emphasized that the fault is more segmented than most

strike-slip faults, with large stepovers between segments. Thus, the zone of deformation at depth cannot be as narrow as a few kilometers in width, as some argue for some major strike-slip faults. More important, the fault follows the volcanic arc. Sieh and Natawidjaja (2000) noted that the fault does not pass beneath all volcanoes, but the volcanoes and the strike-slip fault do share the same zone of activity. McCaffrey et al. (2000) recognized that a belt of volcanoes requires a zone of weakness along the volcanoes, and they suggested that the volcanoes provided a weakness along which oblique convergence could be partitioned into pure strike slip along the Sumatran fault and nearly pure thrust slip along the interface between the Australian plate the forearc. (Molnar and Atwater [1978] argued similarly that inner arc spreading would develop along a zone of weakness created by the volcanic arc and grow into backarc basins). Thus, unlike most intracontinental strike-slip faults, the Sumatran fault inherited a deep zone of weakness.

The Sagaing fault also has a relationship to underthrust lithosphere (Fig. A7). It is a continuation of a transform fault in the Andaman Sea, where active seafloor spreading is occurring (e.g., Curray et al., 1978). This fault passes east of the Indo-Burman Ranges that deform as a thin-skin fold-and-thrust belt with east-west shortening, so that this region moves westward with respect to India. A belt of intermediate depth earthquakes dips eastward beneath the Indo-Burman Ranges, implying that the ranges are underlain by a slab of oceanic lithosphere that dips eastward and is attached to the Indian plate to the west (e.g., Chen and Molnar, 1990; Ni et al., 1989). On a larger scale, however, the India plate moves north-northeast relative to South China, and therefore so must the underthrust lithosphere. Thus, the Sagaing fault absorbs a large fraction, if not all, of the strike-slip component of relative plate motion between India and South China. Moreover, although volcanoes are sparse, the fault passes near two major volcanoes at its northern end (e.g., Le Dain et al., 1984).

We suggest that the Denali fault in Alaska (Figs. 2 and A1), the Philippine fault in the Philippines (Fig. A11), and the Marlboro faults of New Zealand (Fig. A13) may also share such relationships with subduction zones. The Pacific plate underthrusts southern Alaska at a gentle angle. Using receiver functions, Ferris et al. (2003) mapped a sharply defined low-speed zone dipping from 50 to 150 km and reaching its deepest beneath the western end of the Denali fault. They suggested that this zone marks ocean crust on the top of the subducting Pacific lithosphere. If this low-speed zone does mark subducted Pacific lithosphere, it requires that that lithosphere dip gently and underlie most of the crust south of the Denali fault. The Philippine fault, if sharply defined geomorphically and slipping rapidly, remains sufficiently poorly studied that drawing conclusions here seems risky. As discussed in the Appendix, not only is the slip rate uncertain, but additional deformation possibly associated with rapid slip on other faults seems to occur. Nevertheless, slip on the Philippine fault seems to absorb much, if not all, of the component of relative plate motion parallel to the Philippine trench to its east. The Marlboro faults in the northeastern part of the South Island of New Zealand displace slivers of crust that overlie the Pacific plate where it subducts gently and obliquely beneath the island. Although we treat these faults as part of the Alpine fault system, unlike the single, main strand of that fault, the Marlboro faults are underlain by oceanic lithosphere that dips gently westward. Thus, the settings of the Denali, the Philippine, and the Marlboro faults are similar to those of Sagaing fault in Myanmar and the Sumatra fault; they are adjacent to a region that is underlain by subducting oceanic lithosphere.

Slip occurs at ~10 mm/yr or more on 5 other faults in Table 1. That for the Palu-Koro fault in Sulawesi (Figs. 2 and A11) approaches 40 mm/yr. Several aspects, however, make it hardly typical of major intracontinental strike-slip faults, i.e., its relatively short length of 300 km, the distribution of slip onto four separate strands in the one place where it has been studied well, and a large oblique component with ~11–14 mm/yr of extension across the fault zone. Thus, although it clearly stands out as slipping rapidly without an obvious strong region adjacent to most of it, it is hardly a glaring exception to the pattern of a zone of strong lithosphere adjacent to major intracontinental strike-slip faults. Also crossing part of Sulawesi is the Gorontalo fault, which slices obliquely across the northern arm of the island and slips at ~11 mm/yr (Figs. 2 and A11). This fault also is short, and as much as half of its ~200 km length seems to cut through oceanic lithosphere. Thus, it also seems exceptional, but less for not being obviously bounded by a strong zone, than for being a short, and perhaps short-lived, fault in a tectonically complicated setting.

The Xianshuihe and Garzê-Yushu faults (Figs. 2 and A7), which appear to be continuations of one another, stand out as prominent exceptions to the pattern that we suggest here. The southeast end of the Xianshuihe fault passes near the western end of the Sichuan Basin, which seems to be underlain by relatively strong lithosphere (Clark et al., 2005), but most of this fault for its ~300 km length, and all of the Garzê-Yushu fault, which continues west-northwest for another ~300 km, are within the deforming Tibetan Plateau. We can imagine that the Xianshuihe fault developed because of its proximity to the Sichuan Basin, but we suggest that a safer interpretation is that it is an exception to the pattern.

The Darvaz-Karakul fault (Figs. 2 and A7) may also be an exception, but as discussed in the Appendix, its slip rate seems to be poorly constrained. Moreover, it is not clear whether this fault passes only through sedimentary rock and is truncated below by a layer of salt where the sedimentary rock is detached from the basement, or if it passes through the basement. In the latter case, it would be bounded on the west by relatively strong lithosphere underlying the Tajik Depression. We ignore it here, because too little is known.

Table 1 lists many other strike-slip faults that are known well for being sources of major earthquakes or for having been studied thoroughly. Because their slip rates are low we relegate all discussion to the Appendix and ignore them here. Nevertheless, a couple of points do seem worth noting. The most rapid strike slip in Iran seems to be along the eastern margin of the Lut block (Fig. A6), a small fragment of Precambrian crust that had separated from Gondwana and was accreted to Eurasia in Cretaceous to early Cenozoic time (e.g., Stöcklin, 1974; Tirrul et al., 1983). Thus, this fault zone appears to follow a marked contrast in lithospheric strength. Similarly, the Talas-Ferghana fault (Fig. A7), which may slip at a negligibly slow rate (e.g., Mohadjer et al., 2010; Reigber et al., 2001; Zubovich et al., 2007), separates the deforming Tien Shan from the more rigid Ferghana Valley.

DISCUSSION

If one restricts attention to intracontinental strike-slip faults with slip rates of 10 mm/yr or more (Table 1), a large fraction of these faults separates one strong block or plate either from another or from a deforming zone. This pattern is enhanced if we include faults adjacent to subduction zones where oblique convergence occurs.

Among the 14 faults slipping at rates >15 mm/yr, 8 of them (the Fairweather, San Andreas, El Pilar, North Anatolian, Chaman, Longitudinal Valley [if perhaps we overestimate its slip rate], combined Sorong and Yapen, and Alpine) seem to bound strong regions. Four have developed along subduction zones where oblique convergence occurs: the Sagaing, Sumatran, Philippine, and Hope faults. We see the Polochic-Motagua fault as an exception that supports this inference, because as a continuation of the Cayman transform fault it splays out into several strands west of its intersection of

the coast of Central America. Thus, although one may quibble about peculiarities of the various faults, the relatively short Palu-Koro fault, with a substantial component of oblique extension across it, seems to be the only clear exception, and its rather unusual characteristics might make it exceptional in its own right.

We discussed 10 other faults slipping at ~10 mm/yr: the Denali, Garlock, Boconó, East Anatolian, Darvaz-Karakul, Altyn Tagh, Kunlun, Xianshuihe, Garzê-Yushu, and Gorontalo faults. Among these, the Garlock, Boconó, East Anatolian, Altyn Tagh, and Kunlun faults seem to follow the edges of strong blocks, if the slip rate for the Garlock, Boconó, and East Anatolian faults might be overestimated, and the proximity of a strong region to the East Anatolian fault might be stretched too far to be consistent with the pattern we propose. The Denali fault follows closely the edge of Pacific lithosphere subducted at a gentle angle and hence is similar to the Sagaing and Sumatran faults. We contend that we may ignore the short Gorontalo fault, and that too little is known of the Darvaz-Karakul to define it as exceptional or not. As discussed here, the Xianshuihe and Garzê-Yushu faults seem to be the most glaring exceptions to the pattern of strong regions lying close to major faults. Neither is obviously bounded by a strong region, if the Xianshuihe fault does coalesce into a single strand with rapid slip where it diverges from the relatively strong Sichuan Basin. Thus, we suggest that the Xianshuihe and/or Garzê-Yushu faults are "the exception that proves the rule" that major strike-slip faults form at the edges of deforming regions, where a marked contrast in strength facilitates localization of deformation.

As noted in the introduction, localization of strain adjacent to a heterogeneity in strength does not suffice to account for the presence of faulting at the surface, or for the degree to which strain is localized in the crust along major strike-slip faults. Other processes, which include dissipative heating, grain-size reduction, and simply fracturing, must occur. Nevertheless, the summary of major intracontinental strike-slip faults presented here suggests that the presence of heterogeneities in strength facilitates strain localization that then can continue by other mechanisms to become major faults.

ACKNOWLEDGMENTS

This work grew from another study done with G.A. Houseman, and his help, if not specifically associated with this paper, was vital. W. Szeliga shared his analysis in advance of publication. We thank A. Yin and an anonymous reviewer for constructive criticism. This research was supported in part by the National Science Foundation under grant EAR0507730.

APPENDIX. DISCUSSION OF SLIP RATES AND RELEVANT FEATURES OF MAJOR STRIKE-SLIP FAULTS

We discuss strike-slip faults beginning with the Fairweather and Denali faults in Alaska and then the San Andreas system in California. We continue by considering faulting in Central America and South America, and then the Anatolian and Dead Sea faults in western Asia. Continuing eastward, we discuss faults in Iran, Afghanistan, and eastward to Southeast Asia to the Sumatran fault. Next we consider the Longitudinal Valley fault in Taiwan and move south through the Philippines and Sulawesi, and then eastward across the island of New Guinea to New Zealand with the Alpine fault and its splays into the Marlboro fault zone.

Alaska: The Fairweather, Denali, and Totschunda Faults

Pacific–North America plate motion in southeast Alaska is essentially parallel to the Queen Charlotte Islands strike-slip fault, a transform fault. The Pacific plate subducts beneath southern Alaska and at the Aleutian Trench. The dip of the subducting plate is quite gentle (e.g., Ferris et al., 2003), and intermediate depth earthquakes occur beneath the Alaska Range, where the Denali fault trends east-west (Fig. A1). Deformation also extends into Alaska, with slip on the Denali and Totschunda faults accommodating much of the relative plate motion that is not absorbed by subduction in southern Alaska.

Triangulation (Lisowski et al., 1987), GPS measurements (Fletcher and Freymueller, 2003), and preliminary dating of late Holocene offsets of minor streams and a moraine (Plafker et al., 1978) suggest that nearly all Pacific–North America plate motion is absorbed by slip on the Fairweather fault, the continuation of the Queen Charlotte Islands fault onto land. The most accurate rate is that using GPS; Fletcher and Freymueller (2003) inferred 45.6 ± 2.0 mm/yr of right-lateral slip on this fault, and 3.8 ± 1.4 mm/yr of slip on the southeastern end of the Denali fault.

Although most of the slip on the Fairweather fault seems to be absorbed by underthrusting of the Pacific plate beneath southern Alaska, some slip continues on the Totschunda fault to its junction with the Denali fault (Fig. A1) (Lisowski et al., 1987). The trace named the Denali fault in southeast Alaska diverges from the Fairweather fault northeast of where Fletcher and Freymueller (2003) showed that virtually all of the plate motion was absorbed on this latter fault. Widespread seismicity and active faulting suggest that deformation is not confined to slip on the Denali and Totschunda faults (e.g., Freymueller et al., 2008; Page et al., 1995). For example, at the western end of the Denali fault the initial rupture in the large 3 November 2002 earthquake occurred by thrust slip (e.g., Haeussler et al., 2004; Oglesby et al., 2004; Ozacar et al., 2003).

Two detailed studies of late Quaternary slip rates show a westward decrease in rates (Matmon et al., 2006; Mériaux et al., 2009), from 14.4 ± 2.5 mm/yr for the combined slip on the easternmost Denali fault and Totschunda fault (near 143°W), to 12.1 ± 1.7 mm/yr on the Denali fault (near 145°W), to 9.4 ± 1.6 mm/yr (near 148°–149°W), to only 6.7 ± 1.2 mm/yr (just east of 150°W). Biggs et al. (2007) interpreted repeated InSAR (interferometric synthetic aperture radar) measurements from a segment between 147°W and 144°W to suggest a rate of 10.5 ± 5.0 mm/yr. GPS measurements near 149°W give a rate of 9 ± 4 mm/yr (Fletcher, 2002), which Freymueller et al. (2008) refined to 8 ± 1 mm/yr. Freymueller et al. (2008) also reported a relatively low rate of 6 ± 1 mm/yr near

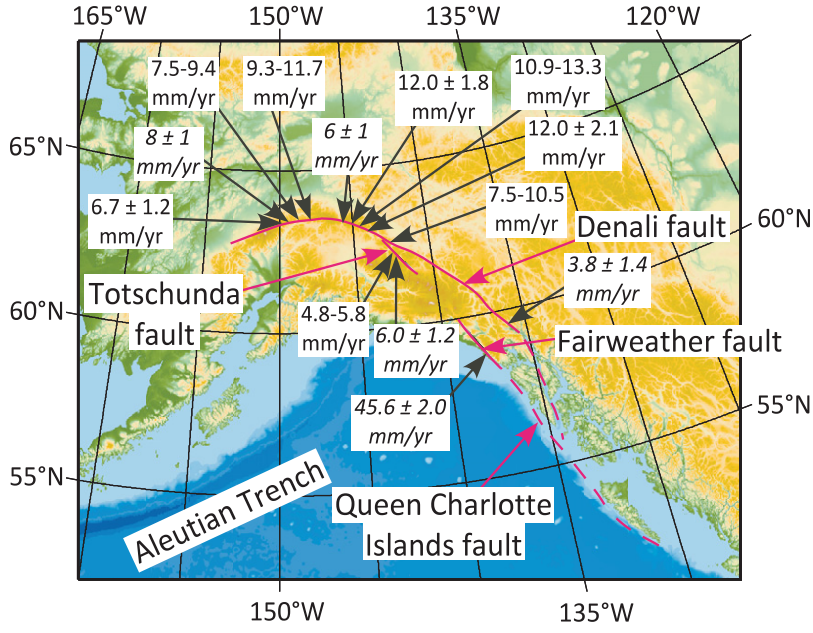

Figure A1. Map of Alaska showing the traces of the Queen Charlotte Islands, Fairweather, Denali, and Totschunda faults. Rates in italics are based on geodetic measurements (Fletcher and Freymueller, 2003; Freymueller et al., 2008), and those in normal fonts are based on dating of Quaternary offsets (Matmon et al., 2006; Mériaux et al., 2009).

146°W, not far from where Matmon et al. (2006) estimated 12.1 ± 1.7 mm/yr. Repeated triangulation along the Totschunda near 142°W suggests a rate of ~10 mm/yr (Lisowski et al., 1987), crudely consistent with what Matmon et al. (2006) reported. Thus, there seems little doubt that a rate of ~10 mm/yr characterizes most of the Denali fault.

California: The San Andreas Fault System

Shortly after plate tectonics was established, Atwater (1970) brought understanding to the tectonic history of western North America by treating the San Andreas (Fig. A2) as the boundary between the Pacific and North America plates. She recognized that not all of the relative motion of the plates manifests itself as slip on that fault, and noted in particular the widespread deformation in the Basin and Range Province to the east. It later became clear that slip on the obliquely oriented San Gregorio–Hosgri fault, west of the San Andreas fault, also accommodates several millimeters/year of slip (e.g., Graham and Dickinson, 1978). Nevertheless, with slip on the San Andreas fault system accounting for ~75% of the relative plate motion and being so close to intact Pacific plate, there seems little doubt that the San Andreas fault developed near the edge of one essentially rigid plate.

The San Andreas fault splays at both ends into a series of nearly parallel strike-slip faults that collectively absorb the same amount of slip as that concentrated on the single trace in central California (e.g., Bennett et al., 1996; Freymueller et al., 1999; Rolandone et al., 2008; Segall, 2002). The nearly parallel faults, in turn, slice the crust of northern and southern California into a number of long narrow blocks tens of kilometers in width. Deformation is localized within a region that is <~100 km wide, and deformation within the mantle lithosphere might be similarly localized.

The slip rate is highest in the central segment of the fault, where slip is confined to one strand, excluding the San Gregorio–Hosgri fault, which is to the west of the San Andreas. Sieh and Jahns (1984) measured average late Quaternary rates of 33.9 ± 2.9 mm/yr for the past 3700 yr and 35.8 +5.4/–4.1 mm/yr for the past 13,250 yr at Wallace Creek. Noriega et al. (2006) corroborated this rate (30–37 mm/yr) from measurements at another site 18 km southeast of Wallace Creek and with GPS measurements across that region. They showed that steady slip at 30–37 mm/yr below a locking depth of 12 km bounds all GPS velocities within the region; this seems to apply to continuously recorded GPS measurements at sites 70 km apart and spanning the fault (Titus et al., 2005). Argus and Gordon (2001) gave a slightly higher rate for this region, 39 ± 2 mm/yr (1σ), but this rate includes slip on the San Gregorio–Hosgri fault. Treating the GPS velocity field in terms of relative movements of blocks, Meade and Hager (2005) inferred rates of 36.0 ± 0.5 and 35.9 ± 0.7 mm/yr in 2 segments. With more recent additional GPS data, Rolandone et al. (2008) reported a rate of 31–35 mm/yr.

Farther north, the San Andreas fault splays into a number of faults that surround San Francisco Bay, as well as a small amount of slip from the San Gregorio–Hosgri fault. Geologic studies suggest a lower rate on the northern strand labeled San Andreas than on the San Andreas fault in central California. Prentice (1989) estimated an upper bound on the Quaternary slip of 25.5 ± 2.5 mm/yr at Point Arena, with a preference for a value closer to 20 mm/yr. Niemi and Hall (1992) reported a lower bound of 24 ± 3 mm/yr from a site 45 km northwest of San Francisco. GPS measurements suggest that slip at the order of 40 mm/yr occurs across this region, with slip on at least three different strands. Assuming purely elastic strain on faults that slip below sensible locking depths, GPS measurements can be fit with a rate comparable to, if possibly slightly slower than, 20 mm/yr on the trace labeled San Andreas (e.g., Argus and Gordon, 2001; d'Alessio et al., 2005; Freymueller et al., 1999; Murray and Segall, 2001; Savage et al., 1999), and rates of ~10 mm/yr on parallel strands to the east. Some geodetic estimates for the Hayward fault (e.g., Murray and Segall, 2001; Prescott et al., 2001; Savage et al., 1999) are larger than Lienkamper and Borchardt's (1996) Holocene rate of 8–9 mm/yr, but a more recent detailed study by Schmidt et al. (2005) gives only ~5 mm/yr. Segall (2002), however, showed that by allowing for viscoelastic deformation below an elastic layer and by including geologic estimates of slip rates, all data fit a rate for the San Andreas strand of ~25 mm/yr and ~8 mm/yr for the Hayward–Rodgers Creek fault, as Lienkamper and Borchardt (1996) inferred.

Similarly, relative movement between the Pacific and North America plates in southern California occurs by strike slip on several faults (Fig. A2) (Bennett et al., 1996), with the segment of the San Andreas adjacent to the Salton Sea slipping the fastest at 23.3 ± 0.3 mm/yr (Meade and Hager, 2005). The remaining plate motion is absorbed by the San Jacinto fault (11.9 ± 1.2 mm/yr), the Elsinore fault (2.7 ± 0.6 mm/yr), and more minor faults. Where these faults coalesce near the northern end of the Gulf of California onto a single strand, the Cerro Prieto fault, the rate reaches 40.0 ± 1.5 mm/yr (Meade and Hager, 2005). Thus, along most of the San Andreas system, present-day and late Quaternary rates exceed 30 mm/yr and approach, if not exceed, 40 mm/yr. Nowhere is deformation spread across a region wider than ~100 km, consistent with a shear zone of comparable width in the mantle.

In central California, part of the relative plate motion occurs by slip on the San Gregorio–Hosgri fault, which crosses bits of the west coast of central

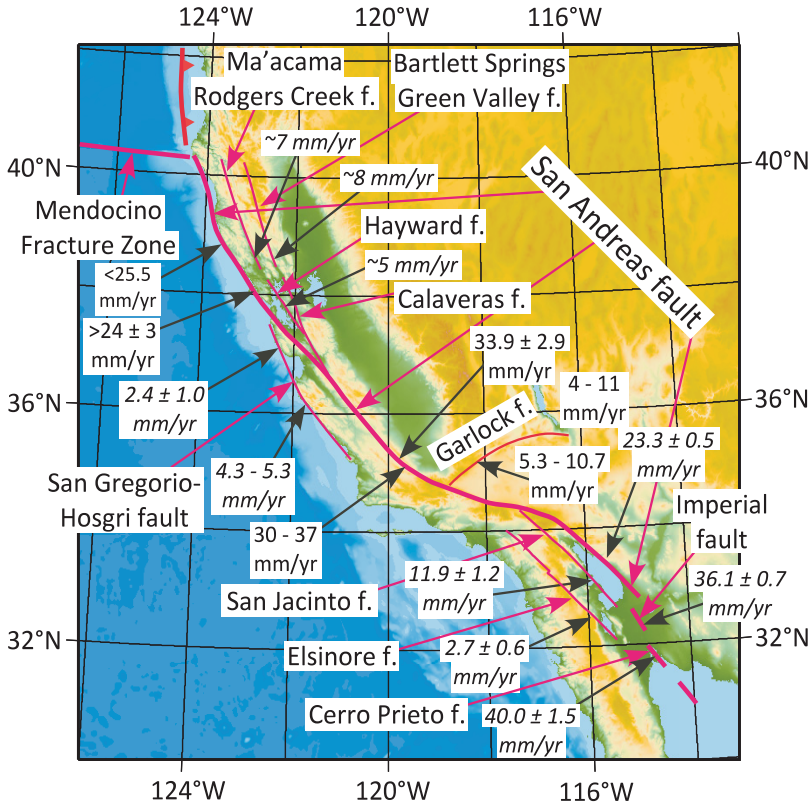

Figure A2. Map of California and adjacent areas showing the traces of the San Andreas fault and adjacent splays in both northern and southern California and the San Gregorio–Hosgri and Garlock faults (f.). Purple lines show right-lateral faults, and the red line shows a left-lateral fault. Teeth show downdip directions of thrust faults. Rates in italics are based on geodetic measurements: those from the Hayward–Rodgers Creek and Green Valley faults are from Segall (2002), that for the Hayward fault is from Schmidt et al. (2005), those from the San Gregorio–Hosgri fault are from d'Alessio et al. (2005) and Rolandone et al. (2008), and those from the southern San Andreas, San Jacinto, Elsinore, Imperial, and Cerro Prieto faults are from Bennett et al. (1996). Rates in normal fonts are based on dating of Quaternary offsets rate: for the northern San Andreas fault from Prentice (1989), for the central San Andreas fault from Sieh and Jahns (1984), and for the Garlock fault from McGill et al. (2009).

California (Fig. A2). In a thorough summary of this fault, Dickinson et al. (2005) argued that 156 ± 4 km of right-lateral slip has occurred since 11 Ma, the age of the youngest unit offset by this amount. Thus, the average rate would be ~14 mm/yr. Essentially all geologic estimates of late Quaternary slip rates, however, are notably lower, as are geodetically constrained rates. For example, Weber and Nolan (1995) reported a late Quaternary rate of 3–9 mm/yr. Dickinson et al. (2005, p. 5) stated: "The estimated late Quaternary slip rate of 6–9 mm/yr (best estimate of ~8 mm/yr) for the San Gregorio segment of the fault on the San Francisco Peninsula," and they noted that this is comparable to the maximum rate given by Hanson and Lettis (1994, p. 145) for the San Simeon segment of the fault. Hanson and Lettis (1994; see also Hanson et al., 2004), however, noted that most of the offset terraces to which they assigned ages yielded notably lower rates. They offered an estimate of 1–3 mm/yr, which overlaps the bounds of 0.9–3.4 mm/yr given by Hall et al. (1994) for the same area. Most studies of GPS velocities also yield low rates of slip on the San Gregorio–Hosgri fault: 3 ± 3 mm/yr (Argus and Gordon, 2001), 2.4–5.1 mm/yr (d'Alessio et al., 2005), 4.3–5.3 mm/yr (Rolandone et al., 2008), and 5.1 ± 3.5 mm/yr (Savage et al., 1999). All of these might be underestimates by a few millimeters/year because of movement of GPS control points on the west coast with respect to the Pacific plate, for presumably strain accumulates offshore (Beavan et al., 2002). In any case, the current rate seems to be <10 mm/yr.

Left-lateral slip occurs on the Garlock fault, which is roughly orthogonal to the San Andreas fault (Fig. A2). Dating of late Quaternary offsets shows that left-lateral slip occurs at ~5.3–10.7 mm/yr in the western segment (McGill et al., 2009) and at 4–9 mm/yr farther east (McGill and Sieh, 1993). GPS measurements show considerably lower rates of only 3 mm/yr or less, but solutions for relative movements of blocks call for substantial extension perpendicular to the fault (Meade and Hager, 2005). Thus, the GPS data seem still to be incomplete. As the prototypical intracontinental transform fault, slip on the Garlock fault slows and dies out to the east as it is absorbed by extension across grabens to its north and by thrust faulting on the south side at its east end (Davis and Burchfiel, 1973). In its western part, where the rate seems highest, the Garlock fault is bounded to the north by the Sierra block, which seems to behave as an essentially rigid object (e.g., Argus and Gordon, 1991).

Guatemala: The Cayman Trough and the El Polochic-Motagua Fault Zone

The Cayman Trough (Fig. A3) behaves as a transform fault separating oceanic lithosphere of the Caribbean and North American plates, and GPS measurements show that slip occurs at ~20 mm/yr (DeMets et al., 2000). GPS measurements in eastern Guatemala also are consistent with slip at 20 mm/yr on its continuation on land, the Motagua fault (Lyon-Caen et al., 2006). Farther westward, however, the fault zone splits into several splays of the Polochic-Motagua fault system. Although we are not aware of studies of Quaternary slip rates for any of these traces, GPS data require slower slip on all strands in western Guatemala and a decrease in the overall rate across the zone (Lyon-Caen et al., 2006).

Clearly, deformation is not localized on a single fault in the western two-thirds of this part of Central America (DeMets et al., 2007; Lyon-Caen et al., 2006; Rodriguez et al., 2009; Rogers and Mann, 2007). Deformation is spread over a zone >~100 km wide, suggesting that deformation at depth also ceases to be confined to the narrow zone that characterizes the Cayman Trough. In a sense, this region provides evidence for the opposite idea: where strength heterogeneity is absent, deformation spreads out, and slip is not concentrated on a single trace.

Northeastern South America: The El Pilar, Boconó, and Oca Faults

The El Pilar fault seems to mark the boundary of the Caribbean and South American plates, if some deformation has occurred south of it. We are not aware of studies of Quaternary slip rates for this fault, but GPS measurements constrain the slip rate at ~20 mm/yr (Pérez et al., 2001; Weber et al., 2001). Virtually all data along the fault can be fit with this rate and with a locking depth of 14 km. Thus, it provides an example of a major fault adjacent to strong lithosphere. To its west, the El Pilar fault splays into the Boconó and Oca faults (Fig. A4), which slip more slowly (e.g., Pérez et al., 2001; Schubert and Sifontes, 1970; Schubert et al., 1992) than the El Pilar fault.

The Boconó fault trends northeast-southwest along the crest of the Mérida (or Venezuelan) Andes (Fig. A4). Schubert and Cifontes (1970) first estimated a rate of 6.6 mm/yr from a 66 m offset of a moraine and an assumed age of 10,700 yr. Later, with a radiocarbon age of ~20 ka, Schubert et al. (1992) reduced this to 3.3 mm/yr, but more recent studies of nearby sites suggest a rate between 7.3 and 10.7 mm/yr, the sum of rates across two overlapping strands, for the past 15 ± 2 ka (Audemard et al., 1999, 2008). Pérez et al. (2001) reported a rate of 9–11 mm/yr from GPS measurements, but their control points come from near the intersection of the El Pilar and Boconó faults. A GPS study by Trenkamp et al. (2002) suggested a rate of 6 ± 2 mm/yr, but they have only a few

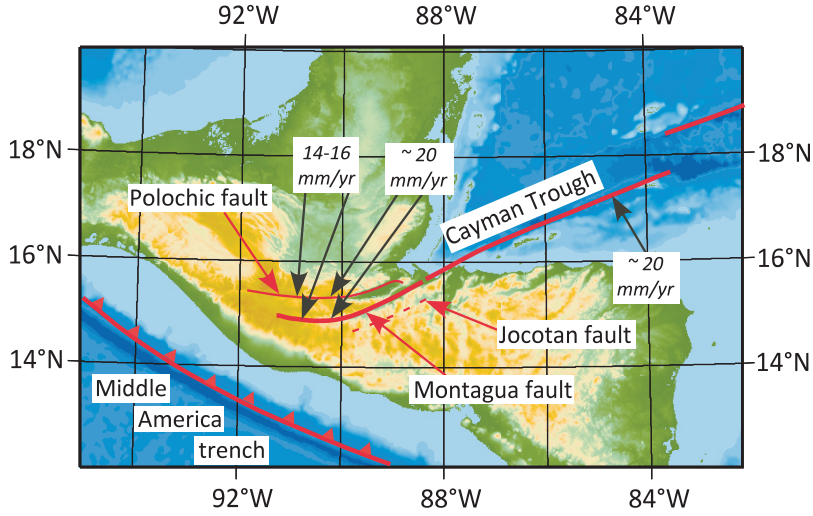

Figure A3. Map of Guatemala and the adjacent Cayman Trough showing the traces of the Polochic, Motaqua, and Jocotan faults and estimates of rates across the entire zone based on global positioning system data from Lyon-Caen et al. (2006).

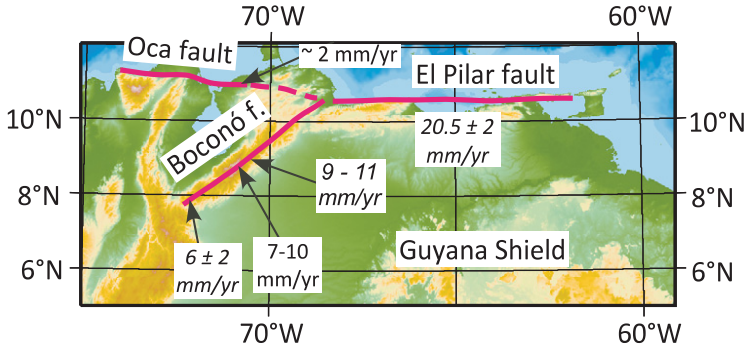

Figure A4. Map of northeastern South America showing the traces of the El Pilar, Boconó, and Oca faults. Rates in italics are based on geodetic measurements (Pérez et al., 2001; Trenkamp et al., 2002), and those in normal fonts are Quaternary slip rates estimated by Audemard et al. (1999, 2008) for the Boconó fault and by Audemard (1996) for the Oca fault.

sites that address this question. In any case, the rate is ~10 mm/yr at most. This fault is bounded on the southeast by the Guyana shield.

The Oca fault continues west of the intersection of the El Pilar and Boconó faults, across the northern edge of Lake Maracaibo, and farther west along the northern edge of the Sierra Nevada de Santa Marta in northern Colombia (Fig. A4). Although sections of this fault can be seen clearly in the topography and as steep gradients in gravity anomalies (e.g., Case and MacDonald, 1973; Kellogg and Bonini, 1982), geologic constraints on rates or amounts of slip are sparse. Tschanz et al (1974) reported at least 65 km of right-lateral slip on the fault, but they offered little supporting evidence. Kellogg (1984) suggested as much as 90–100 km of oblique right-lateral slip, from the correlation of serpentinite in the Sierra and outcrops farther east in Venezuela. Pindell et al. (2005) assumed 120 km of slip. By these standards the fault could hardly be called unimportant in the overall history of the region. Estimates of present-day slip rates, however, suggest that it absorbs only a small fraction of Caribbean–South America relative plate motion. Audemard (1996) inferred from his analysis of trenches across the fault, and across a neighboring fault, a total slip rate of ~2 mm/yr in western Venezuela, an inference supported by Cediel et al. (2003) for the region farther west. For the eastern part in Venezuela, Pérez et. al. (2001) reported no resolvable movement between GPS control points across the Oca fault. We ignore it here, though it may have served as a continuation of the El Pilar fault and the plate boundary between the Caribbean and South America plates in the past.

North Anatolian and East Anatolian Faults, Turkey

GPS measurements give a precise rate of 24 ± 1 mm/yr of right-lateral slip along the North Anatolian fault and a less precisely constrained rate of ~10 mm/yr of left-lateral slip on the East Anatolian fault (McClusky et al., 2000; Reilinger et al., 2006) (Fig. A5). Comparably tight constraints on the late Quaternary average slip rates on either fault do not seem to exist yet. Hubert-Ferrari et al. (2002) placed lower and upper bounds of 12.5 mm/yr and 23 mm/yr on the North Anatolian fault. From another site, Kozaci et al. (2007) estimated average rates of 20.5 ± 5.5 mm/yr and 20.5 ± 8.5 mm/yr for two different durations, and Kozaci et al. (2009) reported a rate of 18.6 +3.5/–3.3 mm/yr from a third site. To the west the fault splays into separate segments, and Pucci et al. (2008) measured an average slip rate for one strand of 15.0 ± 3.2 mm/yr for the past 60 k.y. (Fig. A5). Kozaci et al. (2009) interpreted Quaternary rates lower than those measured with GPS as evidence that the period spanned by the GPS measurements is undergoing a transient phase of high slip. In any case, the rate is clearly high.

The Black Sea, which is underlain by oceanic lithosphere, lies just north of the North Anatolian fault and along most its length the shoreline maintains a constant distance from it. Thus this fault follows the edge of strong lithosphere. We are not aware of evidence of a strong region immediately adjacent to the East Anatolian fault, but the Arabian shield lies to its southeast. In any case, its shorter length of ~400 km and lower rate obviously makes it less important than the North Anatolian fault.

Dead Sea Fault, Israel, Jordan, and Syria

Slip on the Dead Sea fault (Fig. 2) is relatively slow, according to both GPS measurements and studies of late Quaternary faulting. Across the southern part of this fault zone, GPS data from Israel give 3.3–3.7 (± 0.4) mm/yr (Wdowinsky et al., 2004) and 4.9 ± 1.4 mm/yr (Le Beon et al., 2008); those farther north from Lebanon indicate 4–5 mm/yr (Gomez et al., 2007), and measurements throughout this zone yield a northward-increasing rate of 4.5 to 4.8 ± 1 mm/yr (Reilinger et al., 2006). These values accord with a rate of 3.5 mm/yr estimated by Bartov and Sagy (2004) for the past 30 k.y. in the Israeli segment and 4 ± 2 mm/yr in Jordan since 0.5 Ma (Klinger et al., 2000). Across Syria, farther north, Alchalbi et al. (2010) found GPS data to show a lower rate of 1.8–3.3 mm/yr, as well as evidence that north-south shortening across the Palmyride Fold Belt accommodates part of the difference. There seems little doubt that the slip rate is not >~5 mm/yr, but as the Arabia-Africa plate boundary, this clearly is a notable fault.

Main Recent fault and Other Strike-Slip Faults in Iran

Iran (Fig. A6) is host to several major strike-slip faults, many of which are clear in topography seen in aerial photos and space imagery (e.g., Wellman, 1966). With a variety of orientations across the high terrain of Iran and its surroundings, strike-slip faults absorb convergence between Arabia on the south and Eurasia on the north (e.g., Walker and Jackson, 2004). Many of Iran's major earthquakes have occurred on strike-slip faults (Ambraseys and Melville, 1982).

Arguably the most important of these faults is the Main Recent fault, which trends parallel to the Zagros for ~400 km and traverses relatively high terrain northeast of this mountain belt (Fig. A6). Geomorphologic features offset by this fault can be recognized clearly in the field, and deformation measured with InSAR associated with an earthquake in 2006 shows right-lateral slip (Peyret et al., 2006). We are aware of three geological studies that assigned slip rates to this fault. Bachmanov et al. (2004) inferred a rate of ~10 mm/yr from an offset of 110–115 m and an assumed age of 10–12 ka. Talebian and Jackson (2002) recognized much larger offsets of river courses and then divided their amounts by 3–5 m.y. to estimate a rate of 10–17 mm/yr. Authemayou et al. (2009) used concentrations of ^{36}Cl to date a fan across which several channels had been offset and inferred a rate between 2.1 and 5.9 mm/yr. At a second locality, on a separate, roughly parallel trace, they dated a pair of fans offset from their upstream sources and obtained a rate between 1.5 and 6.5 mm/yr. As the two localities seem to be on different strands of the Main Recent fault, they suggested that the rate across the zone could be as large as the sum of these estimates: 3.6–12.4 mm/yr. GPS data, however, concur with the lower bound and give 3 ± 2 mm/yr (Vernant et al., 2004; Walpersdorf et al., 2006). Authemayou et al. (2009) also estimated rates on strands of strike-slip faulting along the Kazerun Line, which crosses the Zagros obliquely. Their measured rates decrease from 2.5–4.1 mm/yr in the north near where the Kazerun Line and Main Recent fault intersect to 1.5–3.5 mm/yr in the central section of the Kazerun Line, to nil in the south near the southern edge of the Zagros. GPS measurements concur with these rates across the Kazerun Line (Tavakoli et al., 2008).

Active strike-slip faults are abundant in Iran, not just in the Zagros (Fig. A6), but most slip at low rates. In northern Iran, Hessami et al. (2003) reported a right-lateral slip rate of 3.1–6.4 mm/yr for Holocene time on the North Tabriz fault, which trends northwest for 200 km in northwestern Iran. Nazari et al. (2009a) deduced a minimum left-lateral slip rate of 0.6–1.6 mm/yr on the Taleghan fault in the Alborz, and Ritz et al. (2006) suggested a left-lateral component of ~2 mm/yr on the Mosha fault. Farther east, in the Kopet Dagh, Trifonov (1978) inferred a right-lateral rate of 1.5–2 mm/yr on the Main Kopet Dagh fault, but he gave little detail in support of that inference. Shabanian et al. (2009a, 2009b) described a network of right-lateral strike-slip faults that continues southeast from the Main Kopet Dagh fault. Along the Bakharden-Quchan fault zone, Shabanian et al. (2009a) reported rates of 2.8 ± 1.0 mm/yr and 4.3 ± 0.6 mm/yr on the two largest strands in this zone. Relying on an estimate for the age of the onset of faulting and their measured total offsets, Shabanian et al. (2009a) inferred rates of 0.5 mm/yr, 1.0 mm/yr, and 1.5 mm/yr for three other faults (see also Shabanian et

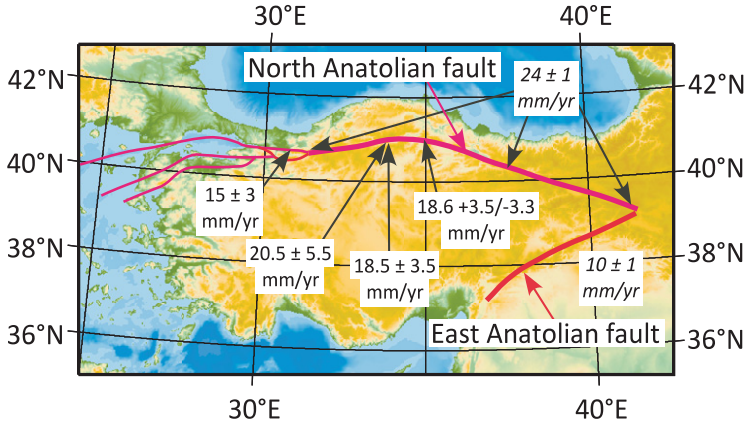

Figure A5. Map of Turkey including the southern Black Sea and showing the traces of the North Anatolian and East Anatolian faults. Purple lines show right-lateral faults, and the red line shows a left-lateral fault. Rates in italics are based on geodetic measurements (Reilinger et al., 2006), and those in normal fonts are from dated Quaternary offsets from Hubert-Ferrari et al. (2002), Kozacı et al. (2007, 2009), and Pucci et al. (2008).

al., 2009b). Accordingly, they offered 9 ± 2 mm/yr as a total rate across the fault zone. In the region southeast of this area, Shabanian et al. (2009b) reported a rate of ~1.2 mm/yr (0.8–1.8 mm/yr on various segments with different orientations) across the Neyshabur and Chakaneh faults and their continuations. Deformation in this area is more complicated than this brief description might imply, but despite many active faults, none seems to slip as rapidly as even 5 mm/yr.

In central Iran, slip on the Doruneh fault (Fig. A6), a major east-northeast–trending left-lateral fault, seems to have occurred at 2.4 ± 0.3 mm/yr during Holocene time (Fattahi et al., 2007). The length of the Doruneh fault is ~200 km, but it can be seen as the eastward continuation of the Great Kavir fault, also ~200 km long, and thus the combined length makes it one of Iran's more important faults. Meyer et al. (2006) and Nazari et al. (2009b) estimated a rate of ~2 mm/yr for the Deshir fault, a north-northwest–trending right-lateral fault ~300 km long in central Iran. East of the Deshir fault, the roughly parallel Anar fault slips at ~0.8 mm/yr (Le Dortz et al., 2009).

In southernmost Iran (Fig. A6), in the transition between underthrusting of ocean floor beneath the Makran of Pakistan and that of the Arabian Peninsula beneath the Zagros, a north-south–trending right-lateral shear zone has developed. Regard et al. (2005) measured right-lateral slip on two relatively short northerly trending fault systems, the Minab-Zendan and the Sabzevaran-Jiroft fault systems, each only tens of kilometers long. They offered bounds of 5.1 ± 1.3 or 6.6 ± 1.5 mm/yr on the slip rate for the former, and 6.2 ± 0.7 mm/yr for the latter (Fig. A6). GPS measurements corroborate rapid slip of ~15 mm/yr across these two fault systems and their surroundings (Peyret et al., 2009).

Strike-slip faults are especially ubiquitous in the region surrounding the Lut block in eastern Iran (Fig. A6). Slip on active strike-slip faults that bound the eastern and western sides of the block presumably accounts for relative movement between the regions east and west of the block (Walker and Jackson, 2004). Sparse GPS measurements suggest that central Iran moves northward at 16 ± 2 mm/yr relative to the region east of the Lut block (Vernant et al., 2004).

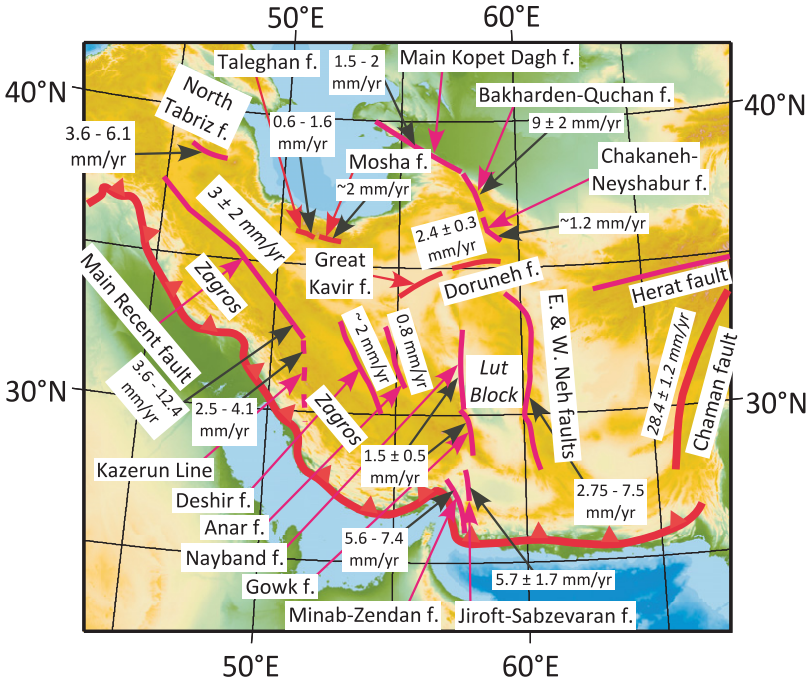

Figure A6. Map of Iran and surrounding regions showing the traces of some of the most important faults (f.) in the region, though none slips as fast as 10 mm/yr. Purple lines show right-lateral faults, and red lines show left-lateral faults. Rates in italics are based on geodetic measurements (Vernant et al., 2004; Walpersdorf et al., 2006), and those in normal fonts are from dated Quaternary offsets. Main Recent fault and Kazerun Line—Authemayou et al. (2009); Doruneh fault—Fattahi et al. (2007); North Tabriz fault—Hessami et al. (2003); East and West Neh faults—Meyer and Le Dortz (2007); Deshir fault—Meyer et al. (2006) and Nazari et al. (2009b); Taleghan fault—Nazari et al. (2009a); Anar fault—Le Dortz et al. (2009); Minab-Zendan and Sabzevaran-Jiroft fault systems—Regard et al. (2005); Mosha fault—Ritz et al. (2006); Bakharden-Quchan fault zone—Shabanian et al. (2009a); Chakaneh-Neyshabur fault zone—Shabanian et al. (2009b); Main Kopet Dagh fault—Trifonov (1978); Gowk-Nayband strike-slip fault—Walker et al. (2009). The rate for the Chaman fault is based on InSAR (interferometric synthetic aperture radar) (W. Szeliga and R. Bilham, 2009, personal commun.).

From a 3 km offset of basalt dated at 2 Ma and a 12 km offset of river courses assumed to have formed at 5 Ma, Walker and Jackson (2002) estimated a rate of 1.5–2.4 mm/yr along the right-lateral Gowk-Nayband strike-slip fault, which follows the west side of the Lut block for 300–400 km. Walker et al. (2009) later refined this to ~1.4 ± 0.5 mm/yr. Walker and Jackson (2002) suggested ~10 mm/yr of slip on the strike-slip fault system on the east side of the Lut block, largely by taking the difference between the GPS rate of Vernant et al. (2004) and their rate for the Gowk-Nayband fault. To assess rates of slip on the east side of the block, Meyer and Le Dortz (2007) assumed ages of 12 ± 2 ka for geomorphic features offset <100 m and reported a rate of only 2.75–7.5 mm/yr for slip along the east side of block, where the north-south–trending East and West Neh faults and other splays can be traced for ~300–400 km. Walker et al. (2009) estimated a minimum slip rate of ~1.2 mm/yr for one of these strands, the East Neh fault, and noted that this rate is a little lower than that given by Meyer and Le Dortz (2007), but not inconsistent with it.

Current data cannot reject slip as rapid as 10 mm/yr along all faults within Iran, but if such a fault exists, it seems unlikely to be as long as 400 km. Thus, although strike-slip faulting plays a dominant role in the active deformation of the Iranian Plateau, no single major fault seems to dominate tectonic activity as can be seen elsewhere.

Chaman Fault, Afghanistan and Pakistan

Although the Chaman fault (Fig. A7) is within active deforming terrain of Pakistan and Afghanistan, it seems to serve as the main boundary between the Indian plate to the east and a southern protrusion of the Eurasian plate to the west. The fault does not strike parallel to relative motion between these plates, and therefore cannot absorb all relative movement, but we suspect that it marks the western edge of the effectively rigid Indian plate. The Sulaiman Ranges, which are south of the Chaman fault and seem to spread out onto the Indian plate, appear to result from folding of thick sediment above intact basement of the Indian plate (e.g., Humayon et al., 1991; Jadoon et al., 1993). In fact, between the fold-and-thrust belt in sedimentary rock of the Sulaiman Ranges and the Chaman fault, ophiolitic mélange crops out at the surface and also has been thrust atop the sedimentary rock to the south. Banks and Warburton (1986) showed that these thrust faults also dip gently north-northwest, and therefore inferred that the Indian plate extends beneath crust near the Chaman fault. Humayon et al. (1991) suggested that the northwestern part of this region might be underlain by oceanic lithosphere that once was north of the Indian subcontinent. Bernard et al. (2000) showed that major earthquakes occur at shallow depths, <~10 km, and hence within the sedimentary layers; fault plane solutions indicate largely thrust faulting with contraction oriented approximately radially to the topography in the Sulaiman region, as if the thickened stack of sedimentary rock flows outward and downslope over the India plate. Thus, we assume that deformation in the Sulaiman Ranges and the region to its northwest occurs in a thin upper crustal layer detached from the underlying lithosphere.

Although the rate of slip on the Chaman fault almost surely is >10 mm/yr and quite likely between 20 and 30 mm/yr, constraints are weak. Beun et al. (1979) argued, from the existence of a north-south fault in volcanic rock dated at ca. 2 Ma and offset ~60–80 km, that the rate is 25–35 mm/yr, but this

requires a large extrapolation of the offset features projected to the fault. Lawrence et al. (1992) noted that four pairs of offset features imply a total offset of 460 ± 10 km. Assuming a date for initiation of slip of 20–25 Ma, they suggested an average slip rate of 19–24 mm/yr, but the brief discussion of the offset features makes this rate tentative. An analysis of InSAR interferograms across a segment of the fault yielded a rate of 28.4 ± 1.2 mm/yr (W. Szeliga and R. Bilham, 2009, personal commun.), close to that of 29.7 mm/yr predicted for relative movement of India toward Eurasia in this region (e.g., Sella et al., 2002). The 22° difference in azimuths between strike of the fault in this region, N34°E, and India-Eurasia relative motions, N12°E, requires some convergence perpendicular to the fault, some of which occurs both north and south of it. In any case, most of the relative movement seems to occur on one trace, and the basement on the east (if not also west) side of the fault seems to behave as part of a strong plate.

At its northern end the Chaman fault splays into at least three segments, including the Gardiz fault (Fig. A7). Differences in velocities of GPS points on opposite sides of it suggest a left-lateral slip rate of 5.4 ± 2 mm/yr (Mohadjer et al., 2010). Differences in velocities between GPS sites spanning most, but not all, of the northern end of the Chaman fault zone place a lower bound on the slip rate of 18 ± 1 mm/yr across that region (Mohadjer et al., 2010).

Darvaz-Karakul Fault, Tajikistan

The Pamir, the high plateau north of the northwest end of the Himalaya, seems to undergo mild deformation as it advances northward toward Eurasia. It slides past the Tajik Depression to its west with slip on the Darvaz-Karakul fault absorbing much of that relative movement (Fig. A7). The Tajik Depression seems to be underlain by thin continental crust (e.g., Burtman and Molnar, 1993; Kulagina et al., 1974), and both seismic refraction (Kulagina et al., 1974) and geological cross sections (Bekker et al., 1974a, 1974b; Zakharov, 1958, 1964) across the depression call for a thick sequence, 10–12 km, of clastic and calcareous sedimentary rock deposited on a thin layer of Jurassic salt. Apparently the lithosphere stretched and thinned in Jurassic time, and subsequent cooling created a basin where thick sediment accumulated on a Jurassic salt horizon (Leith, 1985). Folding and faulting of the overlying strata, as the sedimentary rock slides with little resistance on the weak salt layer, has created ranges and valleys within the Tajik Depression. At the same time, the lithosphere beneath the basin seems to be cold and strong. Whether the Darvaz-Karakul fault penetrates the salt horizon and into the basement is not clear, and thus what role this fault plays in the regional tectonics is still unresolved.

Kuchai and Trifonov (1977) and Trifonov (1978) reported a slip rate of 10–15 mm/yr. They noted offset stream valleys of 5 m and of 20 m; because they found similar offsets of stone walls built during, or possibly since, Sogdian time (sixth to twelfth centuries), they inferred a maximum age of ~1500 yr, which would imply a minimum rate of 13 mm/yr for 20 m offsets. They also mentioned offsets of 60–95 m for late Holocene features, 150–160 m for Holocene features, and 300–350 m for late Pleistocene features, and perhaps 800 m since the beginning of late Pleistocene time, all of which they considered to be consistent with a rate of 10–15 mm/yr. As none of these features have been dated precisely, however, this inferred rate must be considered qualitative at best. Preliminary GPS measurements from continuously recording sites on the west edge of the Pamir and the western part of the Tajik Depression show a component of relative movement parallel to the fault of 11 ± 2 mm/yr (Mohadjer et al., 2010). Thus, this rate is consistent with the estimates of Kuchai and Trifonov (1977), but it is also an upper bound, because it treats all relative movement between the control points as reflecting slip on only one fault. Numerous reports of minor strike-slip faulting within the sedimentary rock of the Tajik Depression (Legler and Przhiyalgovskaya, 1979; Nikonov, 1970; Trifonov, 1978, 1983) allow for some of the 11 ± 2 mm/yr to be absorbed there, but do not place a tight bound on its magnitude.

Because of the likelihood that the Tajik Depression is underlain by strong lithosphere, rapid slip might result from localized strain near the edge of the strong region. Alternatively, if the Darvaz-Karakul fault penetrated only to the salt horizon and separated two deforming regions, it might an exception to the pattern of major strike-slip faults following the edges of strong lithosphere that we report here. Then, because the slip rate is poorly constrained, this fault might not meet our 10 mm/yr criterion for being a major fault. The curved trace of the Darvaz-Karakul fault, its short length of <300 km, and its lack of clarity along much of its trace suggest that it might be a minor feature.

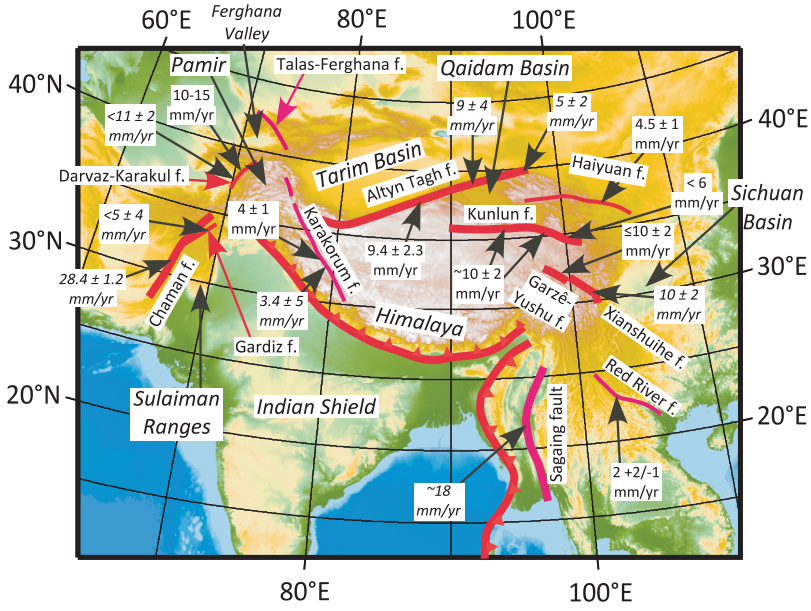

Figure A7. Map of eastern Asia showing the traces of the Chaman, Darvaz-Karakul, Talas-Ferghana, Altyn Tagh, Karakorum, Kunlun, Haiyuan, Xianshuihe, Red River, and Sagaing faults (f.); rates for each are shown. Purple lines show right-lateral faults, and red lines show left-lateral faults. Rates in italics are based on geodetic measurements. Chaman fault—Mohadjer et al. (2010) and W. Szeliga and R. Bilham (2009, personal commun.); Darvaz-Karakul fault—Mohadjer et al. (2010); Karakorum fault—Jade et al. (2004); Altyn Tagh fault—Zhang et al. (2004); Xianshuihe fault—Shen et al. (2005); Sagaing fault—Vigny et al. (2003). Those in normal fonts are based on dating of Quaternary offsets. Darvaz-Karakul fault—Kuchai and Trifonov (1977); Altyn Tagh fault—Cowgill (2007); Kunlun fault —Kirby et al. (2007) and van der Woerd et al. (2002); Haiyuan fault—Li et al. (2009); Garzê-Yushu fault—Wen Xueze et al. (2003); Red River fault—Weldon et al. (1994).

Talas-Ferghana Fault, Kyrgyz Tien Shan

The Talas-Ferghana right-lateral strike-slip fault (Fig. A7) bounds the western end of the Tien Shan and the Ferghana Valley, the underlying lithosphere of which seems to behave as a strong object (e.g., Burov and Molnar, 1998). Relative to Eurasia, the Ferghana Valley seems to rotate about an axis just to its southwest (e.g., Reigber et al., 2001; Thomas et al., 1993). North of the Ferghana Valley crustal shortening within the Chatkal Ranges absorbs northwestward movement of that valley with respect to Eurasia, and south of the valley, the South Tien Shan is thrust over it (e.g., Reigber et al., 2001). Because north-south crustal shortening occurs across the entire Tien Shan east of the Talas-Ferghana fault (e.g., Abdrakhmatov et al., 1996; Thompson et al., 2002), slip on that fault cannot be constant along it. Nevertheless, Burtman (1963, 1964, 1975) showed that Paleozoic belts had been offset along it by at least 180 km, and perhaps 250 km.

Although the Talas-Ferghana is obvious on both aerial photos (e.g., Burtman, 1963, 1964, 1975; Trifonov, 1978) and satellite imagery (e.g., Tapponnier and Molnar, 1979), when the majority of the slip occurred is less obvious. Burtman et al. (1996) measured numerous late Quaternary offset features and obtained bounds on ages of some, nearly all of which suggested an upper bound on the rate of ~10 mm/yr. Because all of these bounds agreed with one another, they inferred that the rate is ~10 mm/yr, but subsequent

GPS measurements require a much lower rate of not >1–3 mm/yr (e.g., Mohadjer et al., 2010; Reigber et al., 2001; Zubovich et al., 2007). Thus, we ignore this fault in further discussion.

Karakorum Fault, Western Tibet

Although some have suggested a rate as high as 30–35 mm/yr for late Quaternary slip on Karakorum fault (Fig. A7) (e.g., Avouac and Tapponnier, 1993; Liu, 1993), recent measurements suggest a much lower rate of 3–5 mm/yr. Brown et al. (2002) surveyed offsets on a debris-flow fan and dated the fan using cosmogenic nuclides to estimate a rate of 4 ± 1 mm/yr. Chevalier et al. (2005) dated cobbles from features that they reported to be moraines, and estimated a rate of 10.7 ± 0.7 mm/yr, but Brown et al. (2005) showed that their dates favor a rate of 4–5 mm/yr. Using GPS control points spanning the fault, Jade et al. (2004) inferred a rate of 3.4 ± 5 mm/yr. With InSAR, Wright et al. (2003) estimated a rate of 1 ± 6 mm/yr (2σ). Because of its low rate, we ignore this fault in further discussion.

Altyn Tagh Fault, Northern Edge of the Tibetan Plateau

Although a wide range of slip rates have been offered for the Altyn Tagh fault (Fig. A7), those based on both late Quaternary offsets and space geodesy now seem to be converging toward a rate of ~10 ± 2 mm/yr. In a thorough study of offset features at two sites, Mériaux et al. (2004) reported an upper bound on the rate of 26.9 ± 6.9 mm/yr, and work by Mériaux et al. (2005) and by Xu Xiwei et al. (2005) suggested relatively high upper bounds on rates, >20 mm/yr, for several other sites along the central part of the fault. In a detailed analysis of one of the sites studied by Mériaux et al. (2004), however, Cowgill (2007) showed that the rate at that site could not be more than roughly half their proposed rate, and he estimated the rate to be only 9.4 ± 2.3 mm/yr. Gold et al. (2009) and Cowgill et al. (2009) inferred a rate between 9.0 ± 1.3 and 15.5 ± 1.7 mm/yr for one site near that studied by Cowgill (2007) and between 9 and 14 mm/yr for another. Zhang et al. (2007) reassessed all of the rates reported by Mériaux et al. (2004, 2005) and Xu et al. (2005), and concluded that all were consistent with 10 mm/yr along the central segment, with the rate diminishing to nil at the eastern end of the fault, as others had inferred (e.g., Chen et al., 2000; Meyer et al., 1996).

GPS measurements consistently show rates of only ~10 mm/yr in the central segment, i.e., 9 ± 5 mm/yr (Bendick et al., 2000), 9 ± 2 mm/yr (Shen et al., 2000); and 9 ± 4 mm/yr (Wallace et al., 2004). A recent assessment using repeated InSAR interferograms gives 11 ± 5 mm/yr (Elliott et al., 2008). From estimates of repeat times of earthquakes and amounts of slip, Washburn et al. (2001a, 2001b) inferred a rate of 10–20 mm/yr, but they seemed to favor a value closer to the lower bound.

We conclude that a rate of 10 ± 2 mm/yr in the central segment of the Altyn Tagh fault is consistent with all data. This fault bounds undeforming, apparently relatively strong, lithosphere beneath Tarim Basin to its north (e.g., Dayem et al., 2009; England and Molnar, 2005; Molnar and Tapponnier, 1981; Reigber et al., 2001; Shen et al., 2001).

Kunlun Fault, Northern Tibet

The Kunlun fault (Fig. A7) trends east-west, emanating from within the northern part of the Tibetan Plateau, passing south of the Qaidam Basin, and dying out near the eastern margin of the plateau. This fault is clear on satellite imagery and in the field (e.g., Kidd and Molnar, 1988; Tapponnier and Molnar, 1977). Early analysis suggested a rate of ~10 mm/yr (e.g., Kidd and Molnar, 1988) and subsequent detailed examination of late Quaternary faulting (e.g., van der Woerd et al., 1998, 2000, 2002) and GPS measurements (e.g., Hilley et al. 2005; Zhang et al., 2004) have confirmed this rate for the segment just south of the Qaidam Basin.

In a particularly thorough study, van der Woerd et al. (2002) presented evidence for slip along the fault at five sites, all of which are south of the Qaidam Basin. For most, they exploited upper bounds on rates, and in all cases these are ~11 ± 2 mm/yr; van der Woerd et al. (2002) also gave enough data to estimate lower bounds, which in most cases are 7–9 mm/yr. Thus a rate of 10 ± 2 mm/yr seems sensible. Li Haibing et al. (2005) estimated the rate at another site near the west end of the trace, ~300 km southwest of the Qaidam Basin. They gave an upper bound on the rate of 10.7 ± 3.5 mm/yr. Using their age for the terrace above the offset riser, however, gives a lower bound of only 5.2 ± 1.7 mm/yr. Thus, the rate might decrease toward the west end of the trace, where it diverges from the Qaidam Basin. Kirby et al. (2007) and Harkins and Kirby (2008) showed that the rate decreases markedly toward the eastern end of the fault, dropping from ~10 mm/yr to nil over a distance of ~200 km, in the segment that is south and east of the eastern end of the Qaidam Basin. GPS measurements near the eastern end also show that localized slip on the Kunlun fault disappears where the fault trace disappears (Kirby et al., 2007).

Slip seems to occur rapidly where the fault is close to, and hence essentially bounds, the Qaidam Basin, a region of relatively low elevation (~3000 m) compared to the surroundings and with only mild deformation (e.g., Chen et al., 1999; Tapponnier and Molnar, 1977). To the west, the slip rate on the Kunlun fault eventually must decrease, for the fault cannot be traced clearly west of ~90°E, but whether a lower rate pertains to where Li Haibing et al. (2005) worked cannot yet be ascertained. To the east, where the fault is within deforming crust to its north and south, the rate decreases, and strain occurs over a wide zone (Kirby et al., 2007). Thus the high slip rate appears to characterize the section where the fault bounds the apparently relatively strong Qaidam Basin, which apparently is underlain by Precambrian basement (Yin et al., 2007, 2008a, 2008b). Where the fault is within deforming crust on both sides, however, strain is spread over a wide region.

Haiyuan Fault, Northeastern Margin of Tibet

The Haiyuan fault (Fig. A7) emanates from within the northeastern margin of Tibet, west of the Qilian Shan, and trends east to east-southeast for ~1000 km before terminating in the Liupanshan, a minor north-south range that marks the northeastern edge of Tibet (e.g., Burchfiel et al., 1991; Zhang Peizhen et al., 1990, 1991). The eastern ~200 km of the fault ruptured in a devastating earthquake in 1920, with coseismic offsets of ~8 m in the central segment (Zhang Weiqi et al., 1987). The entire length of the fault can be seen clearly on satellite imagery (e.g., Deng Qidong et al., 1984; Tapponnier and Molnar 1977) and in the field. Although prominent as a topographic feature, the total slip on the Haiyuan fault appears to be modest, only 11–16 km (Burchfiel et al., 1991).

From offset landforms and radiocarbon dates of them, Zhang et al. (1988) estimated a rate of 8 ± 2 mm/yr for the eastern segment of this fault, but subsequent work showed this rate to be an overestimate. Lasserre et al. (1999, 2002) carried out detailed work in sites farther west, and they obtained estimates of 12 ± 4, 10.5 ± 1.4, and 19 ± 5 mm/yr from three sites. One of us (Molnar) visited the three sites, and suspects that these are upper bounds on rates. For the first, in fact, the reported offset stream valley might not be displaced by slip on the fault; the stream crosses where the fault steps, and a ridge formed by compression in the step has blocked the stream (Lasserre et al., 1999). In any case, the radiocarbon sample was taken from a terrace sufficiently low that its age yields an upper bound on the rate. For the second (Lasserre et al., 1999), I question whether the date assumed for the offset feature actually applies to that feature, and in any case it too would yield an upper bound on the rate. For the third, Lasserre et al. (2002) dated what they assumed to be a moraine, but in the field I found no moraine to be obvious.

Li et al. (2009) studied three sites along the eastern part of the Haiyuan fault, including the one that Zhang et al. (1988) had considered most important, and estimated both upper and lower bounds on slip rates and determined rates of 4.2 ± 0.8, 4.5 ± 0.7, and 5.0 ± 2.5 mm/yr. Moreover, they found this to match the rates obtained from repeated GPS measurements of 4.3 ± 1.5 mm/yr and from repeated satellite interferometry measurements of 4.2–8 mm/yr (Cavalié et al., 2008). Thus, in the eastern segment of the fault, the rate seems to be not >~5 mm/yr.

The sites considered by Li et al. (2009) are hundreds of kilometers east of those studied by Lasserre et al. (1999, 2002). Thus, despite the doubts expressed here, the work of Li et al. (2009) does not rule out the possibility that a higher rate characterizes the fault farther west. Unpublished work by Yuan Dao-yang and by Zhang Peizhen (2004, 2008, personal communs.), however, does yield relatively low rates of 5 mm/yr or less for sites near those studied by Lasserre et al. (1999, 2002) and yet lower rates farther west toward the western end of the fault. We conclude that slip on this fault is definitely slower than 10 mm/yr and unlikely to exceed ~5 mm/yr.

Xianshuihe and Garzê-Yushu Faults, Eastern Tibet and Western Sichuan

To a first approximation, the Xianshuihe and Garzê-Yushu faults (Fig. A7) are continuations of one another, offset from each other by a pull-apart basin (e.g., Allen et al., 1991; Tapponnier and Molnar, 1977; Zhou et al., 1983). Their somewhat different strikes allows them to be major contributors to deformation that is distributed over a broad region, and hence to behave somewhat independently of one another. Each can be traced clearly for ~300 km; the Garzê-Yushu fault dies out to the west within Tibet. The Xianshuihe fault splays into three strands at its eastern end (Allen et al., 1991), where it curves southward and is given a different name, and where the rate seems to be lower than that along the main northwest-southeast–trending strand (e.g., Wang et al., 1998).

Despite intensive study, definitive evidence for a late Quaternary slip rate has not yet been published. From a compilation of offsets and published radiocarbon dates of some features, Allen et al. (1991) suggested a rate of 15 ± 5 mm/yr. Wen Xueze, R.J. Weldon, and others subsequently carried out detailed work, with much radiocarbon dating: Weldon (1997–1999, personal communs.) stated that preliminary results suggested a rate of <9 mm/yr, and possibly as low as 4 mm/yr, but he has allowed that inconsistencies in such dates in some trenches do not permit a tight constraint on

the rate (R.J. Weldon, 2007, personal commun.). In a study of the Garzê-Yushu fault, Wen Xueze et al. (2005) placed an upper bound on the rate of that fault of 10 ± 2 mm/yr. From dates that they gave for terraces above offset terrace risers, our assessment is that the lower bound would be ~8 mm/yr. Initial GPS measurements suggested a rate of ~10 mm/yr for the Xianshuihe fault (Chen et al., 2000), and results from a denser network yield a rate of 10 ± 2, 10 ± 2, and 11 ± 2 mm/yr across the western, central, and eastern sections of that fault (Shen et al., 2005). GPS data from the Garzê-Yushu fault, however, are too sparse to constrain the rate. Recent analysis of InSAR data from 1998 to 2008 yields a rate of 9–12 mm/yr for the Xianshuihe fault (Wang et al., 2009).

The relatively high slip rate for the Xianshuihe fault, and its westward continuation, the Garzê-Yushu fault, make it the most glaring exception to the pattern that we propose. Both flanks of these faults appear to be undergoing active deformation, mostly left-lateral strike slip parallel to this main system (e.g., Shen et al., 2005; Tapponnier and Molnar, 1977; Wang et al., 1998). Neither flank seems to be bounded by an effectively rigid block, except at the southeastern end of the Xianshuihe fault where it approaches the Sichuan Basin (Fig. A7).

Red River Fault, Southwest China and Vietnam

Tight constraints on the slip rate of the Red River fault (Fig. A7) do not yet exist, but all call for a maximum of 10 mm/yr and most suggest as few as 1–3 mm/yr. Estimating a rate is made difficult by there being more than one strand of active faulting along some segments of the fault (e.g., Allen et al., 1984; Replumaz et al., 2001; Schoenbohm et al., 2006). Allen et al. (1984) reported offsets of ~5.5 km in one locality, and Schoenbohm et al. (2006) found others with this offset. Allen et al. (1984) suggested an age of 2–3 Ma, and deduced a rate of 2–3 mm/yr, but allowed for a rate as fast as 5 mm/yr. Replumaz et al. (2001) suggested that stream offsets of 25 km characterize slip on the fault, and they suggested an age of 5 Ma for the incision of the streams to give an average rate of 5 mm/yr. Schoenbohm et al. (2006) preferred this interpretation to that of Allen et al. (1984). By contrast, from a detailed trenching at one site, Weldon et al. (1994) inferred a rate of 1.6 ± 0.5 mm/yr.

GPS measurements favor the lower rates. Using a large-scale array but without sites near the fault, Simons et al. (2007) inferred a rate of 1.6 ± 0.5 mm/yr. From campaign measurements spanning only 2 yr, Duong and Feigl (1998) suggested a rate of 1–5 mm/yr but with low confidence in the southeast part of the fault in Vietnam. With longer durations and many sites, Shen et al. (2005) reported 2 ± 2 mm/yr in the northwest segment and 1 ± 2 mm/yr in the central segment. On the basis of the low rates from both GPS and some geologic studies, we do not consider the Red River fault further.

Sagaing Fault, Myanmar

The Sagaing (Fig. A7) is obviously a major fault. Historical seismicity has been high (Chhibber, 1934). It connects to a major transform fault within the Andaman Sea (e.g., Curray et al., 1978). Curray et al. (1978) gave a spreading rate of ~40 mm/yr for opening of the Andaman Sea and hence also to the slip rate on the transform fault that connects it to the Sagaing fault. In reassessing the magnetic anomalies, with guidance from S. Cande, Curray (2005, p. 212) found the best, but "not truly compelling," match to be 118 km of opening since 4 Ma. Accordingly, Curray (2005) deferred to Raju et al. (2004), who suggested rates of 16 mm/yr between ca. 4 and ca. 2 Ma, and 38 mm/yr since that time, or an average of ~18–19 mm/yr. We do not find these identifications of magnetic anomalies to be very convincing, and hence we do not find these data to constrain the slip rate well.

From geologic study on land, Bertrand et al. (1998) dated a basalt flow (0.25–0.31 Ma), the northern and southern edges of which were offset by the fault 6.5 km and 2.7 km, respectively. They offered lower and upper bounds of 10 ± 1 and 23 ± 3 mm/yr, bounds that, although not tight, seem to eliminate rates of 30 mm/yr or more. GPS data also call for a rate lower than 30 mm/yr; Vigny et al. (2003) fitted velocities on two profiles across the fault with a rate of 18 mm/yr, but they noted that the fault trace is displaced to the east of the middle of arc-tangent fit to the velocities, which might suggest that the rate is yet lower. Although the rate might be somewhat <20 mm/yr, the GPS data clearly rule out a rate as low as 10 mm/yr.

Sumatran Fault, Sumatra

The Australian plate moves nearly due north relative to the Sunda block in the region of Indonesia, but subduction of the Australian plate includes a large northeastward component of slip. To compensate for that obliquity, the wedge of lithosphere above the downgoing Australian plate and southwest of the volcanoes slides northwest relative to Sundaland to the northeast along a major strike-slip fault, the Sumatran fault (Fig. A8), which strikes parallel to the belt of volcanoes (e.g., Fitch, 1972). McCaffrey (1991, 1992) showed further that the variation in slip vectors of earthquakes along the Sunda arc adjacent to Sumatra required that the forearc wedge deform and that the slip rate on the Sumatran fault increase toward the northwest. Both GPS measurements (e.g., Bock et al., 2003; Genrich et al., 2000; Prawirodirdjo et al., 1997, 2000) and estimates of slip rates on segments of the fault (e.g., Bellier and Sébrier, 1995; Bellier et al., 1999; Sieh and Natawidjaja, 2000) corroborate McCaffrey's (1991, 1992) inferences that strain occurs within the forearc and that the slip rate of the Sumatran fault increases northwestward. Bellier and Sébrier (1995) reported a relatively precise rate of 23 ± 2 mm/yr from offsets of streams as large as 1660 ± 30 m cut into the Toba Tuff dated at 73 ± 4 ka. From less precisely dated stream offsets, they inferred a less precise rate of 17 ± 6 mm/yr for central Sumatra and 11 ± 5 mm/yr for southern Sumatra (Fig. A8). In southernmost Sumatra, Bellier et al. (1999) dated a tuff at 0.55 ± 0.15 Ma; the tuff was incised by streams

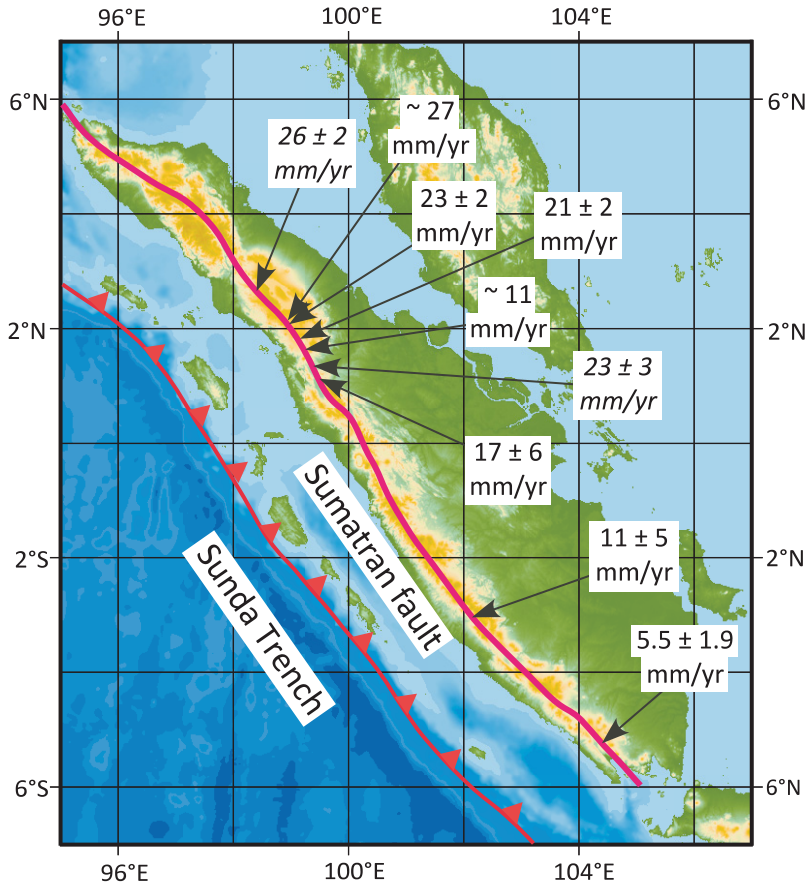

Figure A8. Map of Sumatra showing the trace of the Sunda Trench and the Sumatran fault. Rates in italics are based on geodetic measurements (Genrich et al., 2000; Prawirodirdjo et al., 2000), and those in normal fonts are from dated Quaternary offsets from Bellier and Sébrier (1995), Bellier et al. (1999), and Sieh and Natawidjaja (2000).

that have subsequently been offset as much as 2550 ± 100 m, and thus they determined a rate of only 5.5 ± 1.9 mm/yr. Citing their own work (presented only in abstracts), Sieh and Natawidjaja (2000) reported rates of ~27 mm/yr in northern Sumatra and ~11 mm/yr in the central part. Using GPS measurements, Genrich et al. (2000) found that the rate in northern Sumatra decreased from 26 ± 2 mm/yr at 2.7°N to 23 ± 3 mm/yr at 0.8°S. Using much of the same data but with earlier geodetic surveys that allow a 100 yr time span, Prawirodirdjo et al. (2000) reported similar rates.

Longitudinal Valley Fault, Taiwan

The Longitudinal Valley fault (Fig. A9) follows a linear trough separating high mountains to the west from low hills to the east, but it is by no means a simple strike-slip fault (e.g., Shyu et al., 2005). Geologic studies show that in places thrust faults dip both east and west from the Valley (e.g., Shyu et al., 2005, 2006a, 2006b). Moreover, geodetic data show that along much of the valley the component of convergent motion across the valley is not only faster than the strike-slip component parallel to it (e.g., Angelier et al., 1997; Bos et al., 2003; Lee et al., 2003; Yu et al., 1990, 1997, 1999), but also that the rate of strike-slip varies along the fault (e.g., Bos et al., 2003; Yu et al., 1990, 1997, 1999). Several authors have claimed that the strike-slip component is minor; for example, Barrier and Angelier (1986, p. 39) stated, "The Longitudinal Valley fault is a thrust, with a minor left-lateral strike-slip component (20% of the total movement)"; others (e.g., Yu and Kuo, 2001; Yu et al., 1990, 1997, 1999) have reiterated that assertion. At the same time, geodetic data, including those presented by some of these same authors, call for components of left-lateral slip of 10–20 mm/yr (e.g., Angelier et al., 1997; Lee et al., 2003; Yu et al., 1990, 1997, 1999). In addition, an analysis of geodetic data before and after the largest earthquake to occur in the Longitudinal Valley in the past 75 yr, that in 1951, shows variations in the proportion of strike-slip and thrust components of slip along the fault (Lee et al., 2008). In only rare segments of the Longitudinal Valley does there appear to be strike slip on a vertical plane; in much of the region deformation occurs by oblique slip on a plane that dips eastward (e.g., Angelier et al., 1997; Hsu et al., 2003). At the southern end of the Longitudinal Valley, however, slip seems to be partitioned into thrust and strike slip, but with the strike-slip strand trending north-south, not parallel to the valley (e.g., Lee et al., 1998; Shyu et al., 2008).

The variation in style and rates of deformation along the Longitudinal Valley fault reflects, at least in part, the rapid evolution of underthrusting of the Asia southeastern margin beneath the arc that extends north from Luzon to the Ryukyu Islands (e.g., Shyu et al., 2005, 2006a, 2006b, 2008). Such underthrusting, and related deformation across the entire island, began in northern Taiwan and has been propagating southward.

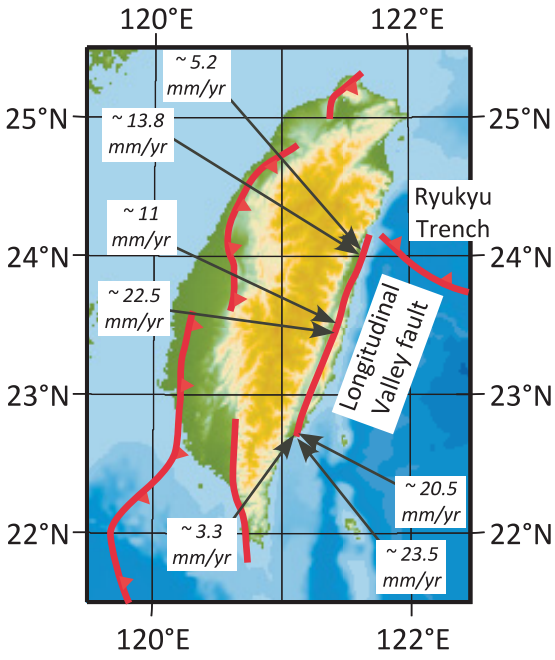

Figure A9. Map of Taiwan showing the trace of the Longitudinal Valley fault and some of the thrust faults on the west side of the island (e.g., Shyu et al., 2005). Rates in italics are based on geodetic measurements (Bos et al., 2003; Hu et al., 2001; Yu et al., 1990).

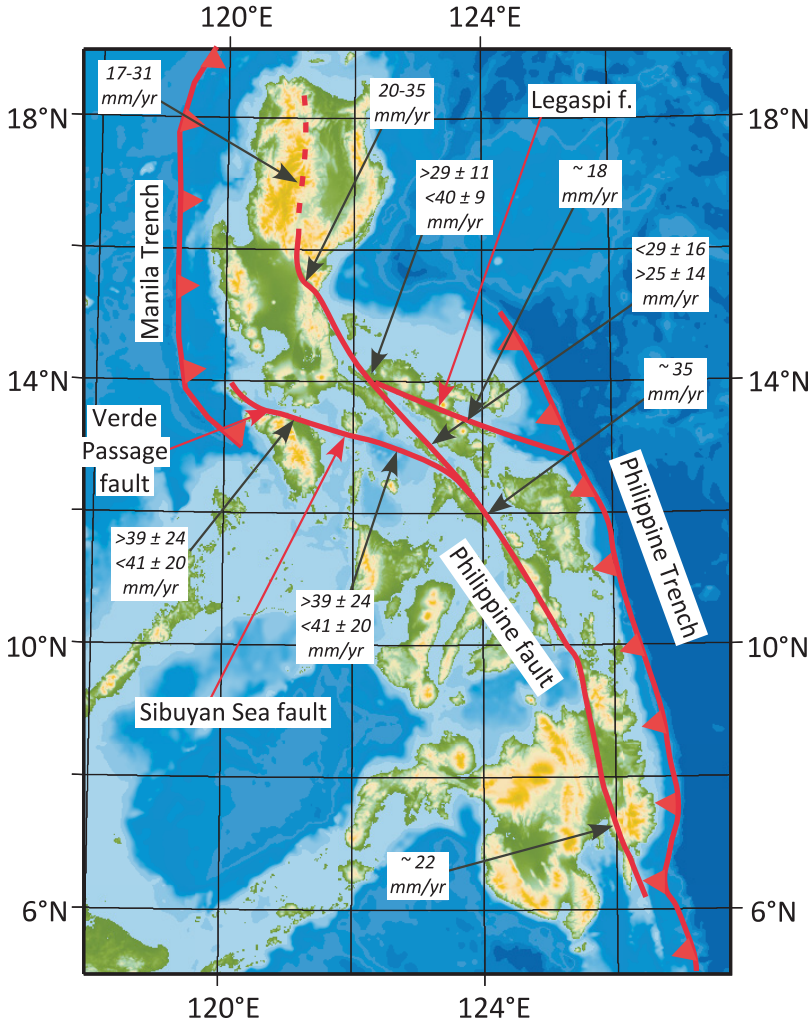

Figure A10. Map of the Philippines showing the trace of the Philippine fault as given by Allen (1962), the Sibuyan Sea fault according to Beavan et al. (2001), and the Verde Passage and Legaspi faults from Rangin et al. (1999). All rates are based on geodetic measurements (Beavan et al., 2001; Galgana et al., 2007; Rangin et al., 1999; Yu et al., 1999).

As a result the style of deformation at any locality in Taiwan has evolved with time during the past few million years. Because intact southeast Asian lithosphere underthrusts the island of Taiwan, none of the fault strands that reach the surface in the Longitudinal Valley continues to depths >~20 km (e.g., Hsu et al., 2003); hence none seems to penetrate the mantle, except as a splay from the main underthrust zone. Thus, although strike slip may be rapid, its variation along strike and the absence of a clear vertical fault along most of the Longitudinal Valley make it so different from the other cases discussed here that we do not consider it to be particularly enlightening about intracontinental strike-slip faulting. Nevertheless, it is obviously bounded by strong Philippine Sea lithosphere to the east.

Philippine Fault, Philippines

The existence of a major strike-slip fault crossing the Philippines (Fig. A10) and trending parallel to deep-sea trenches on both sides of the belt of islands has been known for many years (e.g., Allen, 1962), but detailed geologic constraints on slip rates do not seem to have been published. GPS measurements show rapid slip of 20–40 mm/yr along the trace, with the rate varying along the fault (e.g., Beavan et al., 2001; Galgana et al., 2007; Rangin et al., 1999; Yu et al., 1999). Rangin et al. (1999) reported a decrease in rate from 22 mm/yr at 7°N to 35 mm/yr near 12°N. Beavan et al. (2001) found that rates differed markedly depending on whether strain was treated as elastic or viscoelastic; with the latter their data suggested a rate of 40 mm/yr at the northern end of the fault, but with the former, the rate could be as little as 15–22 mm/yr. Galgana et al. (2007) subdivided the northern part of the region in Figure A10 into blocks, and using GPS velocities they solved for relative movement of them. Their block boundaries included the Verde Passage and Sibuyan Sea faults (Fig. A10), and they allowed for differences in rates along the Philippine fault and for slip on these faults. By contrast, although Rangin et al. (1999) inferred 40 mm/yr of left-lateral slip on Verde Passage fault, consistent with what Galgana et al. (2007) deduced, they did not include the Sibuyan fault. Moreover, Rangin et al. (1999) reported 13 mm/yr of each left-lateral slip on and extension across the Legaspi fault, but Galgana et al. (2007) did not include a block boundary at it. The large uncertainties, typically 10–20 mm/yr, do not allow blocks or other faults to be delineated unambiguously or variations in slip rates to be constrained precisely. Obviously, the large uncertainties allow a variety of interpretations. Nonetheless, the Philippine fault clearly is a major fault.

Palu-Koro and Gorontalo Faults, Sulawesi, Indonesia

Two relatively short, fast-slipping faults cross northwestern and northeastern Sulawesi obliquely. The left-lateral Palu-Koro fault (~300 km long)

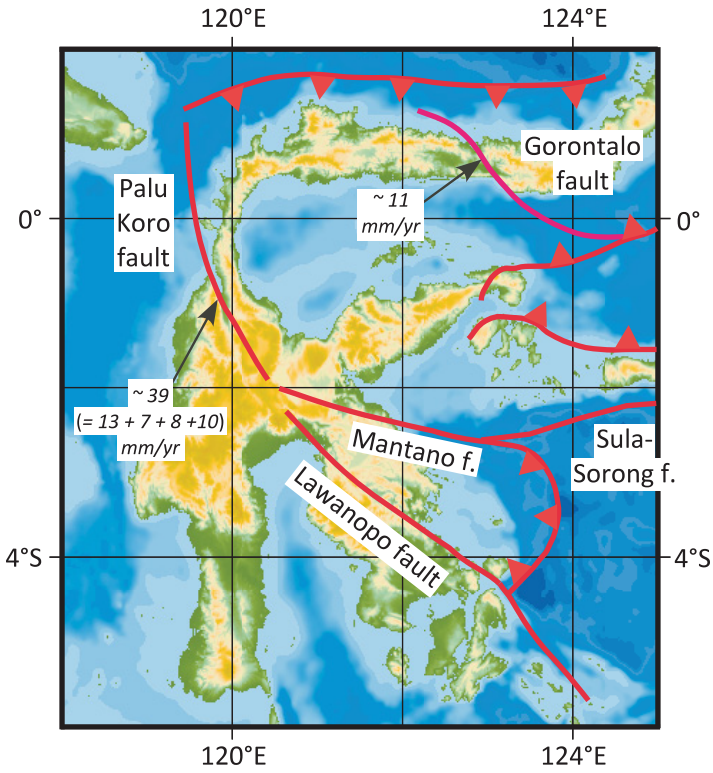

Figure A11. Map of Sulawesi showing the traces of the Palu Koro, Gorontalo, and other faults (f.). Purple line shows right-lateral fault, and red lines show left-lateral faults. Names and locations of faults and rates for the Palu Koro and Gorontalo faults are from Socquet et al. (2006). The sum of 13, 7, 8, and 10 mm/yr does not equal 39 mm/yr, presumably because of round-off errors. Moreover, the speed of one flank with respect to the other is 42 mm/yr, because of a large normal component on at least one trace and a component of extension across the Palu Koro fault zone.

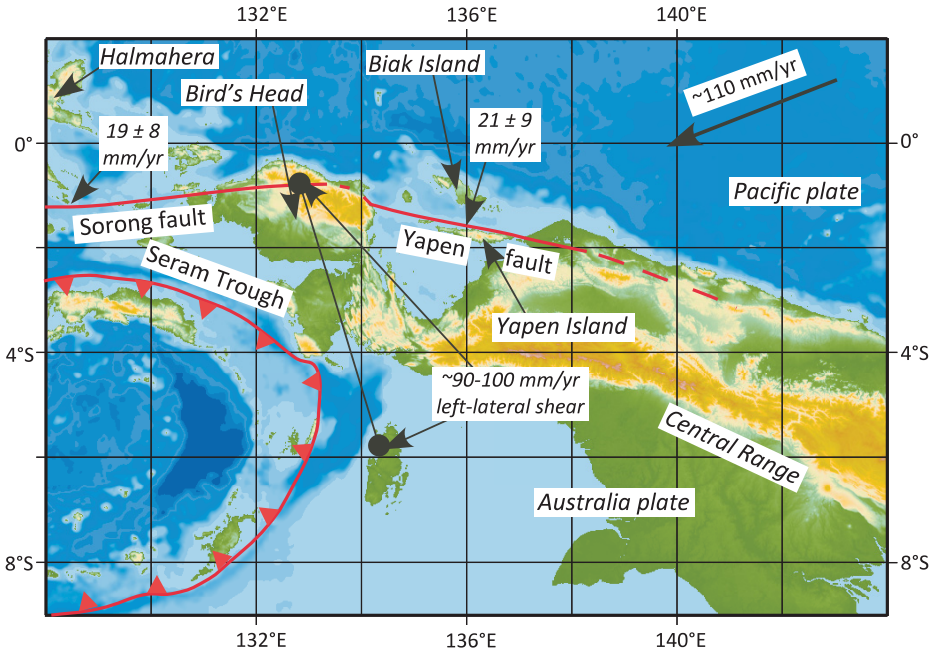

Figure A12. Map of western New Guinea showing the traces of the Sorong and Yapen faults, slip rates of which are constrained by global positioning system measurements (e.g., Bock et al., 2003), and the region where shear occurs across a broad region with no obvious faults (Stevens et al., 2002).

transforms into a subduction zone to the north, where seafloor plunges southward beneath the western part of the northern arm of Sulawesi (e.g., Beaudouin et al., 2003; Silver et al., 1983; Walpersdorf et al., 1998a) (Fig. A11). Much of its trace is under water, and presumably cuts through thin crust, surely oceanic crust near its northern extremity. To the south, it splays into at least two faults, one of which connects with the Sorong fault, which in turn links with a shear zone across northwestern New Guinea (Fig. A12) (e.g., Rangin et al., 1999; Socquet et al., 2006). Slip on the Palu-Koro fault accommodates rotation of the Sula block or microplate, which is to its east, with respect to the region to the west and north, Sundaland. The axis of rotation is quite close to the region, just east of the northern arm of Sulawesi (e.g., Surmont et al., 1994; Silver et al., 1983; Walpersdorf et al., 1998a, 1998b). The right-lateral Gorontalo fault, only ~200 km in length, seems to mark the eastern end of the same small Sula block (Socquet et al., 2006).

Both geologic studies of Quaternary faulting (e.g., Bellier et al., 2001, 2006) and GPS measurements (e.g., Socquet et al., 2006; Stevens et al., 1999; Walpersdorf et al., 1998b) call for slip rates of ~40 mm/yr across the Palu-Koro fault zone. Detailed field investigations, however, suggest that slip on the main trace is not pure strike slip, but includes a substantial normal component (e.g., Bellier et al., 2006), and detailed GPS data indicate a rate of extension of ~11–14 mm/yr across the fault zone (Socquet et al., 2006). Moreover, the fault zone seems to include at least 4 major traces separated by ~10–20 km, slipping at rates of 7–13 mm/yr (Socquet et al., 2006). GPS data also show right-lateral slip at ~11 mm/yr on the Gorontalo fault (Socquet et al., 2006).

Although these faults slip rapidly, their relevance to our study is marginalized by several aspects. First, the nature of rapid relative movement in this region and repeated collisions of microcontinents with one another require rapid evolution of relative movement and loci of boundaries between blocks (e.g., Genrich et al., 1996). Thus, these faults could be transient features in an evolving deformation field and not long-lived faults. Second, to some extent the faults are plate boundaries between oceanic plates, even if the oceanic part of the Sula block might be small. Third, the obliquity of slip and the width of the Palu-Koro fault zone of ~50 km compared to its length of only ~300 km make it hardly typical of a major strike-slip fault.

Sorong and Yapen Faults, Irian Jaya, Indonesia

Shear must occur rapidly in northwestern New Guinea as the Pacific plate moves west-southwest relative to Australia at ~110 mm/yr. GPS control points in the northwestern part of New Guinea move rapidly, at 90–100 mm/yr, westward with respect to Australia (e.g., Puntodewo et al., 1994; Rangin et al., 1999; Stevens et al., 2002). Although seismicity is high, and large earthquakes that show strike slip occur in this region (e.g., Abers and McCaffrey, 1988; Okal, 1999; Stevens et al., 2002), it appears that major faults, if they exist at all, have not been studied in detail. Just west of New Guinea, slip on a major strike-slip fault, the Sorong fault (Fig. A12), displaces Halmahera north of the fault with respect to much of the Bird's Head south of it at ~20 mm/yr: 19 ± 8 mm/yr (Bock et al., 2003) or 20 ± 11 mm/yr (Stevens et al., 2002). This fault seems to enter the Bird's Head of northwestern New Guinea. Farther east, seismicity and fault plane solutions show strike-slip faulting on the Yapen fault, just north of Yapen Island and south of Biak Island (Fig. A12); GPS measurements suggest slip at 21 ± 9 mm/yr. The sparse number of control points does not allow the rate to be tightly constrained, or even to be assigned unambiguously to a single fault trace.

The ~110 mm/yr of relative movement between the Pacific and Australia plates seems to be spread over a zone ~300 km wide, and cannot be fit by elastic strain associated with slip at depth on a single fault. For example, Stevens et al. (2002) showed that the GPS velocities cannot be fit if slip occurred on a fault locked to a depth of 50 km, which would necessarily be >100 km south of the Sorong and Yapen faults. They show that the ~100 mm/yr of relative movement can, however, be matched if shear is distributed so that large-scale rotation about a vertical axis occurs. Farther east, much of this deformation seems to occur within the Central Range, and how the Yapen fault continues eastward does not seem to be known.

Alpine Fault, New Zealand

The South Island of New Zealand straddles the boundary of the Pacific and Australian plates, and most of the relative plate motion is absorbed by slip on the Alpine fault (Fig. A13). The angular velocity describing relative motion of the Pacific and Australian plates calls for 39–40 mm/yr parallel to the Alpine fault and 9–10 mm/yr perpendicular to it (Beavan et al., 2002). Both active faulting (e.g., Norris and Cooper, 2001; Sutherland et al., 2006) and geodetic studies (e.g., Beavan et al., 1999; Walcott, 1984; Wallace et al., 2007) imply that roughly two-thirds of the strike-slip component occurs by slip on the Alpine fault, and the remainder is spread across the South Island and perhaps slightly offshore (Beavan et al., 2002). Norris and Cooper (2001), in a comprehensive summary of work by Berryman et al. (1998), Cooper and Norris (1994, 1995), Norris and Cooper (1995), and Sutherland and Norris (1995), offered a rate of 27 ± 5 mm/yr for the Alpine fault. Sutherland et al. (2006) inferred from numerous offsets of different ages that slip along the southwestern end of the fault occurs at 23 ± 2 mm/yr. Barnes (2009) presented evidence of submerged moraines and outwash fans that have been offset by slip on the Alpine fault at its southwest, offshore end. From dates of 17 +2/–1 ka for the outwash fans and assuming the same ages for the offset moraines, he inferred rates of 27.2 (–3.0/+1.8) mm/yr increasing southwest to 31.4 (–3.5/+2.1) mm/yr (Fig. A13).

In the northeastern part of the South Island, the Alpine fault splays into four crudely parallel

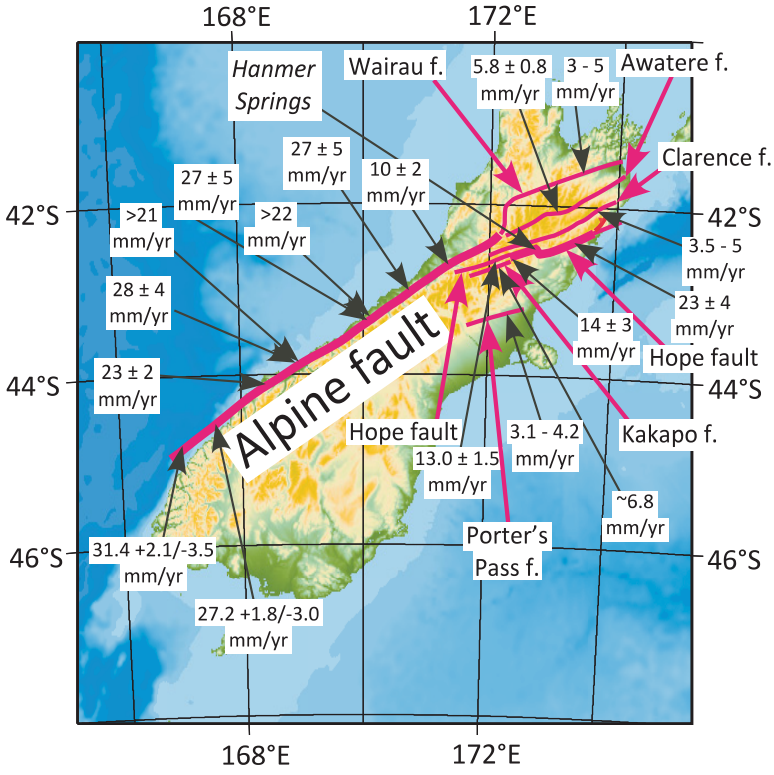

Figure A13. Map of the South Island of New Zealand, showing the traces of the Alpine fault and the Marlboro faults in the northern part of the island and slip rates. Rates for the Alpine fault are from Barnes (2009), Norris and Cooper (2001), and Sutherland et al. (2006). The other faults (f.) include the Wairau (Zachariasen et al., 2006), the Awatere (Mason et al., 2006), the Clarence (Nicol and Van Dissen, 2002), the Hope (Cowan, 1990; Langridge and Berryman, 2005; Langridge et al., 2003), the Kakapo (Yang, 1991), and the Porters Pass (Howard et al., 2005). We omit rates constrained by global positioning system measurements here because of space, but most agree with geologically measured rates.

strike-slip faults, and a fifth to their southeast. The vast majority of the ~480 km of right-lateral slip seems to have occurred by slip on the Wairau fault, the northwesternmost strand, suggesting that slip on the others began much more recently than it did on the Alpine-Wairau strand. Present-day slip rates on most of these faults are not fast; for example, in solving for rates using GPS constraints on relative movements of blocks, Wallace et al. (2007) reported 3.5 mm/yr on the Wairau fault, 5.7 mm/yr on the Awatere fault, 5.3 mm/yr on the Clarence fault, ~18 mm/yr on the Hope fault, and 6.5–7.5 mm/yr on the Porters Pass fault (Fig. A13). By comparison, using fewer data and a different approach, Bourne et al. (1998) reported rates of 9, 6, 5, and 19 mm/yr for the Wairau, Awatere, Clarence, and Hope faults, respectively. Most of these rates accord with geological estimates (e.g., Knuepfer, 1992). Zachariasen et al. (2006) reported 3–5 mm/yr for the Wairau fault. Mason et al. (2006) gave 5.6 ± 0.8 mm/yr for the Awatere fault, a slight modification to rates of 6 ± 1.5 mm/yr (Benson et al., 2001) and 7 ± 1 mm/yr (Little et al., 1998). Nicol and Van Dissen (2002) gave a rate of 3.5–5 mm/yr for the Clarence fault.

For the Hope fault, most rates have been determined west of Hanmer Springs, and they are notably less than the ~18 mm/yr given above: 14 ± 3 mm/yr (Cowan, 1990), 10.5 ± 0.5 mm/yr (Cowan and McGlone, 1991), or 8.1–11.0 mm/yr to 13.0 ± 1.5 mm/yr (Langridge and Berryman, 2005). Where these lower rates have been measured, however, the Hope fault is nearly parallel to another fault, the Kakapo fault, with a slip rate of ~6.8 mm/yr (and possibly 8.1–12.1 mm/yr) (Yang, 1991). Thus, the sum of slip rates on this segment of the Hope fault and on the Kakapo fault is consistent with a combined rate of ~20 mm/yr. Moreover, Langridge et al. (2003) determined a maximum bound of 23 ± 4 mm/yr on the rate for the segment east of Hanmer Springs, consistent with earlier estimates for late Quaternary time of 20–25 mm/yr (Van Dissen and Yeats, 1991) and 18 or 19 mm/yr based on GPS measurements (Bourne et al., 1998; Wallace et al., 2007). Thus, the high rate east of Hanmer Springs is consistent with these geologic estimates to the west. Farther northeast, much of the slip on the Hope fault seems to end in thrust faults near the coast (Van Dissen and Yeats, 1991), and although evidence of the Hope fault can be traced offshore (e.g., Barnes and Audru, 1999), that segment does not seem to a major fault.

Geologic estimates suggest a slip rate of only 3.1–4.2 mm/yr for the Porters Pass fault (Howard et al., 2005).

REFERENCES CITED

Abdrakhmatov, K.Y., Aldazhanov, S.A., Hager, B.H., Hamburger, M.W., Herring, T.A., Kalabaev, K.B., Makarov, V.I., Molnar, P., Panasyuk, S.V., Prilepin, M.T., Reilinger, R.E., Sadybakasov, I.S., Souter, B.J., Trapeznikov, Y.A., Tsurkov, V.Y., and Zubovich, A.V., 1996, Relatively recent construction of the Tien Shan inferred from GPS measurements of present-day crustal deformation rates: Nature, v. 384, p. 450–453, doi: 10.1038/384450a0.

Abers, G., and McCaffrey, R., 1988, Active deformation in the New Guinea fold-and-thrust belt: Seismological evidence for strike-slip faulting and basement-involved thrusting: Journal of Geophysical Research, v. 93, p. 13,332–13,354, doi: 10.1029/JB093iB11p13332.

Alchalbi, A., Daoud, M., Gomez, F., McClusky, S., Reilinger, R., Romeyeh, M.A., Alsouod, A., R.Y., Ballani, B., Darawcheh, R., Sbeinati, R., Radwan, Y., Al Masri, R., Bayerly, M., Al Ghazzi, R., and Barazangi, M., 2010, Crustal deformation in northwestern Arabia from GPS measurements in Syria: Slow slip rate along the northern Dead Sea fault: Geophysical Journal International, v. 180, p. 125–135, doi: 10.1111/j.1365-246X.2009.04431.x.

Allen, C.R., 1962, Circum-Pacific faulting in the Philippines-Taiwan region: Journal of Geophysical Research, v. 67, p. 4795–4812, doi: 10.1029/JZ067i012p04795.

Allen, C.R., Gillespie, A.R., Yuan, H., Sieh, K.E., Buchang, Z., and Chengnan, Z., 1984, Red River and associated faults, Yunnan Province, China: Quaternary geology, slip rates, and seismic hazard: Geological Society of America Bulletin, v. 95, p. 686–700, doi: 10.1130/0016-7606(1984)95<686:RRAAFY>2.0.CO;2.

Allen, C.R., Zhuoli, L., Hong, Q., Xueze, W., Huawei, Z., and Weishi, H., 1991, Field study of a highly active fault zone: The Xianshuihe fault of southwestern China: Geological Society of America Bulletin, v. 103, p. 1178–1199, doi: 10.1130/0016-7606(1991)103<1178:FSOAHA>2.3.CO;2.

Ambraseys, N.N., and Melville, C.P., 1982, A history of Persian earthquakes: New York, Cambridge University Press, 244 p.

Angelier, J., Chu, H.-T., and Lee, J.-C., 1997, Shear concentration in a collision zone: Kinematics of the Chihshang fault as revealed by outcrop-scale quantification of active faulting, Longitudinal Valley, eastern Taiwan: Tectonophysics, v. 274, p. 117–143, doi: 10.1016/S0040-1951(96)00301-0.

Argus, D.F., and Gordon, R.G., 1991, Current Sierra Nevada–North America motion from very long baseline interferometry: Implications for the kinematics of the western United States: Geology, v. 19, p. 1085–1088, doi: 10.1130/0091-7613(1991)019<1085:CSNNAM>2.3.CO;2.

Argus, D.F., and Gordon, R.G., 2001, Present tectonic motion across the Coast Ranges and San Andreas fault system in central California: Geological Society of America Bulletin, v. 113, p. 1580–1592, doi: 10.1130/0016-7606(2001)113<1580:PTMATC>2.0.CO;2.

Atwater, T., 1970, Implications of plate tectonics for the Cenozoic evolution of western North America: Geological Society of America Bulletin, v. 81, p. 3513–3536, doi: 10.1130/0016-7606(1970)81[3513:IOPTFT]2.0.CO;2.

Audemard, F.A.M., 1996, Paleoseismicity studies on the Oca-Ancón fault system, northwestern Venezuela: Tectonophysics, v. 259, p. 67–80, doi: 10.1016/0040-1951(95)00144-1.

Audemard, F., Pantosti, D., Machette, M., Costa, C., Okumura, K., Cowan, H., Diederix, H., and Ferrer, C., and Participants of the South American Field Workshop on Paleoseismology, 1999, Trench investigation along the Mérida section of the Boconó fault (central Venezuelan Andes), Venezuela: Tectonophysics, v. 308, p. 1–21.

Audemard, M.F.A., Ollaves, R., Bechtold, M., Díaz, G., Beck, C., Carrillo, E., Pantosti, D., and Diederix, H., 2008, Trench investigation on the main strand of the Boconó fault in its central section, at Mesa del Caballo, Mérida Andes, Venezuela: Tectonophysics, v. 459, p. 38–53.

Authemayou, C., Bellier, O., Chardon, D., Benedetti, L., Malekzade, Z., Claude, C., Angeletti, B., Shabanian, E., and Abbassi, M.R., 2009, Quaternary slip-rates of the Kazerun and the main recent faults: Active strike-slip partitioning in the Zagros fold-and-thrust belt: Geophysical Journal International, v. 178, p. 524–540, doi: 10.1111/j.1365-246X.2009.04191.x.

Avouac, J.-P., and Tapponnier, P., 1993, Kinematic model of active deformation in Central Asia: Geophysical Research Letters, v. 20, p. 895–898, doi: 10.1029/93GL00128.

Bachmanov, D.M., Trifonov, V.G., Hessami, K.T., Kozhurin, A.I., Ivanova, T.P., Rogozhin, E.A., Hademi, M.C., and Jamali, F.H., 2004, Active faults in the Zagros and central Iran: Tectonophysics, v. 380, p. 221–241, doi: 10.1016/j.tecto.2003.09.021.

Banks, C.J., and Warburton, J., 1986, "Passive-roof" duplex geometry in the frontal structures of the Kirthar and Sulaiman mountain belts, Pakistan: Journal of Structural Geology, v. 8, p. 229–237, doi: 10.1016/0191-8141(86)90045-3.

Barnes, P.M., 2009, Postglacial (after 20 ka) dextral slip rate of the offshore Alpine fault, New Zealand: Geology, v. 37, p. 3–6, doi: 10.1130/G24764A.1.

Barnes, P.M., and Audru, J.-C., 1999, Recognition of active strike-slip faulting from high-resolution marine seismic reflection profiles; eastern Marlborough fault system, New Zealand: Geological Society of America Bulletin, v. 111, p. 538–559, doi: 10.1130/0016-7606(1999)111<0538:ROASSF>2.3.CO;2.

Barrier, E., and Angelier, J., 1986, Active collision in eastern Taiwan: The Coastal Range: Tectonophysics, v. 125, p. 39–72, doi: 10.1016/0040-1951(86)90006-5.

Beaudouin, T., Bellier, O., and Sébrier, M., 2003, Champs de contrainte et de déformation déduits de l'analyse des mécanismes au foyer des séismes de la région de Sulawesi (Indonésie): Implications géodynamiques: Bulletin de la Société Géologique de France, v. 174, p. 305–317, doi: 10.2113/174.3.305.

Beavan, J., Moore, M., Pearson, C., Henderson, M., Parsons, B., Bourne, S., England, P., Walcott, D., Blick, G., Darby, D., and Hodgkinson, K., 1999, Crustal deformation during 1994–1998 due to oblique continental collision in the central Southern Alps, New Zealand, and implications for seismic potential of the Alpine fault: Journal of Geophysical Research, v. 104, p. 25,233–25,255, doi: 10.1029/1999JB900198.

Beavan, J., Silcock, D., Hamburger, M., Ramos, E., Thibault, C., and Feir, R., 2001, Geodetic constraints on postseismic deformation following the 1990 M_s 7.8 Luzon earthquake and implications for Luzon tectonics and Philippine Sea plate motion: Geochemistry Geophysics Geosystems, v. 2, p. 1015, doi: 10.1029/2000GC000100.

Beavan, J., Tregoning, P., Bevis, M., Kato, T., and Meertens, C., 2002, Motion and rigidity of the Pacific plate and implications for plate boundary deformation: Journal of Geophysical Research, v. 107, 2261, doi: 10.1029/2001JB000282.

Bekker, Y.A., Koshlakov, G.V., and Kuznetsov, Y.S., 1974a, Deep structure of southwest Tadjikistan from geologic and geophysical data, *in* Searches for precursors of earthquakes in prediction polygons: Moscow, Nauka, p. 16–23 (in Russian).

Bekker, Y.A., Koshlakov, G.V., Kuznetsov, E.C., Murchaidze, D.P., and Orlov, E.S., 1974b, Toward the tectonics of the region of the city of Dushanbe (Gissar Valley) from the results of geological-geophysical investigations (in Russian), *in* Searches for Precursors of earthquakes in prediction polygons: Moscow, Nauka, p. 24–29 (in Russian).

Bell, M.L., Crough, S.T., and Nur, A., 1977, Non-Newtonian antiplane flow and its application to plate deformation: Tectonophysics, v. 39, p. 501–514, doi: 10.1016/0040-1951(77)90150-0.

Bellier, O., and Sébrier, M., 1995, Is the slip rate variation on the Great Sumatran fault accommodated by forearc stretching?: Geophysical Research Letters, v. 22, p. 1969–1972, doi: 10.1029/95GL01793.

Bellier, O., Bellon, H., Sébrier, M., Sutanto, and Maury, R.C., 1999, K-Ar age of the Ranau Tuffs, implications for the Ranau caldera emplacement and slip-partitioning in Sumatra (Indonesia): Tectonophysics, v. 312, p. 347–359, doi: 10.1016/S0040-1951(99)00198-5

Bellier, O., Sébrier, M., Beaudouin, T., Villeneuve, M., Braucher, R., Bourlès, D., Siame, L., Putranto, E., and Pratomo, I., 2001, High slip rate for a low seismicity along the Palu-Koro active fault in central Sulawesi (Indonesia): Terra Nova, v. 13, p. 463–470, doi: 10.1046/j.1365-3121.2001.00382.x.

Bellier, O., Sébrier, M., Seward, D., Beaudouin, T., Villeneuve, M., and Putranto, E., 2006, Fission track and fault kinematics analyses for new insight into the late Cenozoic tectonic regime changes in west-central Sulawesi (Indonesia): Tectonophysics, v. 413, p. 201–220, doi: 10.1016/j.tecto.2005.10.036.

Bendick, R., Bilham, R., Freymueller, J., Larson, K., and Yin, G., 2000, Geodetic evidence for a low slip rate on the Altyn Tagh fault system: Nature, v. 404, p. 69–72, doi: 10.1038/35003555.

Bennett, R.A., Rodi, W.A., and Reilinger, R.E., 1996, Global positioning system constraints on fault slip rates in

southern California and northern Baja, Mexico: Journal of Geophysical Research, v. 101, p. 21,943–21,960, doi: 10.1029/96JB02488.

Benson, A.M., Little, T.A., Van Dissen, R.J., Hill, N., and Townsend, D.B., 2001, Late Quaternary paleoseismic history and surface rupture characteristics of the eastern Awatere strike-slip fault, New Zealand: Geological Society of America Bulletin, v. 113, p. 1079–1091, doi: 10.1130/0016-7606(2001)113<1079:LQPHAS>2.0.CO;2.

Bernard, M., Shen-Tu, B., Holt, W.E., and Davis, D.M., 2000, Kinematics of active deformation in the Sulaiman lobe and range, Pakistan: Journal of Geophysical Research, v. 105, p. 13,253–13,279, doi: 10.1029/1999JB900405.

Berryman, K., Cooper, A.F., Norris, R.J., Sutherland, R., and Villamor, P., 1998, Paleoseismic investigation of the Alpine fault at Haast and Okuru: Geological Society of New Zealand Miscellaneous Publication 101A, 44 p.

Bertrand, G., Rangin, C., Maury, R.C., Htun, H.M., Bellon, H., and Guillaud, J.P., 1998, Les basaltes de Singu (Myanmar): Nouvelles contraintes sur le taux de décrochement récent de la faille de Sagaing: Paris, Académie des Sciences Comptes Rendus, v. 327, p. 479–484.

Beun, N., Bordet, P., and Carbonnel, J.-P., 1979, Première données quantitatives relatives au coulissages du décrochement de Chaman (Afghanistan du Sud-Est): Paris, Académie des Sciences Comptes Rendus, v. 288, p. 931–934.

Biggs, J., Wright, T., Lu, Z., and Parsons, B., 2007, Multi-interferogram method for measuring interseismic deformation: Denali fault, Alaska: Geophysical Journal International, v. 170, p. 1165–1179, doi: 10.1111/j.1365-246X.2007.03415.x.

Bock, Y., Prawirodirdjo, L., Genrich, J.F., Stevens, C.W., McCaffrey, R., Subarya, C., Puntodewo, S.S.O., and Calais, E., 2003, Crustal motion in Indonesia from global positioning system measurements: Journal of Geophysical Research, v. 108, no. B8, 2367, doi: 10.1029/2001JB000324.

Bos, A.G., Spakman, W., and Nyst, M.C.J., 2003, Surface deformation and tectonic setting of Taiwan inferred from a GPS velocity field: Journal of Geophysical Research, v. 108, no. B10, 2458, doi: 10.1029/2002JB002336.

Brown, E.T., Bendick, R., Bourlès, D.L., Gaur, V.K., Molnar, P., Raisbeck, G.M., and Yiou, F., 2002, Slip rates of the Karakorum fault, Ladakh, India, determined using cosmic ray exposure dating of debris flows and moraines: Journal of Geophysical Research, v. 107, no. B9, 2192, doi: 10.1029/2000JB000100.

Brown, E.T., Molnar, P., and Bourlès, D.L., 2005, Slip-rate measurements on the Karakorum fault may imply secular variations in fault motion: Technical comment: Science, v. 309, p. 1326b, doi: 10.1126/science.1112508.

Bourne, S.J., Árnadóttir, T., Beavan, J., Darby, D.J., England, P.C., Parsons, B., Walcott, R.I., and Wood, P.R., 1998, Crustal deformation of the Marlborough fault zone in the South Island of New Zealand: Geodetic constraints over the interval 1982–1994: Journal of Geophysical Research, v. 103, p. 30,147–30,165, doi: 10.1029/98JB02228.

Burchfiel, B.C., Zhang Peizhen, Wang Yipeng, Zhang Weiqi, Song Fangmin, Deng Qidong, Molnar, P., and Royden, L., 1991, Geology of the Haiyuan fault zone, Ningxia-Hui Autonomous Region, China, and its relation to the evolution of the northeastern margin of the Tibetan plateau: Tectonics, v. 10, p. 1091–1110, doi: 10.1029/90TC02685.

Burov, E.B., and Molnar, P., 1998, Gravity anomalies over the Ferghana Valley (Central Asia) and intracontinental deformation: Journal of Geophysical Research, v. 103, p. 18,137–18,152, doi: 10.1029/98JB01079.

Burtman, V.S., 1963, The Talaso-Fergana and San Andreas strike-slip faults, *in* Peive, A.V., ed., Faults and horizontal movements of the Earth's crust: Moscow, Nauka, Trudy Geological Institute, Akademi Nauk USSR, Volume 80, p. 128–151 (in Russian).

Burtman, V.S., 1964, The Talaso-Fergana strike-slip fault: Moscow, Nauka, Trudy Geological Institute, Akademi Nauk USSR, Volume 104, 143 p. (in Russian).

Burtman, V.S., 1975, Structural geology of the Variscan Tien Shan, USSR: American Journal of Science, v. 272A, p. 157–186.

Burtman, V.S., and Molnar, P., 1993, Geological and geophysical evidence for deep subduction of continental crust beneath the Pamir: Geological Society of America Special Paper 281, 76 p.

Burtman, V.S., Skobelev, S.F., and Molnar, P., 1996, Late Cenozoic slip on the Talas-Ferghana fault, the Tien Shan, central Asia: Geological Society of America Bulletin, v. 108, p. 1004–1021, doi: 10.1130/0016-7606(1996)108<1004:LCSOTT>2.3.CO;2.

Case, J.E., and MacDonald, W.D., 1973, Regional gravity anomalies and crustal structure in northern Colombia: Geological Society of America Bulletin, v. 84, p. 2905–2916, doi: 10.1130/0016-7606(1973)84<2905:RGAACS>2.0.CO;2.

Cavalié, O., Lasserre, C., Doin, M.-P., Peltzer, G., Sun, J., Xu, X., and Shen, Z.-K., 2008, Measurement of interseismic strain across the Haiyuan fault (Gansu, China), by InSAR: Earth and Planetary Science Letters, v. 275, p. 246–257, doi: 10.1016/j.epsl.2008.07.057.

Cediel, F., Shaw, R.P., and Cáceres, C., 2003, Tectonic assembly of the Northern Andean block, *in* Bartolini, C.R.T., et al., eds., The Circum-Gulf of Mexico and the Caribbean: Hydrocarbon habitats, basin formation, and plate tectonics: American Association of Petroleum Geologists Memoir 79, p. 815–848.

Chen, W.-P., and Molnar, P., 1990, Source parameters of earthquakes and intraplate deformation beneath the Shillong Plateau and northern Indoburman Ranges: Journal of Geophysical Research, v. 95, p. 12,527–12,552, doi: 10.1029/JB095iB08p12527.

Chen, W.P., Chen, C.-Y., and Náb lek, J.L., 1999, Present-day deformation of the Qaidam basin with implications for intra-continental tectonics: Tectonophysics, v. 305, p. 165–181, doi: 10.1016/S0040-1951(99)00006-2.

Chen, Z., Burchfiel, B.C., Liu, Y., King, R.W., Royden, L.H., Tang, W., Wang, E., Zhao, J., and Zhang, X., 2000, Global positioning system measurements from eastern Tibet and their implications for India/Eurasia intracontinental collision: Journal of Geophysical Research, v. 105, p. 16,215–16,227, doi: 10.1029/2000JB900092.

Chester, J.S., Chester, F.M., and Kroenenberg, A.K., 2005, Fracture surface energy of the Punch bowl fault, San Andreas system: Nature, v. 437, p. 133–136.

Chevalier, M.-L., Ryerson, F.J., Tapponnier, P., Finkel, R.C., Van Der Woerd, J., Li, H., and Liu, Q., 2005, Slip-rate measurements on the Karakorum fault may imply secular variations in fault motion: Science, v. 307, p. 411–414, doi: 10.1126/science.1105466.

Chhibber, H.L., 1934, Geology of Burma: London, McMillan, 538 p.

Clark, M.K., Bush, J.W.M., and Royden, L.H., 2005, Dynamic topography produced by lower crustal flow against rheological strength heterogeneities bordering the Tibetan Plateau: Geophysical Journal International, v. 162, p. 575–590, doi: 10.1111/j.1365-246X.2005.02580.x.

Cooper, A.F., and Norris, R.J., 1994, Anatomy, structural evolution, and slip rate of a plate-boundary thrust: The Alpine fault at Gaunt Creek, Westland, New Zealand: Geological Society of America Bulletin, v. 106, p. 627–633, doi: 10.1130/0016-7606(1994)106<0627:ASEASR>2.3.CO;2.

Cooper, A.F., and Norris, R.J., 1995, Displacement on the Alpine fault at Haast River, South Westland, New Zealand: New Zealand Journal of Geology and Geophysics, v. 38, p. 509–514.

Cowan, H.A., 1990, Late Quaternary displacements on the Hope fault at Glynn Wye, North Canterbury: New Zealand Journal of Geology and Geophysics, v. 33, p. 285–293.

Cowan, H.A., and McGlone, M.S., 1991, Late Holocene displacements and characteristic earthquakes on the Hope River segment of the Hope fault, New Zealand: Royal Society of New Zealand Journal, v. 21, p. 373–384.

Cowgill, E., 2007, Impact of riser reconstructions on estimation of secular variation in rates of strike-slip faulting: Revisiting the Cherchen River site along the Altyn Tagh fault, NW China: Earth and Planetary Science Letters, v. 254, p. 239–255, doi: 10.1016/j.epsl.2006.09.015.

Cowgill, E., Gold, R.D., Chen Xuanhua, Wang Xiao-Feng, Arrowsmith, J R., and Southon, J., 2009, Low Quaternary slip rate reconciles geodetic and geologic rates along the Altyn Tagh fault, northwestern Tibet: Geology, v. 37, p. 647–650, doi: 10.1130/G25623A.1.

Curray, J.R., 2005, Tectonics and history of the Andaman Sea region: Journal of Asian Earth Sciences, v. 25, p. 187–232, doi: 10.1016/j.jseaes.2004.09.001.

Curray, J.R., Moore, D.G., Lawver, L.A., Emmel, F.J., Raitt, R.W., Henry, M., and Kieckhefer, R., 1978, Tectonics of the Andaman Sea and Burma, *in* Watkins, J.S.L., et al., eds., Geological and geophysical investigations of continental margins: American Association of Petroleum Geologists Memoir 29, p. 189–198.

d'Alessio, M.A., Johanson, I.A., Bürgmann, R., Schmidt, D.A., and Murray, M.H., 2005, Slicing up the San Francisco Bay area: Block kinematics and fault slip rates from GPS-derived surface velocities: Journal of Geophysical Research, v. 110, B06403, doi: 10.1029/2004JB003496.

Davis, G.A., and Burchfiel, B.C., 1973, Garlock fault: An intracontinental transform structure, southern California: Geological Society of America Bulletin, v. 84, p. 1407–1422, doi: 10.1130/0016-7606(1973)84<1407:GFAITS>2.0.CO;2.

Davis, P., England, P., and Houseman, G., 1997, Comparison of shear wave splitting and finite strain from the India-Asia collision zone: Journal of Geophysical Research, v. 102, p. 27,511–27,522, doi: 10.1029/97JB02378.

Dayem, K.E., Houseman, G.A., and Molnar, P., 2009, Localization of shear along a lithospheric strength discontinuity: Application of a continuous deformation model to the boundary between Tibet and the Tarim Basin: Tectonics, v. 28, TC3002, doi: 10.1029/2008TC002264.

DeMets, C., Jansma, P.E., Mattioli, G.S., Dixon, T.H., Farina, F., Bilham, R., Calais, E., and Mann, P., 2000, GPS geodetic constraints on Caribbean–North American plate motion: Geophysical Research Letters, v. 27, p. 437–440, doi: 10.1029/1999GL005436.

DeMets, C., Mattioli, G., Jansma, P., Rogers, R., Tenorio, C., and Turner, H.L., 2007, Present motion and deformation of the Caribbean plate: Constraints from new GPS geodetic measurements from Honduras and Nicaragua, *in* Mann, P., ed., Geologic and yectonic development of the Caribbean plate in northern Central America: Geological Society of America Special Paper 428, p. 21–36, doi: 10.1130/2007.2428(01).

Deng Qidong, Song Fangmin, Zhu Shilong, Li Mengluan, Wang Tielin, Zhang Weiqi, Burchfiel, B.C., Molnar, P., and Zhang Peizhen, 1984, Active faulting and tectonics of the Ningxia-Hui Autonomous Region, China: Journal of Geophysical Research, v. 89, p. 4427–4445, doi: 10.1029/JB089iB06p04427.

Dickinson, W.R., Ducea, M., Rosenberg, L.I., Green, H.G., Graham, S.A., Clark, J.C., Weber, G.E., Kidder, S., Ernst, W.G., and Brabb, E.E., 2005, Net dextral slip, Neogene San Gregorio–Hosgri fault zone, coastal California: Geologic evidence and tectonic implications: Geological Society of America Special Paper 391, 43 p.

Duong, C.C., and Feigl, K., 1998, Geodetic measurement of horizontal strain across the Red River fault near Thac Ba, Vietnam, 1963–1994: Journal of Geodesy, v. 73, p. 298–310.

Elliott, J.R., Biggs, J., Parsons, B., and Wright, T.J., 2008, InSAR slip rate determination on the Altyn Tagh fault, northern Tibet, in the presence of topographically correlated atmospheric delays: Geophysical Research Letters, v. 35, L12309, doi: 10.1029/2008GL033659.

England, P., and Houseman, G., 1986, Finite strain calculations of continental deformation 2. Comparison with the India-Asia Collision: Journal of Geophysical Research, v. 91, p. 3664–3676, doi: 10.1029/JB091iB03p03664.

England, P., and Molnar, P., 1990, Right-lateral shear and rotation as the explanation for strike-slip faulting in eastern Tibet: Nature, v. 344, p. 140–142, doi: 10.1038/344140a0.

England, P., and Molnar, P., 1997, The field of crustal velocity in Asia calculated from Quaternary rates of slip on faults: Geophysical Journal International, v. 130, p. 551–582, doi: 10.1111/j.1365-246X.1997.tb01853.x.

England, P., and Molnar, P., 2005, Late Quaternary to decadal velocity fields in Asia: Journal of Geophysical Research, v. 110, B12401, doi: 10.1029/2004JB003541.

England, P., Engdahl, R., and Thatcher, W., 2004, Systematic variation in the depths of slabs beneath arc volcanoes: Geophysical Journal International, v. 156, p. 377–408, doi: 10.1111/j.1365-246X.2003.02132.x.

Evans, B., and Goetze, C., 1979, The temperature variation of hardness of olivine and its implication for polycrystalline yield stress: Journal of Geophysical Research, v. 84, p. 5505–5524, doi: 10.1029/JB084iB10p05505.

Fattahi, M., Walker, R.T., Khatib, M.M., Dolati, A., and Bahroudi, A., 2007, Slip-rate estimate and past earthquakes on the Doruneh fault, eastern Iran: Geophysical Journal International, v. 168, p. 691–709, doi: 10.1111/j.1365-246X.2006.03248.x.

Ferris, A., Abers, G.A., Christensen, D.H., and Veenstra, E., 2003, High-resolution image of the subducted Pacific plate (?) beneath central Alaska, 50–150 km depth: Earth and Planetary Science Letters, v. 214, p. 575–588, doi: 10.1016/S0012-821X(03)00403-5.

Fitch, T.J., 1972, Plate convergence, transcurrent faults, and internal deformation adjacent to southeast Asia and the western Pacific: Journal of Geophysical Research, v. 77, p. 4432–4460, doi: 10.1029/JB077i023p04432.

Fleitout, L., and Froidevaux, C., 1980, Thermal and mechanical evolution of shear zones: Journal of Structural Geology, v. 2, p. 159–164, doi: 10.1016/0191-8141(80)90046-2.

Flesch, L.M., Haines, A.J., and Holt, W.E., 2001, Dynamics of the India-Eurasia collision zone: Journal of Geophysical Research, v. 106, p. 16,435–16,460, doi: 10.1029/2001JB000208.

Flesch, L.M., Holt, W.E., Silver, P.G., Stephenson, M., Wang, C.-Y., and Chan, W.W., 2005, Constraining the extent of crust upper mantle coupling in central Asia using GPS, geologic, and shear-wave splitting data: Earth and Planetary Science Letters, v. 238, p. 248–268, doi: 10.1016/j.epsl.2005.06.023.

Fletcher, H.J., 2002, Crustal deformation in Alaska measured using the global positioning system [Ph.D. thesis]: Fairbanks, University of Alaska, 135 p.

Fletcher, H.J., and Freymueller, J.T., 2003, New constraints on the motion of the Fairweather fault, Alaska, from GPS observations: Geophysical Research Letters, v. 30, p. 1139, doi: 10.1029/2002GL016476.

Fletcher, R.C., and Hallet, B., 1983, Unstable extension of the lithosphere: A mechanical model for Basin-and-Range structure: Journal of Geophysical Research, v. 88, p. 7457–7466, doi: 10.1029/JB088iB09p07457.

Freymueller, J.T., Murray, M.H., Segall, P., and Castillo, D., 1999, Kinematics of the Pacific–North America plate boundary zone, northern California: Journal of Geophysical Research, v. 104, p. 7419–7441, doi: 10.1029/1998JB900118.

Freymueller, J.T., Woodard, H., Cohen, S.C., Cross, R., Elliott, J., Larsen, C.F., Hreinsdottir, S., and Zweck, C., 2008, Active deformation processes in Alaska, based on 15 years of GPS measurements, *in* Freymueller, J.T., et al., eds., Active tectonics and seismic potential of Alaska: American Geophysical Union Geophysical Monograph 179, p. 1–42.

Froidevaux, C., 1986, Basin and Range large-scale tectonics: Constraints from gravity and reflection seismology: Journal of Geophysical Research, v. 91, p. 3625–3632, doi: 10.1029/JB091iB03p03625.

Galgana, G., Hamburger, M., McCaffrey, R., Corpuz, E., and Chen, Q.-Z., 2007, Analysis of crustal deformation of Luzon Island, Philippines, using geodetic observations and earthquake focal mechanisms: Tectonophysics, v. 432, p. 63–87, doi: 10.1016/j.tecto.2006.12.001.

Genrich, J.F., Bock, Y., McCaffrey, R., Prawirodirdjo, L., Stevens, C.W., Puntodewo, S.S.O., Subarya, C., and Wdowinski, S., 2000, Distribution of slip at the northern Sumatran fault system: Journal of Geophysical Research, v. 105, p. 28,327–28,341, doi: 10.1029/2000JB900158.

Gomez, F., Karam, G., Khawlie, M., McClusky, S., Vernant, P., Reilinger, R., Jaafar, R., Tabet, C., Khair, K., and Barazangi, M., 2007, Global positioning system measurements of strain accumulation and slip transfer through the restraining bend along the Dead Sea fault system in Lebanon: Geophysical Journal International, v. 168, p. 1021–1028, doi: 10.1111/j.1365-246X.2006.03328.x.

Graham, S.A., and Dickinson, W.R., 1978, Evidence for 115 kilometers of right slip on the San Gregorio–Hosgri fault trend: Science, v. 199, p. 179–181, doi: 10.1126/science.199.4325.179.

Haeussler, P.J., Schwartz, D.P., Dawson, T.E., Stenner, H.D., Lienkaemper, J.J., Sherrod, B., Cinti, F.R., Montone, P., Craw, P.A., Crone, A.J., and Personius, S.F., 2004, Surface rupture and slip distribution of the Denali and Totschunda faults in the 3 November 2002 M 7.9 earthquake, Alaska: Seismological Society of America Bulletin, v. 94, p. 23–52, doi: 10.1785/0120040626.

Hall, N.T., Hunt, T.D., and Vaughn, P., 1994, Holocene behavior of the San Simeon fault zone, south-central coastal California, *in* Alterman, I.B., et al., eds., Seismotectonics of the central California Coast Ranges: Geological Society of America Special Paper 292, p. 167–190.

Hanson, K.L., and Lettis, W.R., 1994, Estimated Pleistocene slip rate for the San Simeon fault zone, south-central California *in* Alterman, I.B., et al., eds., Seismotectonics of the central California Coast Ranges: Geological Society of America Special Paper 292, p. 133–150.

Hanson, K.L., Lettis, W.R., McLaren, M.K., Savage, W.U., and Hall, N.T., 2004, Style and rate of Quaternary deformation of the Hosgri fault zone, offshore southern California: U.S. Geological Survey Bulletin 1995-BB, 33 p.

Harkins, N., and Kirby, E., 2008, Fluvial terrace riser degradation and determination of slip rates on strike-slip faults: An example from the Kunlun fault, China: Geophysical Research Letters, v. 35, L05406, doi: 10.1029/2007GL033073.

Hessami, K., Pantosti, D., Tabassi, H., Shabanian, E., Abbassi, M.R., Feghhi, K., and Solaymani, S., 2003, Paleoearthquakes and slip rates of the North Tabriz fault, NW Iran: Preliminary results: Annals of Geophysics, v. 46, p. 903–915.

Hilley, G.E., Bürgmann, R., Zhang, P.-Z., and Molnar, P., 2005, Bayesian inference of plastosphere viscosities near the Kunlun fault, northern Tibet: Geophysical Research Letters, v. 32, L01302, doi: 10.1029/2004GL021658.

Holt, W.E., 2000, Correlated crust and mantle strain fields in Tibet: Geology, v. 28, p. 67–70, doi: 10.1130/0091-7613(2000)28<67:CCAMSF>2.0.CO;2.

Holt, W.E., Ni, J.F., Wallace, T.C., and Haines, A.J., 1991, The active tectonics of the eastern Himalayan syntaxis and surrounding regions: Journal of Geophysical Research, v. 96, p. 14,595–14,632, doi: 10.1029/91JB01021.

Howard, M., Nicol, A., Campbell, J., and Pettinga, J.R., 2005, Holocene paleoearthquakes on the strike-slip Porters Pass fault, Canterbury: New Zealand Journal of Geology and Geophysics, v. 48, p. 59–74.

Hsu, Y.-J., Simons, M., Yu, S.-B., Kuo, L.-C., and Chen, H.-Y., 2003, A two-dimensional dislocation model for interseismic deformation of the Taiwan mountain belt: Earth and Planetary Science Letters, v. 211, p. 287–294, doi: 10.1016/S0012-821X(03)00203-6.

Hu, J.-C., Angelier, J., Homberg, C., Lee, J.-C., and Chu, H.-T., 2001, Three-dimensional modeling of the behavior of the oblique convergent boundary of southeast Taiwan: Friction and strain partitioning: Tectonophysics, v. 333, p. 261–276.

Hubert-Ferrari, A., Armijo, R., King, G., Meyer, B., and Barka, A., 2002, Morphology, displacement, and slip rates along the North Anatolian fault, Turkey: Journal of Geophysical Research, v. 107, doi: 10.1029/2001JB000393.

Humayon, M., Lillie, R.J., and Lawrence, R.D., 1991, Structural interpretation of the eastern Sulaiman foldbelt and foredeep, Pakistan: Tectonics, v. 10, p. 299–324, doi: 10.1029/90TC02133.

Jade, S., Bhatt, B.C., Bendick, R., Gaur, V.K., Molnar, P., Anand, M.B., and Kumar, D., 2004, GPS measurements from the Ladakh Himalaya, India: Preliminary tests of plate-like or continuous deformation in Tibet: Geological Society of America Bulletin, v. 116, p. 1385–1391, doi: 10.1130/B25357.1.

Jadoon, I.A.K., Lawrence, R.D., and Lillie, R.J., 1993, Evolution of foreland structures: An example from the Sulaiman thrust lobe of Pakistan, southwest of the Himalayas, *in* Treloar, P.J., and Searle, M.P., eds., Himalayan tectonics: Geological Society of London Special Publication 74, p. 589–602.

Kellogg, J.N., 1984, Cenozoic tectonic history of the Sierra de Perijá, Venezuelan-Colombia, and adjacent basins, *in* Bonini, W.E., et al., eds., The Caribbean–South America plate boundary and regional tectonics: Geological Society of America Memoir 162, p. 239–262.

Kellogg, J.N., and Bonini, W.E., 1982, Subduction of the Caribbean plate and basement uplifts in the overriding South American plate: Tectonics, v. 1, p. 251–276, doi: 10.1029/TC001i003p00251.

Kidd, W.S.F., and Molnar, P., 1988, Quaternary and active faulting observed on the 1985 Academia Sinica-Royal Society geotraverse of Tibet: Royal Society of London Philosophical Transactions, ser. A, v. 327, p. 337–363.

Kirby, E., Harkins, N., Wang, E.-Q., Shi, X.-H., Fan, C., and Burbank, D., 2007, Slip rate gradients along the eastern Kunlun fault: Tectonics, v. 26, TC2010, doi: 10.1029/2006TC002033.

Klemperer, S.L., Hauge, T.A., Hauser, E.C., Oliver, J.E., and Potter, C.J., 1986, The Moho in the northern Basin and Range Province, Nevada, along the COCORP 40°N seismic-reflection transect: Geological Society of America Bulletin, v. 97, p. 603–618, doi: 10.1130/0016-7606(1986)97<603:TMITNB>2.0.CO;2.

Knuepfer, P.L.K., 1992, Temporal variations in latest Quaternary slip across the Australian-Pacific plate boundary, northeastern South Island, New Zealand: Tectonics, v. 11, p. 449–464, doi: 10.1029/91TC02890.

Kozacž, Ö., Dolan, J., Finkel, R., and Hartleb, R., 2007, Late Holocene slip rate for the North Anatolian fault, Turkey, from cosmogenic ^{36}Cl geochronology: Implications for the constancy of fault loading and strain release rates: Geology, v. 35, p. 867–870, doi: 10.1130/G23187A.1.

Kozacž, Ö., Dolan, J., and Finkel, R.C., 2009, A late Holocene slip rate for the central North Anatolian fault, at Tahtaköprü, Turkey, from cosmogenic ^{10}Be geochronology: Implications for fault loading and strain release rates: Journal of Geophysical Research, v. 114, doi: 10.1029/2008JB005760.

Kuchai, V.K., and Trifonov, V.G., 1977, Young left-lateral strike slip along the zone of the Darvaz-Karakul' fault: Geotektonika (Moskva), no. 3, p. 91–105.

Kulagina, M.V., Lukk, A.A., and Kulagin, B.K., 1974, Block structure of the Earth's crust of Tadjikistan, *in* Searches for precursors of earthquakes in prediction polygons: Moscow, Nauka, p. 70–84 (in Russian).

Langridge, R.M., and Berryman, K.R., 2005, Morphology and slip rate of the Hurunui section of the Hope fault, South Island, New Zealand: New Zealand Journal of Geology and Geophysics, v. 48, p. 43–57.

Langridge, R., Campbell, J., Pettinga, J., Hill, N., Pere, V., Pope, J., Pettinga, J., Estrada, B., and Berryman, K., 2003, Preliminary paleoseismic data for the Conway segment of the Hope fault from Greenburn Stream, South Island, New Zealand: Annals of Geophysics, v. 46, p. 1119–1139.

Lasserre, C., Morel, P.-H., Gaudemer, Y., Tapponnier, P., Ryerson, F.J., King, G.C.P., Métivier, F., Kasser, M., Kashgarian, M., Liu Baichi, Lu Taiya, and Yuan Daoyang, 1999, Postglacial left slip rate and past occurrence of $M \geq 8$ earthquakes on the western Haiyuan fault, Gansu, China: Journal of Geophysical Research, v. 104, p. 17,633–17,651, doi: 10.1029/1998JB900082.

Lasserre, C., Gaudemer, Y., Tapponnier, P., Mériaux, A.-S., Van der Woerd, J., Yuan Daoyang, Ryerson, F.J., Finkel, R.C., and Caffee, M.W., 2002, Fast late Pleistocene slip rate on the Leng Long Ling segment of the Haiyuan fault, Qinghai, China: Journal of Geophysical Research, v. 107, no. B11, 2276, doi: 10.1029/2000JB000060.

Lawrence, R.D., Khan, S.H., and Nakata, T., 1992, Chaman fault, Pakistan-Afghanistan: Annales Tectonicae, v. 6, p. 196–223.

Le Beon, M., Klinger, Y., Amrat, A.Q., Agnon, A., Dorbath, L., Baer, G., Ruegg, J.-C., Charade, O., and Mayyas, O., 2008, Slip rate and locking depth from GPS profiles across the southern Dead Sea Transform: Journal of Geophysical Research, v. 113, B11403, doi: 10.1029/2007JB005280.

Le Dain, A.Y., Tapponnier, P., and Molnar, P., 1984, Active faulting and tectonics of Burma and surrounding regions: Journal of Geophysical Research, v. 89, p. 453–472, doi: 10.1029/JB089iB01p00453.

Le Dortz, K., Meyer, B., Sébrier, M., Nazari, H., Braucher, R., Fattahi, M., Benedetti, L., Foroutan, M., Siame, L., Bourlès, D., Talebian, M., Bateman, M.D., and Ghoraishi, M., 2009, Holocene right-slip rate determined by cosmogenic and OSL dating on the Anar fault, Central Iran: Geophysical Journal International, v. 179, p. 700–710, doi: 10.1111/j.1365-246X.2009.04309.x.

Lee, J.-C., Angelier, J., Chu, H.-T., Yu, S.-B., and Hu, J.-C., 1998, Plate-boundary strain partitioning along the sinistral collision suture of the Philippine and Eurasian plates: Analysis of geodetic data and geological observation in southeastern Taiwan: Tectonics, v. 17, p. 859–871, doi: 10.1029/98TC02205.

Lee, J.-C., Angelier, J., Chu, H.-T., Hu, J.-C., Jeng, F.-S., and Rau, R.-J., 2003, Active fault creep variations at Chihshang, Taiwan, revealed by creep meter monitoring, 1998–2001: Journal of Geophysical Research, v. 108, no. B11, 2528, doi: 10.1029/2003JB002394.

Lee, Y.-H., Chen, G.-T., Rau, R.-J., and Ching, K.-E., 2008, Coseismic displacement and tectonic implication of 1951 Longitudinal Valley earthquake sequence, eastern Taiwan: Journal of Geophysical Research, v. 113, B04305, doi: 10.1029/2007JB005180.

Legler, B.A., and Przhiyalgovskaya, I.A., 1979, The interaction of the Indian and Asian lithospheric plates and tectonics of the Tadjik Depression (in Russian), *in* Structure of lithospheric plates: Moscow, Institute of Oceanology, Academy of Sciences, USSR, p. 125–188.

Leloup, P.-H., Ricard, Y., Battaglia, J., and Lacassin, R., 1999, Shear heating in continental strike-slip shear zones: Numerical modeling and case studies: Geophysical Journal International, v. 136, p. 19–40, doi: 10.1046/j.1365-246X.1999.00683.x.

Li, C.-Y., Zhang, P.-Z., Yin, J.-H., and Min, W., 2009, Late Quaternary left-lateral slip rate of the Haiyuan fault, northeastern margin of the Tibetan Plateau: Tectonics, v. 28, TC5010, doi: 10.1029/2008TC002302.

Li Haibing, Van der Woerd, J., Tapponnier, P., Klinger, Y., Qi Xuexiang, Yang Jingsui, and Zhu Yintang, 2005, Slip rate on the Kunlun fault at Hongshui Gou, and recurrence time of great events comparable to the 14/11/2001, Mw~7.9 Kokoxili earthquake: Earth and Planetary Science Letters, v. 237, p. 285–299, doi: 10.1016/j.epsl.2005.05.041.

Lienkaemper, J.J., and Borchardt, G., 1996, Holocene slip rate of the Hayward fault at Union City, California: Journal of Geophysical Research, v. 101, p. 6099–6108, doi: 10.1029/95JB01378.

Lisowski, M., Savage, J.C., and Burford, R.O., 1987, Strain accumulation across the Fairweather and Totschunda faults, Alaska: Journal of Geophysical Research, v. 92, p. 11,552–11,560, doi: 10.1029/JB092iB11p11552.

Little, T.A., Grapes, R., and Berger, G.W., 1998, Late Quaternary strike-slip on the eastern part of the Awatere fault, South Island, New Zealand: Geological Society of America Bulletin, v. 110, p. 127–148, doi: 10.1130/0016-7606(1998)110<0127:LQSSOT>2.3.CO;2.

Liu, Q., 1993, Paléoclimat et contraintes chronologiques sur les mouvements récent dans l'Ouest du Tibet: Failles du Karakorum et de Longmu Co-Gozha Co, lacs en pull-apart de Longmu Co et de Sumxi Co: Thèse de Doctorat de l'Université Paris VII, 358 p.

Lockner, D.A., and Okubo, P.G., 1983, Measurements of frictional heating in granite: Journal of Geophysical Research, v. 88, p. 4313–4320, doi: 10.1029/JB088iB05p04313.

Lyon-Caen, H., Barrier, E., Lasserre, C., Franco, A., Arzu, I., Chiquin, L., Chiquin, M., Duquesnoy, T., Flores, O., Galicia, O., Luna, J., Molina, E., Porras, O., Requena, J., Robles, V., Romero, J., and Wolf, R., 2006, Kinematics of the North American–Caribbean–Cocos plates in Central America from new GPS measurements across the Polochic-Motagua fault system: Geophysical Research Letters, v. 33, L19309, doi: 10.1029/2006GL027694.

Mason, D.P.M., Little, T.A., and Van Dissen, R.J., 2006, Rates of active faulting during late Quaternary fluvial terrace formation at Saxton River, Awatere fault, New Zealand: Geological Society of America Bulletin, v. 118, p. 1431–1446, doi: 10.1130/B25961.1.

Matmon, A., Schwartz, D.P., Haeussler, P.J., Finkel, R., Lienkaemper, J.J., Stenner, H.D., and Dawson, T.E., 2006, Denali fault slip rates and Holocene–late Pleistocene kinematics of central Alaska: Geology, v. 34, p. 645–648, doi: 10.1130/G22361.1.

McCaffrey, R., 1991, Slip vectors and stretching of the Sumatran forearc: Geology, v. 19, p. 881–884, doi: 10.1130/0091-7613(1991)019<0881:SVASOT>2.3.CO;2.

McCaffrey, R., 1992, Oblique plate convergence, slip vectors, and forearc deformation: Journal of Geophysical Research, v. 97, p. 8905–8915, doi: 10.1029/92JB00483.

McCaffrey, R., Zwick, P.C., Bock, Y., Prawirodirdjo, L., Genrich, J.F., Stevens, C.W., Puntodewo, S.S.O., and Subarya, C., 2000, Strain partitioning during oblique plate convergence in northern Sumatra: Geodetic and seismologic constraints and numerical modeling: Journal of Geophysical Research, v. 105, p. 28,363–28,376, doi: 10.1029/1999JB900362.

McClusky, S., and 27 others, 2000, Global positioning system constraints on plate kinematics and dynamics in the eastern Mediterranean and Caucasus: Journal of Geophysical Research, v. 105, no. B3, p. 5695–5719.

McGill, S.F., Wells, S.G., Fortner, S.K., Kuzma, H.A., and McGill, J.D., 2009, Slip rate of the western Garlock fault, at Clark Wash, near Lone Tree Canyon, Mojave Desert, California: Geological Society of America Bulletin, v. 121, p. 536–554, doi: 10.1130/B26123.1.

Mériaux, A.-S., Ryerson, F.J., Tapponnier, P., Van der Woerd, J., Finkel, R.C., Xu, X., Xu, Z., and Caffee, M.W., 2004, Rapid slip along the central Altyn Tagh fault: Morphochronologic evidence from Cherchen He and Sulamu Tagh: Journal of Geophysical Research, v. 109, B06401, doi: 10.1029/2003JB002558.

Mériaux, A.-S., Tapponnier, P., Ryerson, F.J., Xu Xiwei, King, G., Van der Woerd, J., Finkel, R.C., Li Haibing, Caffee, M.W., Xu Zhiqin, and Chen Wenbin, 2005, The Aksay segment of the northern Altyn Tagh fault: Tectonic geomorphology, landscape evolution, and Holocene slip rate: Journal of Geophysical Research, v. 110, B04404, doi: 10.1029/2004JB003210.

Mériaux, A.-S., Sieh, K., Finkel, R.C., Rubin, C.M., Taylor, M.H., Meltzner, A.J., and Ryerson, F.J., 2009, Kinematic behavior of southern Alaska constrained by westward decreasing postglacial slip rates on the Denali fault, Alaska: Journal of Geophysical Research, v. 114, B03404, doi: 10.1029/2007JB005053.

Meyer, B., and Le Dortz, K., 2007, Strike-slip kinematics in Central and Eastern Iran: Estimating fault slip-rates averaged over the Holocene: Tectonics, v. 26, TC5009, doi: 10.1029/2006TC002073.

Meyer, B., Tapponnier, P., Gaudemer, Y., Peltzer, G., Guo Shunmin, and Chen Zhitai, 1996, Rate of left-lateral movement along the easternmost segment of the Altyn Tagh fault, east of 96°E (China): Geophysical Journal International, v. 124, p. 29–44, doi: 10.1111/j.1365-246X.1996.tb06350.x.

Meyer, B., Mouthereau, F., Lacombe, O., and Agard, P., 2006, Evidence for Quaternary activity along the Deshir fault: Implication for the Tertiary tectonics of Central Iran: Geophysical Journal International, v. 164, p. 192–201, doi: 10.1111/j.1365-246X.2005.02784.x.

Mohadjer, S., Bendick, R., Ischuk, A., Kuzikov, S., Kostuk, A., Saydullaev, U., Lodi, S., Kakar, D.M., Wasy, A., Khan, A., Molnar, P., Bilham, R., and Zubovich, A.V., 2010, Partitioning of India-Eurasia convergence in the Pamir-Hindu Kush from GPS measurements: Geophysical Research Letters, v. 37, L04305, doi: 10.1029/2009GL041737.

Molnar, P., and Atwater, T., 1978, Interarc spreading and cordilleran tectonics as alternates related to the age of subducted oceanic lithosphere: Earth and Planetary Science Letters, v. 41, p. 330–340, doi: 10.1016/0012-821X(78)90187-5.

Molnar, P., and Tapponnier, P., 1981, A possible dependence of tectonic strength on the age of the crust in Asia: Earth and Planetary Science Letters, v. 52, p. 107–114, doi: 10.1016/0012-821X(81)90213-2.

Murray, M.H., and Segall, P., 2001, Modeling broadscale deformation in northern California and Nevada from plate motions and elastic strain accumulation: Geophysical Research Letters, v. 28, p. 4315–4318, doi: 10.1029/2001GL013373.

Nazari, H., Ritz, J.-F., Salamati, R., Shafei, A., Ghassemi, A., Michelot, J.-L., Massault, M., and Ghorashi, M., 2009a, Morphological and palaeoseismological analysis along the Taleghan fault (central Alborz, Iran): Geophysical Journal International, v. 178, p. 1028–1041, doi: 10.1111/j.1365-246X.2009.04173.x.

Nazari, H., Fattahi, M., Meyer, B., Sébrier, M., Talebian, M., Foroutan, M., Le Dortz, K., Bateman, M.D., and Ghorashi, M., 2009b, First evidence for large earthquakes on the Deshir fault, Central Iran Plateau: Terra Nova, v. 21, p. 417–426, doi: 10.1111/j.1365-3121.2009.00892.x.

Ni, J.F., Guzman-Speziale, M., Bevis, M., Holt, W.E., Wallace, T.C., and Seager, W.R., 1989, Accretionary tectonics of Burma and the three-dimensional geometry of the Burma subduction zone: Geology, v. 17, p. 68–71, doi: 10.1130/0091-7613(1989)017<0068:ATOBAT>2.3.CO;2.

Nicol, A., and Van Dissen, R., 2002, Dip-dip partitioning of displacement components on the oblique-slip Clarence fault, New Zealand: Journal of Structural Geology, v. 24, p. 1521–1535, doi: 10.1016/S0191-8141(01)00141-9.

Niemi, T.M., and Hall, N.T., 1992, Late Holocene slip rate and recurrence of great earthquakes on the San Andreas fault in northern California: Geology, v. 20, p. 195–198, doi: 10.1130/0091-7613(1992)020<0195:LHSRAR>2.3.CO;2.

Nikonov, A.A., 1970, Differential analysis of the Quaternary tectonics of the Afghan-Tadjik Depression: Geotektonika (Moskva), no. 1, p. 101–107.

Noriega, G.R., Arrowsmith, J.R., Grant, L.B., and Young, J.J., 2006, Stream channel offset and late Holocene slip rate of the San Andreas fault at the Van Matre Ranch site, Carrizo Plain, California: Seismological Society of America Bulletin, v. 96, p. 33–47, doi: 10.1785/0120050094.

Norris, R.J., and Cooper, A.F., 1995, Origin of small-scale segmentation and transpressional thrusting along the Alpine fault, New Zealand: Geological Society of America Bulletin, v. 107, p. 231–240, doi: 10.1130/0016-7606(1995)107<0231:OOSSSA>2.3.CO;2.

Norris, R.J., and Cooper, A.F., 2001, Late Quaternary slip rates and slip partitioning on the Alpine fault, New Zealand: Journal of Structural Geology, v. 23, p. 507–520, doi: 10.1016/S0191-8141(00)00122-X.

Oglesby, D.D., Dreger, D.S., Harris, R.A., Ratchkovski, N., and Hansen, R., 2004, Inverse kinematic and forward dynamic models of the 2002 Denali fault earthquake, Alaska: Seismological Society of America Bulletin, v. 94, p. 214–233, doi: 10.1785/0120040620.

Okal, E.A., 1999, Historical seismicity and seismotectonic context of the great 1979 Yapen and 1996 Biak, Irian Jaya earthquakes: Pure and Applied Geophysics, v. 154, p. 633–675, doi: 10.1007/s000240050247.

Olgaard, D.L., and Brace, W.F., 1983, The microstructure of gouge from a mining-induced seismic shear zone: International Journal of Rock Mechanics and Mining Sciences, v. 20, p. 11–19, doi: 10.1016/0148-9062(83)91610-8.

Ozacar, A.A., Beck, S.L., and Christensen, D.H., 2003, Source process of the 3 November 2002 Denali fault earthquake (central Alaska) from teleseismic observations: Geophysical Research Letters, v. 30, 1638, doi: 10.1029/2003GL017272.

Page, R.A., Plafker, G., and Pulpan, H., 1995, Block rotation in east-central Alaska: A framework for evaluating earthquake potential?: Geology, v. 23, p. 629–632, doi: 10.1130/0091-7613(1995)023<0629:BRIECA>2.3.CO;2.

Peltzer, G., and Tapponnier, P., 1988, Formation and evolution of strike-slip faults, rifts, and basins, during the India-Asia collision: An experimental approach: Journal of Geophysical Research, v. 93, p. 15,085–15,117, doi: 10.1029/JB093iB12p15085.

Pérez, O.J., Bilham, R., Bendick, R., Velandia, J.R., Hernández, N., Moncayo, C., Hoyer, M., and Kozuch, M., 2001, Velocity field across the southern Caribbean plate boundary and estimates of Caribbean/South-American

plate motion using GPS geodesy 1994–2000: Geophysical Research Letters, v. 28, p. 2987–2990, doi: 10.1029/2001GL013183.

Peyret, M., Rolandone, F., Dominguez, S., Djamour, Y., and Meyer, B., 2008, Source model for the Mw 6.1, 31 March 2006, Chalan-Chulan earthquake (Iran) from InSAR: Terra Nova, v. 20, p. 126–133.

Peyret, M., Djamour, Y., Hessami, K., Regard, V., Bellier, O., Vernant, P., Daignières, M., Nankali, H., Van Gorp, S., Goudarzi, M., Chéry, J., Bayer, R., and Rigoulay, M., 2009, Present-day strain distribution across the Minab-Zendan-Palami fault system from dense GPS transects: Geophysical Journal International, v. 179, p. 751–762, doi: 10.1111/j.1365-246X.2009.04321.x.

Pindell, J., Kennan, L., Maresch, W.V., Stanek, K.-P., Draper, G., and Higgs, R., 2005, Plate-kinematics and crustal dynamics of circum-Caribbean arc-continent interactions: Tectonic controls on basin development in Proto-Caribbean margins, *in* Avé Lallemant, H.G., and Sisson, V.B., eds., Caribbean–South American plate interactions, Venezuela: Geological Society of America Special Paper 394, p. 7–52.

Plafker, G., Hudson, T., Bruns, T., and Rubin, M., 1978, Late Quaternary offsets along the Fairweather fault and crustal plate interactions: Canadian Journal of Earth Sciences, v. 15, p. 805–816.

Prawirodirdjo, L., Bock, Y., McCaffrey, R., Genrich, J., Calais, E., Stevens, C., Puntodewo, S.S.O., Subarya, C., Rais, J., Zwick, P., and Fauzi, 1997, Geodetic observations of interseismic strain segmentation at the Sumatra subduction zone: Geophysical Research Letters, v. 24, p. 2601–2604, doi: 10.1029/97GL52691.

Prawirodirdjo, L., Bock, Y., Genrich, J.F., Puntodewo, S.S.O., Rais, J., Subarya, C., and Sutisna, S., 2000, One century of tectonic deformation along the Sumatran fault from triangulation and GPS surveys: Journal of Geophysical Research, v. 105, p. 28,343–28,361, doi: 10.1029/2000JB900150.

Prentice, C.S., 1989, Earthquake geology of the northern San Andreas fault near Point Arena California [Ph.D. thesis]: Pasadena, California Institute of Technology, 252 p.

Prescott, W.H., Savage, J.C., Svarc, J.L., and Manaker, D., 2001, Deformation across the Pacific–North America plate boundary near San Francisco, California: Journal of Geophysical Research, v. 106, p. 6673–6682, doi: 10.1029/2000JB900397.

Pucci, S., De Martini, P.M., and Pantosti, D., 2008, Preliminary slip rate estimates for the Düzce segment of the North Anatolian fault zone from offset geomorphic markers: Geomorphology, v. 97, p. 538–554, doi: 10.1016/j.geomorph.2007.09.002.

Puntodewo, S.S.O., McCaffrey, R., Calais, E., Bock, Y., Rais, J., Subarya, C., Poewariardi, R., Stevens, C., Genrich, J., Fauzi, Zwick, P., and Wdowinski, S., 1994, GPS measurements of crustal deformation within the Pacific-Australia plate boundary in Irian Jaya, Indonesia: Tectonophysics, v. 237, p. 141–153.

Raju, K.A.K., Ramprasad, T., Rao, P.S., Ramalingeswara Rao, B., and Varghese, J., 2004, New insights into the tectonic evolution of the Andaman basin, northeast Indian Ocean: Earth and Planetary Science Letters, v. 221, p. 145–162, doi: 10.1016/S0012-821X(04)00075-5.

Rangin, C., Le Pichon, X., Mazzotti, S., Pubellier, M., Chamot-Rooke, N., Aurelio, M., Walpersdorf, A., and Quebral, R., 1999, Plate convergence measured by GPS across the Sundaland/Philippine Sea plate deformed boundary: the Philippines and eastern Indonesia: Geophysical Journal International, v. 139, p. 296–316, doi: 10.1046/j.1365-246x.1999.00969.x.

Raterron, P., Wu, Y.-J., Weidner, D.J., and Chen, J.-H., 2004, Low-temperature olivine rheology at high pressure: Physics of the Earth and Planetary Interiors, v. 145, p. 149–159, doi: 10.1016/j.pepi.2004.03.007.

Regard, V., Bellier, O., Thomas, J.-C., Bourlès, D., Bonnet, S., Abbassi, M.R., Braucher, R., Mercier, J., Shabanian, E., Soleymani, S., and Feghhi, K., 2005, Cumulative right-lateral fault slip rate across the Zagros–Makran transfer zone: Role of the Minab–Zendan fault system in accommodating Arabia–Eurasia convergence in southeast Iran: Geophysical Journal International, v. 162, p. 177–203, doi: 10.1111/j.1365-246X.2005.02558.x.

Reigber, C., Michel, G.W., Galas, R., Angermann, D., Klotz, J., Chen, J.Y., Papschev, A., Arslanov, R., Tzurkov, V.E., and Ishanov, M.C., 2001, New space geodetic constraints on the distribution of deformation in Central Asia: Earth and Planetary Science Letters, v. 191, p. 157–165, doi: 10.1016/S0012-821X(01)00414-9.

Reilinger, R., and 24 others, 2006, GPS constraints on continental deformation in the Africa-Arabia-Eurasia continental collision zone and implications for the dynamics of plate interactions: Journal of Geophysical Research, v. 111, B05411, doi: 10.1029/2005JB004051.

Replumaz, A., Lacassin, R., Tapponnier, P., and Leloup, P.H., 2001, Large river offsets and Plio-Quaternary dextral slip rate on the Red River fault (Yunnan, China): Journal of Geophysical Research, v. 106, p. 819–836, doi: 10.1029/2000JB900135.

Ritz, J.-F., Nazari, H., Ghassemi, A., Salamati, R., Shafei, Al., Solaymani, S., and Vernant, P., 2006, Active transtension inside central Alborz: A new insight into northern Iran-southern Caspian geodynamics: Geology, v. 34, p. 477–480.

Rodriguez, M., DeMets, C., Rogers, R., Tenorio, C., and Hernandez, D., 2009, A GPS and modelling study of deformation in northern Central America: Geophysical Journal International, v. 178, p. 1733–1754, doi: 10.1111/j.1365-246X.2009.04251.x.

Rogers, R.D., and Mann, P., 2007, Transtensional deformation of the western Caribbean–North America plate boundary zone, *in* Mann, P., ed., Geologic and tectonic development of the Caribbean plate boundary in northern Central America: Geological Society of America Special Paper 428, p. 37–64, doi: 10.1130/2007.2428(02).

Rolandone, F., Bürgmann, R., Agnew, D.C., Johanson, I.A., Templeton, D.C., d'Alessio, M.A., Titus, S.J., DeMets, C., and Tikoff, B., 2008, Aseismic slip and fault-normal strain along the central creeping section of the San Andreas fault: Geophysical Research Letters, v. 35, L14305, doi: 10.1029/2008GL034437.

Savage, J.C., Svarc, J.L., and Prescott, W.H., 1999, Geodetic estimates of fault slip rates in the San Francisco Bay region: Journal of Geophysical Research, v. 104, p. 4995–5002, doi: 10.1029/1998JB900108.

Schmidt, D.A., Bürgmann, R., Nadeau, R.M., and d'Alessio, M., 2005, Distribution of aseismic slip rate on the Hayward fault inferred from seismic and geodetic data: Journal of Geophysical Research, v. 110, B08406, doi: 10.1029/2004JB003397.

Schoenbohm, L.M., Burchfiel, B.C., Chen Liangzhong, and Yin Jiyun, 2006, Miocene to present activity along the Red River fault, China, in the context of continental extrusion, upper-crustal rotation, and lower-crustal flow: Geological Society of America Bulletin, v. 118, p. 672–688, doi: 10.1130/B25816.1.

Schubert, C., and Sifontes, R.S., 1970, Boconó fault, Venezuelan Andes, evidence of postglacial movement: Science, v. 170, p. 66–69, doi: 10.1126/science.170.3953.66.

Schubert, C., Estévez, R., and Henneberg, H., 1992, The Boconó fault, western Venezuela: Annales Tectonicae, v. VI, supplement, p. 238–260.

Segall, P., 2002, Integrating geologic and geodetic estimates of slip rate on the San Andreas fault system: International Geology Review, v. 44, p. 62–82, doi: 10.2747/0020-6814.44.1.62.

Sella, G.F., Dixon, T.H., and Mao, A., 2002, REVEL: A model for recent plate velocities from space geodesy: Journal of Geophysical Research, v. 107, 2081, doi: 10.1029/2000JB000033.

Shabanian, E., Siame, L., Bellier, O., Benedetti, L., and Abbassi, M.R., 2009a, Quaternary slip rates along the northeastern boundary of the Arabia–Eurasia collision zone (Kopeh Dagh Mountains, northeast Iran): Geophysical Journal International, v. 178, p. 1055–1077, doi: 10.1111/j.1365-246X.2009.04183.x.

Shabanian, E., Bellier, O., Siame, L., Arnaud, N., Abbassi, M.R., and Cochemé, J.-J., 2009b, New tectonic configuration in NE Iran: Active strike-slip faulting between the Kopeh Dagh and Binalud mountains: Tectonics, v. 28, TC5002, doi: 10.1029/2008TC002444.

Shen, Z.-K., Wang, M., Li, Y., Jackson, D.D., Yin, A., Dong, D., and Fang, P., 2001, Crustal deformation along the Altyn Tagh fault system, western China, from GPS: Journal of Geophysical Research, v. 106, p. 30,607–30,621, doi: 10.1029/2001JB000349.

Shen, Z.-K., Lü, J.-N., Wang, M., and Bürgmann, R., 2005, Contemporary crustal deformation around the southeast borderland of the Tibetan Plateau: Journal of Geophysical Research, v. 110, B11409, doi: 10.1029/2004JB003421.

Shyu, J.B.H., Sieh, K., Chen, Y.-G., and Liu, C.-S., 2005, Neotectonic architecture of Taiwan and its implications for future large earthquakes: Journal of Geophysical Research, v. 110, B08402, doi: 10.1029/2004JB003251.

Shyu, J.B.H., Sieh, K., Avouac, J.-P., Chen, W.-S., and Chen, Y.-G., 2006a, Millennial slip rate of the Longitudinal Valley fault from river terraces: Implications for convergence across the active suture of eastern Taiwan: Journal of Geophysical Research, v. 111, B08403, doi: 10.1029/2005JB003971.

Shyu, J.B.H., Sieh, K., Chen, Y.-G., and Chung, L.-H., 2006b, Geomorphic analysis of the Central Range fault, the second major active structure of the Longitudinal Valley suture, eastern Taiwan: Geological Society of America Bulletin, v. 118, p. 1447–1462, doi: 10.1130/B25905.1.

Shyu, J.B.H., Sieh, K., Chen, Y.-G., Chuang, R.Y., Wang, Y., and Chung, L.-H., 2008, Geomorphology of the southernmost Longitudinal Valley fault: Implications for evolution of the active suture of eastern Taiwan: Tectonics, v. 27, TC1019, doi: 10.1029/2006TC002060.

Sieh, K.E., and Jahns, R.H., 1984, Holocene activity of the San Andreas fault at Wallace Creek, California: Geological Society of America Bulletin, v. 95, p. 883–896, doi: 10.1130/0016-7606(1984)95<883:HAOTSA>2.0.CO;2.

Sieh, K., and Natawidjaja, D., 2000, Neotectonics of the Sumatran fault, Indonesia: Journal of Geophysical Research, v. 105, p. 28,295–28,326, doi: 10.1029/2000JB900120.

Silver, E.A., McCaffrey, R., and Smith, R.B., 1983, Collision, rotation, and the initiation of subduction in the evolution of Sulawesi, Indonesia: Journal of Geophysical Research, v. 88, p. 9407–9418, doi: 10.1029/JB088iB11p09407.

Simons, W.J.F., Socquet, A., Vigny, C., Ambrosius, B.A.C., Haji Abu, S., Promthong, C., Subarya, C., Sarsito, D.A., Matheussen, S., Morgan, P., and Spakman, W., 2007, A decade of GPS in Southeast Asia: Resolving Sundaland motion and boundaries: Journal of Geophysical Research, v. 112, B06420, doi: 10.1029/2005JB003868.

Socquet, A., Simons, W., Vigny, C., McCaffrey, R., Subarya, C., Sarsito, D., Ambrosius, B., and Spakman, W., 2006, Microblock rotations and fault coupling in SE Asia triple junction (Sulawesi, Indonesia) from GPS and earthquake slip vector data: Journal of Geophysical Research, v. 111, B08409, doi: 10.1029/2005JB003963.

Stevens, C., McCaffrey, R., Bock, Y., and Genrich, J., Endang, Subarya, C., Puntodewo, S.S.O., Fauzi, and Vigny, C., 1999, Rapid rotations about a vertical axis in a collisional setting revealed by the Palu fault, Sulawesi, Indonesia: Geophysical Research Letters, v. 26, p. 2677–2680.

Stevens, C., McCaffrey, R., Bock, Y., Genrich, J.F., Pubellier, M., and Subarya, C., 2002, Evidence for block rotations and basal shear in the world's fastest slipping continental shear zone in NW New Guinea, *in* Stein, S., and Freymueller, J., eds., Plate boundary zones: American Geophysical Union Geodynamics Series Volume 30, p. 87–99.

Stöcklin, J., 1974, Possible ancient continental margins in Iran, *in* Burke, C.A., and Drake, C.L., eds., The geology of continental margins: New York, Springer-Verlag, p. 873–887.

Surmont, J., Laj, C., Kissel, K., Rangin, C., Bellon, H., and Priadi, B., 1994, New palaeomagnetic constraints on the Cenozoic tectonic evolution of the north arm of Sulawesi, Indonesia: Earth and Planetary Science Letters, v. 121, p. 629–638, doi: 10.1016/0012-821X(94)90096-5.

Sutherland, R., and Norris, R.J., 1995, Late Quaternary displacement rate, paleoseismicity, and geomorphic evolution of the Alpine fault: Evidence from Hokuri Creek, South Westland, New Zealand: New Zealand Journal of Geology and Geophysics, v. 38, p. 419–430.

Sutherland, R., Berryman, K., and Norris, R., 2006, Quaternary slip rate and geomorphology of the Alpine fault: Implications for kinematics and seismic hazard in southwest New Zealand: Geological Society of America Bulletin, v. 118, p. 464–474, doi: 10.1130/B25627.1.

Talebian, M., and Jackson, J., 2002, Offset of the Main recent fault of NW Iran and implications for the late Cenozoic tectonics of the Arabia–Eurasia collision zone: Geophysical Journal International, v. 150, p. 422–439, doi: 10.1046/j.1365-246X.2002.01711.x.

Tapponnier, P., and Molnar, P., 1977, Active faulting and tectonics in China: Journal of Geophysical Research, v. 82, p. 2905–2930, doi: 10.1029/JB082i020p02905.

Tapponnier, P., and Molnar, P., 1979, Active faulting and Cenozoic tectonics of the Tien Shan, Mongolia and Baykal regions: Journal of Geophysical Research, v. 84, p. 3425–3459, doi: 10.1029/JB084iB07p03425.

Tapponnier, P., Peltzer, G., and Armijo, R., 1986, On the mechanics of the collision between India and Asia, *in* Coward, M.P., and Ries, A.C., eds., Collision tectonics: Geological Society of London Special Publication 19, p. 115–157.

Tapponnier, P., Meyer, B., Avouac, J.P., Peltzer, G., Gaudemer, Y., Guo Shunmin, Xiang Hongfa, Yin Kelun, Chen Zhitai, Cai Shuahua, and Dai Huagang, 1990, Active thrusting and folding in the Qilian Shan, and decoupling between upper crust and mantle in northeastern Tibet: Earth and Planetary Science Letters, v. 97, p. 382–403, doi: 10.1016/0012-821X(90)90053-Z.

Tapponnier, P., Xu Zhiqin, Roger, F., Meyer, B., Arnaud, N., Wittlinger, G., and Yang Jingsui, 2001, Oblique stepwise rise and growth of the Tibet Plateau: Science, v. 294, p. 1671–1677, doi: 10.1126/science.105978.

Tavakoli, F., Walpersdorf, A., Authemayou, C., Nankali, H.R., Hatzfeld, D., Tatar, M., Djamour, Y., Nilforoushan, F., and Cotte, N., 2008, Distribution of the right-lateral strike-slip motion from the Main Recent fault to the Kazerun fault system (Zagros, Iran): Evidence from present-day GPS velocities: Earth and Planetary Science Letters, v. 275, p. 342–347, doi: 10.1016/j.epsl.2008.08.030.

Thatcher, W., and England, P.C., 1998, Ductile shear zones beneath strike-slip faults: Implications for the thermomechanics of the San Andreas fault zone: Journal of Geophysical Research, v. 103, p. 891–905, doi: 10.1029/97JB02274.

Thomas, J.-C., Perroud, H., Cobbold, P.R., Bazhenov, M.L., Burtman, V.S., Chauvin, A., and Sadybakasov, E., 1993, A paleomagnetic study of Tertiary formations from the Kyrgyz Tien-Shan and its tectonic implications: Journal of Geophysical Research, v. 98, p. 9571–9589, doi: 10.1029/92JB02912.

Thompson, S.C., Weldon, R.J., Rubin, C.M., Abdrakhmatov, K., Molnar, P., and Berger, G.W., 2002, Late Quaternary slip rates across the central Tien Shan, Kyrgyzstan, Central Asia: Journal of Geophysical Research, v. 107, no. B9, 2203, doi: 10.1029/2001JB000596.

Tirrul, R., Bell, I.R., Griffis, R.J., and Camp, V.E., 1983, The Sistan suture zone of eastern Iran: Geological Society of America Bulletin, v. 94, p. 134–150, doi: 10.1130/0016-7606(1983)94<134:TSSZOE>2.0.CO;2.

Titus, S.J., DeMets, C., and Tikoff, B., 2005, New slip rate estimates for the creeping segment of the San Andreas fault: California Geology, v. 33, p. 205–208.

Trenkamp, R., Kellogg, J.N., Freymueller, J.T., and Mora, P.H., 2002, Wide plate margin deformation, southern Central America and northwestern South America, CASA GPS observations: Journal of South American Earth Sciences, v. 15, p. 157–171, doi: 10.1016/S0895-9811(02)00018-4.

Trifonov, V.G., 1978, Late Quaternary tectonic movements of western and Central Asia: Geological Society of America Bulletin, v. 89, p. 1059–1072, doi: 10.1130/0016-7606(1978)89<1059:LQTMOW>2.0.CO;2.

Trifonov, V.G., 1983, Late Quaternary tectogenesis: Moscow, Nauka, 224 p. (in Russian).

Tschanz, C.M., Marvin, R.F., Cruz, B.J., Mehnert, H.H., and Cebula, G.T., 1974, Geologic evolution of the Sierra Nevada de Santa Marta, northeastern Colombia: Geological Society of America Bulletin, v. 85, p. 273–284, doi: 10.1130/0016-7606(1974)85<273:GEOTSN>2.0.CO;2.

Van der Woerd, J., Ryerson, F.J., Tapponnier, P., Gaudemer, Y., Finkel, R., Meriaux, A.S., Caffee, M., Zhao Guoguang, and He Qunlu, 1998, Holocene left-slip rate determined by cosmogenic surface dating on the Xidatan segment of the Kunlun fault (Qinghai, China): Geology, v. 26, p. 695–698, doi: 10.1130/0091-7613(1998)026<0695:HLSRDB>2.3.CO;2.

Van der Woerd, J., Ryerson, F.J., Tapponnier, P., Meriaux, A.-S., Gaudemer, Y., Meyer, B., Finkel, R.C., Caffee, M.W., Zhao Guoguang, and Xu Zhuqin, 2000, Uniform slip rate along the Kunlun fault: Implications for seismic behaviour and large-scale tectonics: Geophysical Research Letters, v. 27, p. 2353–2356, doi: 10.1029/1999GL011292.

Van Der Woerd, J., Tapponnier, P., Ryerson, F.J., Meriaux, A.-S., Meyer, B., Gaudemer, Y., Finkel, R.C., Caffee, M.W., Zhao Guoguang, and Xu Zhuqin, 2002, Uniform postglacial slip-rate along the central 600 km of the Kunlun fault (Tibet), from ^{26}Al, ^{10}Be, and ^{14}C dating of riser offsets, and climatic origin of the regional morphology: Geophysical Journal International, v. 148, p. 356–388, doi: 10.1046/j.1365-246x.2002.01556.x.

Van Dissen, R., and Yeats, R.S., 1991, Hope fault, Jordan thrust, and uplift of the Seaward Kaikoura Range, New Zealand: Geology, v. 19, p. 393–396, doi: 10.1130/0091-7613(1991)019<0393:HFJTAU>2.3.CO;2.

Vernant, P., Nilforoushan, F., Hatzfeld, D., Abbassi, M.R., Vigny, C., Masson, F., Nankali, H., Martinod, J., Ashtiani, A., Bayer, R., Tavakoli, F., and Chéry, J., 2004, Present-day crustal deformation and plate kinematics in the Middle East constrained by GPS measurements in Iran and northern Oman: Geophysical Journal International, v. 157, p. 381–398, doi: 10.1111/j.1365-246X.2004.02222.x.

Vigny, C., Socquet, A., Rangin, C., Chamot-Rooke, N., Pubellier, M., Bouin, M.-N., Bertrand, G., and Becker, M., 2003, Present-day crustal deformation around Sagaing fault, Myanmar: Journal of Geophysical Research, v. 108, no. B11, 2533, doi: 10.1029/2002JB001999.

Walcott, R.I., 1984, The kinematics of the plate boundary zone through New Zealand: A comparison of short- and long-term deformations: Royal Astronomical Society Geophysical Journal, v. 79, p. 613–633.

Walker, R., and Jackson, J., 2002, Offset and evolution of the Gowk fault, SE Iran: A major intra-continental strike-slip system: Journal of Structural Geology, v. 24, p. 1677–1698, doi: 10.1016/S0191-8141(01)00170-5.

Walker, R., and Jackson, J., 2004, Active tectonics and late Cenozoic strain distribution in central and eastern Iran: Tectonics, v. 23, TC5010, doi: 10.1029/2003TC001529.

Walker, R.T., Gans, P., Allen, M.B., Jackson, J., Khatib, M., Marsh, N., and Zarrinkoub, M., 2009, Late Cenozoic volcanism and rates of active faulting in eastern Iran: Geophysical Journal International, v. 177, p. 783–805.

Wallace, K., Yin, G., and Bilham, R., 2004, Inescapable slow slip on the Altyn Tagh fault: Geophysical Research Letters, v. 31, L09613, doi: 10.1029/2004GL019724.

Wallace, L.M., Beavan, J., McCaffrey, R., Berryman, K., and Denys, P., 2007, Balancing the plate motion budget in the South Island, New Zealand using GPS, geological and seismological data: Geophysical Journal International, v. 168, p. 332–352, doi: 10.1111/j.1365-246X.2006.03183.x.

Walpersdorf, A., Rangin, C., and Vigny, C., 1998a, GPS compared to long-term geologic motion of the north arm of Sulawesi: Earth and Planetary Science Letters, v. 159, p. 47–55, doi: 10.1016/S0012-821X(98)00056-9.

Walpersdorf, A., Vigny, C., Manurung, P., Subarya, C., and Sutisna, S., 1998b, Determining the Sula block kinematics in the triple junction area of Indonesia with GPS: Geophysical Journal International, v. 135, p. 351–361, doi: 10.1046/j.1365-246X.1998.00641.x.

Walpersdorf, A., Hatzfeld, D., Nankali, H., Tavakoli, F., Nilforoushan, F., Tatar, M., Vernant, P., Chéry, J., and Masson, F., 2006, Difference in the GPS deformation pattern of north and central Zagros (Iran): Geophysical Journal International, v. 167, p. 1077–1088, doi: 10.1111/j.1365-246X.2006.03147.x.

Wang, E., Burchfiel, B.C., Royden, L.H., Chen Liangzhong, Chen Jishen, Li Wenxin, and Chen Zhiliang, 1998, Late Cenozoic Xianshuihe-Xiaojiang, Red River, and Dali fault systems of southwestern Sichuan and central Yunnan, China: Geological Society of America Special Paper 327, 108 p.

Wang, H., Wright, T.J., and Biggs, J., 2009, Interseismic slip rate of the northwestern Xianshuihe fault from InSAR data: Geophysical Research Letters, v. 36, L03302, doi: 10.1029/2008GL036560.

Washburn, Z., Arrowsmith, J.R., Forman, S.L., Cowgill, E., Wang Xiaofeng, Zhang Yueqiao, and Chen Zhengle, 2001a, Late Holocene earthquake history of the central Altyn Tagh fault, China: Geology, v. 29, p. 1051–1054, doi: 10.1130/0091-7613(2001)029<1051:LHEHOT>2.0.CO;2.

Washburn, Z., Arrowsmith, J.R., Dupont-Nivet, G., Wang Xiaofeng, Zhang Yueqiao, and Chen Zhengle, 2001b, Paleoseismology of the Xorxol segment of the central Altyn Tagh fault, Xinjiang, China: Annals of Geophysics, v. 46, p. 1015–1034.

Wdowinski, S., Bock, Y., Baer, G., Prawirodirdjo, L., Bechor, N., Naaman, S., Knafo, R., Forrai, Y., and Melzer, Y., 2004, GPS measurements of current crustal movements along the Dead Sea fault: Journal of Geophysical Research, v. 109, B05403, doi: 10.1029/2003JB002640.

Weber, G.E., and Nolan, J.M., 1995, Determination of late Pleistocene–Holocene slip rates along the San Gregorio fault zone, San Mateo County, California, *in* Jacobson, M.L., compiler, National Earthquake Hazards Reduction Program annual project summaries: XXXVI: Volume 1: U.S. Geological Survey Open-File Report OFR 95-210, p. 805–807.

Weber, J., Dixon, T., DeMets, C., Ambeh, W., Jansma, P.E., Mattioli, G., Saleh, J., Sella, G., Bilham, R., and Pérez, O., 2001, GPS estimate of relative motion between the Caribbean and South-American plates, and geological implications for Trinidad and Venezuela: Geology, v. 29, p. 75–78, doi: 10.1130/0091-7613(2001)029<0075:GEORMB>2.0.CO;2.

Weldon, R.J., Sieh, K.E., Zhu, C., Han, Y., Yang, J., and Robinson, S., 1994, Slip rate and recurrence interval of earthquake on the Hong He (Red River) fault, Yunnan, P.R.C., *in* International Workshop on Seismotectonics and Seismic Hazard in SE Asia: Hanoi, Vietnam, p. 244–248.

Wellman, H.W., 1966, Active wrench faults in Iran, Afghanistan and Pakistan: Geologische Rundschau, v. 55, p. 716–735, doi: 10.1007/BF02029650.

Wen Xueze, Xu Xiwei, Zheng Rongzhang, Xie Yingqing, and Wan Chuang, 2003, Average slip-rate and recent large earthquake ruptures along the Garzê-Yushu fault: Science in China, v. 46, p. 276–288.

Wilson, B., Dewers, T., Reches, Z., and Brune, J., 2005, Particle size and energetics of gouge from earthquake rupture zones: Nature, v. 434, p. 749–752, doi: 10.1038/nature03433.

Wright, T.J., Parsons, B., England, P.C., and Fielding, E.J., 2004, InSAR observations of low slip rates on the major faults of western Tibet: Science, v. 305, p. 236–239, doi: 10.1126/science.1096388.

Xu Xiwei, Tapponnier, P., Van Der Woerd, J., Ryerson, F.J., Wang Feng, Zheng Rongzhang, Chen Wenbin, Ma Wentao, Yu Guihua, Chen Guihua, and Meriaux, A.S., 2005, Late Quaternary sinistral slip rate along the Altyn Tagh fault and its structural transformational model: Science in China, Earth Science, v. 48, p. 384–397.

Yang, J.S., 1991, The Kakapo fault—A major active dextral fault in the central North Canterbury–Buller regions of New Zealand: New Zealand Journal of Geology and Geophysics, v. 34, p. 137–143.

Yin, A., and Nie, S.-Y., 1994, A Phanerozoic palinspastic reconstruction of China and its neighboring regions, *in* Yin, A., and Harrison, M., eds., The tectonic evolution

of Asia: World and Regional Geology 8: Cambridge, Cambridge University Press, p. 442–485.

Yin, A., Dang, Y.-Q., Zhang, M., McRivette, M.W., Burgess, W.P., and Chen, X.-H., 2007, Cenozoic tectonic evolution of Qaidam basin and its surrounding regions (Part 2): Wedge tectonics in southern Qaidam basin and the Eastern Kunlun Range, *in* Sears, J.W., et al., eds., Whence the Mountains? Inquiries into the evolution of orogenic systems: A volume in honor of Raymond A. Price: Geological Society of America Special Paper 433, p. 369–390, doi: 10.1130/2007.2433(18).

Yin, A., Dang, Y.-Q., Wang, L.-C., Jiang, W.-M., Zhou, S.-P., Chen, X.-H., Gehrels, G.E., and McRivette, M.W., 2008a, Cenozoic tectonic evolution of Qaidam basin and its surrounding regions (Part 1): The southern Qilian Shan-Nan Shan thrust belt and northern Qaidam basin: Geological Society of America Bulletin, v. 120, p. 813–846, doi: 10.1130/B26180.1.

Yin, A., Dang, Y.-Q., Zhang, M., Chen, X.-H., and McRivette, M.W., 2008b, Cenozoic tectonic evolution of the Qaidam basin and its surrounding regions (Part 3): Structural geology, sedimentation, and regional tectonic reconstruction: Geological Society of America Bulletin, v. 120, p. 847–876, doi: 10.1130/B26232.1.

Yu, S.-B., and Kuo, L.-C., 2001, Present-day crustal motion along the Longitudinal Valley fault, eastern Taiwan: Tectonophysics, v. 333, p. 199–217, doi: 10.1016/S0040-1951(00)00275-4.

Yu, S.-B., Jackson, D.D., Yu, G.-K., and Liu, C.-C., 1990, Dislocation model for crustal deformation in the Longitudinal Valley area, eastern Taiwan: Tectonophysics, v. 183, p. 97–109, doi: 10.1016/0040-1951(90)90190-J.

Yu, S.-B., Chen, H.-Y., and Kuo, L.-C., 1997, Velocity field of GPS stations in the Taiwan area: Tectonophysics, v. 274, p. 41–59, doi: 10.1016/S0040-1951(96)00297-1.

Yu, S.-B., Kuo, L.-C., Punongbayan, R.S., and Ramos, E.G., 1999, GPS observation of crustal motion in the Taiwan-Luzon region: Geophysical Research Letters, v. 26, p. 923–926, doi: 10.1029/1999GL900148.

Yuen, D.A., Fleitout, L., Schubert, G., and Froidevaux, C., 1978, Shear deformation zones along transform faults and subducting slabs: Royal Astronomical Society Geophysical Journal, v. 54, p. 93–119.

Zachariasen, J., Berryman, K., Langridge, R., Prentice, C., Rymer, M., Stirling, M., and Villamor, P., 2006, Timing of late Holocene surface rupture of the Wairau fault, Marlborough, New Zealand: New Zealand Journal of Geology and Geophysics, v. 49, p. 159–174.

Zakharov, S.A., 1958, Sediment structure of the Mesozoic and Cenozoic of the Tadjik Depression: Stalinabad, Donish, 230 p. (in Russian).

Zakharov, S.A., 1964, Cardinal questions of tectogenesis in connection with the direction of searches for oil and gas in the Tadjik Depression and the bases of seismotectonic regionalization of southern Tadjikistan (in Russian), *in* Problems of the geology of Tadjikistan: Dushanbe, Donish, p. 33–78.

Zhang Huilan, Liu, H.-L., and Kanamori, H., 1983, Source processes of large earthquakes along the Xianshuihe fault in southwestern China: Seismological Society of America Bulletin, v. 73, p. 537–551.

Zhang Peizhen, Molnar, P., Burchfiel, B.C., Royden, L., Wang Yipeng, Deng Qidong, Song Fangmin, Zhang Weiqi, and Jiao Decheng, 1988, Bounds on the Holocene slip rate of the Haiyuan fault, north-central China: Quaternary Research, v. 30, p. 151–164, doi: 10.1016/0033-5894(88)90020-8.

Zhang Peizhen, Burchfiel, B.C., Molnar, P., Zhang Weiqi, Jiao Decheng, Deng Qidong, Wang Yipeng, Royden, L., and Song Fangmin, 1990, Late Cenozoic tectonic evolution of the Ningxia-Hui Autonomous Region, China: Geological Society of America Bulletin, v. 102, p. 1484–1498, doi: 10.1130/0016-7606(1990)102<1484:LCTEOT>2.3.CO;2.

Zhang Peizhen, Burchfiel, B.C., Molnar, P., Zhang Weiqi, Jiao Dechen, Deng Qidong, Wang Yipeng, Royden, L., and Song Fangmin, 1991, Amount and style of late Cenozoic deformation in the Liupan Shan area, Ningxia Autonomous Region, China: Tectonics, v. 10, p. 1111–1129, doi: 10.1029/90TC02686.

Zhang, Peizhen, Shen, Z.-K., Wang, M., Gan, W.-J., Bürgmann, R., Molnar, P., Wang, Q., Niu, Z.-J., Sun, J.-Z., Wu, J.-C., Hanrong, S., and Xinzhao, Y., 2004, Continuous deformation of the Tibetan Plateau from global positioning system data: Geology, v. 32, p. 809–812, doi: 10.1130/G20554.1.

Zhang, Peizhen, Molnar, P., and Xu, X.-w., 2007, Late Quaternary and present-day rates of slip along the Altyn Tagh fault, northern margin of the Tibetan Plateau: Tectonics, v. 26, TC5010, doi: 10.1029/2006TC002014.

Zhang Weiqi, Jiao Decheng, Zhang Peizhen, Molnar, P., Burchfiel, B.C., Deng Qidong, and Wang Yipeng, 1987, Displacement along the Haiyuan fault associated with the great 1920 Haiyuan, China, earthquake: Seismological Society of America Bulletin, v. 77, p. 117–181.

Zubovich A.V., Makarov, V.I., Kuzikov, S.I., Mosienko, O.I., and Shchelochkov, G.G., 2007, Intracontinental mountain building in Central Asia as inferred from satellite geodetic data: Geotectonics, v. 41, p. 13–25.

Manuscript Received 05 May 2009
Revised Manuscript Received 21 December 2009
Manuscript Accepted 23 January 2010